IDENTIFICATION OF NOVEL TRANSCRIPTION FACTORS REGULATING RECOVERY OF THE ENDOTHELIAL LINEAGE IN AVASCULAR MUTANTS

Christopher E. Schmitt

A dissertation submitted to the faculty of the University of North Carolina at Chapel Hill in partial fulfillment of the requirements for the degree of Doctor of Philosophy in the Curriculum in Genetics and Molecular Biology.

Chapel Hill
2012

Approved by:

Victoria Bautch, PhD
Suk-Won Jin, PhD
John Rawls, PhD
Bob Goldstein, PhD
Frank Conlon, PhD

ABSTRACT

CHRISTOPHER SCHMITT: Identification of Novel Transcription Factors Regulating Recovery of the Endothelial Lineage in Avascular Mutants
(Under the direction of Dr. Suk-Won Jin)

Multiple mesodermal tissues are known to give rise to endothelial cells during development. Furthermore, markers for functionally distinct endothelium are well established. Therefore, it is likely that multiple distinct populations of endothelial cells exist during development and into adulthood. Two zebrafish mutants, *clo*che and *groom of cloche* provide a unique opportunity to interrogate the heterogeneous origin of the endothelial lineage. Homozygous mutant embryos lack the majority of the endothelial lineage at early developmental stages, however, generate rudimentary vessels at later stages, indicating that they retain the ability to generate endothelial cells despite this initial lack of early endothelial progenitors. To delineate the developmental source of the endothelial cells in these avascular mutant embryos, we first performed lineage tracing from early gastrula to determine the fate of mesoderm. Consistent with their phenotype, we found an increase of *kdrl*$^{-}$ unspecified mesoderm, indicating that much of the mesoderm apportioned to become angioblasts fails to become specified. Conversely, endothelial differentiation from the tailbud, a proposed secondary source of endothelial cells during development, was largely unperturbed. Consistent with this finding, the majority of the early *kdrl*$^{+}$ cells found in avascular mutant embryos are specified from tailbud. To better elucidate the molecular basis of endothelial recovery in avascular mutant embryos, we analyzed the gene expression profile using microarray analysis on isolated mutant endothelial cells. We find that the expression of the genes characteristic of other mesodermal lineages are substantially elevated in *kdrl*$^{+}$ cells isolated from avascular mutant embryos. Subsequent validation identified two transcription factors, *sox11b* and *pax9,* both of which have not previously implicated in vascular development. Yet, we confirmed that both genes

are expressed in the vasculature and knockdown of either gene results in a vascular phenotype. Additionally, we found that the function of Pax9 appears to be evolutionarily conserved. Taken together, our analyses illustrate a complex regulation of endothelial specification and differentiation during vertebrate development. Furthermore, we have identified two new key transcription factors involved in vascular development.

ACKNOWLEDGEMENTS

I would like to thank:

My advisor, Suk-Won Jin

The Jin Lab, past and present members:

Hyeseon Kang, Samantha Lee, Jose Cardona-Costa, Will Dunworth, Jun-Dae Kim, Sophie Dal-Pra

My Committee Members

Vicki Bautch
Frank Conlon
John Rawls
Bob Goldstein

My Parents, Ed and Barbara Schmitt

Developmental Biology Training Grant

University of North Carolina-Chapel Hill
Curriculum in Genetics and Molecular Biology

TABLE OF CONTENTS

LIST OF FIGURES

Figure

LIST OF ABBREVIATIONS

BMP	bone morphogenetic protein
BrdU	bromodeoxyuridine
BSA	bovine serum albumin
cas	*casanova*
clo	*cloche*
CVP	caudal vein plexus
EDTA	Ethylenediaminetetraacetic acid
eGFP	enhanced green fluorescent protein (GFP)
EG-VEGF	endocrine-gland-derived vascular endothelial growth factor
etv2	*ets variant 2*. The zebrafish homolog of mouse *ER71*
FACS	fluorescence-activated cell sorting
FBS	fetal bovine serum
FGF	fibroblast growth factor
gata1	*GATA binding protein 1*
gata2	*GATA binding protein 2*
grc	*groom of cloche*
HBSS	Hank's balanced salt solution
hlx-1	*H2.0-like homeobox 1*
HPF	hours post-fertilization
HUVEC	Human umbilical vein endothelial cells
ISV	intersegmental vessel

kdrl	*kinase insert domain receptor like.* The functional zebrafish ortholog of VEGFR2.
msx1	*msh homeobox 1*
pax9	*paired box 9*
PBS	phosphate buffered saline
PCR	polymerase chain reaction
pu.1(*spi1*)	spleen focus forming virus (SFFV) proviral integration oncogene
qRT-PCR	quantitative reverse transcription-polymerase chain reaction
RIN	RNA integrity number
RT-PCR	reverse transcription-polymerase chain reaction
SAM	Significance analysis of microarrays
sox11b	*SRY-related HMG-box transcription factor 11b*
sox17	*SRY-related HMG-box transcription factor 17*
tal1	*T-cell acute lymphocytic leukemia protein 1*
tbx20	T-box protein 20
TUNEL	terminal deoxynucleotidyl transferase mediated dUTP nick end labeling
VEGF	vascular endothial growth factor
WNT	wingless-type MMTV integration site family
WT	wild-type

Chapter 1

Introduction

Emergence of the vascular system.

The vascular system is comprised of multiple cell types that allow for circulation of blood, nutrients, water and waste. Vascular smooth muscle cells, mural cells, and endothelial cells make up this complex system that is essential for the development, growth, and survival of a vertebrate organism. Endothelial cells line the vessels and mediate the exchange of oxygen between blood and surrounding tissues. In addition to diseases directly involving the vasculature such as thrombosis, numerous pathologies are exacerbated by aberrant vascular patterning or regulation [1]. During development, endothelial cells undergo morphogenetic events, which can be separated into two different processes: vasculogenesis and angiogenesis. Vasculogenesis is characterized by the formation of new blood vessels de novo, during mid-stages of somitogenesis, while subsequent formation of blood vessels from pre-existing vessels is collectively referred to as angiogenesis.

During development, endothelial cells are specified from the mesoderm during early stages of gastrulation in close proximity to hematopoietic cells [2]. In mouse, *er71/etv2* is shown to be necessary for the proper specification

endothelial cells [3], as is T-cell acute lymphocytic leukemia protein 1 (TAL1) [4]. Similarly, in zebrafish, it has been shown that prior to *kdrl* expression, angioblasts express the ets-domain transcription factor, *etv2* within the lateral plate mesoderm [5]. Subsequently, angioblasts express *kdrl* and migrate into the midline. These angioblasts coalesce and form a primitive vascular cord in the midline of the embryo [6, 7]. During development, the vertebrate endothelial lineage arises from mesodermal tissues. It has been reported that diverse mesodermal tissues including lateral plate mesoderm[8], blood islands within the yolk sac[9, 10], allantois[11], somitic mesoderm[12], as well as placenta[13, 14], can produce endothelial cells during development. Moreover, the entire mesoderm excluding notochord and prechordal mesoderm can serve as sources for endothelial cells[15], suggesting that angiogenic potential might be one of the intrinsic properties of the developing mesoderm. In addition, almost every cell in a 16 or 32-cell stage *Xenopus* embryos was fate-mapped and shown to give rise to endothelial cells, indicating the diverse origin of endothelial cells [16]. In addition, lineage tracing studies have indicated that a small portion of the endothelial lineage comes from hemangioblast, a common progenitor of both hematopoietic and vascular lineages [17]. Subsequently, endothelial cells further differentiate as arterial, venous or lymphatic endothelial cells, each of which possesses unique molecular and cellular characteristics.

Not only do endothelial cells originate from spatially distinct populations, they emerge during separate waves of differentiation during development. For instance, previous works in zebrafish have shown that endothelial progenitors

migrate from the lateral plate mesoderm at multiple time points during development [6], suggesting that the differentiation of endothelial progenitors is also regulated in a temporal manner. During development, lateral plate mesoderm-derived angioblasts have been shown to give rise to the majority of trunk vasculature [6]. In zebrafish, it has been shown that the tailbud also contributes to the endothelial lineage in a WNT-dependant manner [18]. That is, Wnt signaling regulates the formation of the endothelial lineage within the tailbud mesoderm, without obvious effects on the lateral plate mesoderm [18]. In fact the majority of caudal vasculature is derived from tailbud (Schmitt et al, submitted).

Subsequent processes, termed angiogenesis include arterio-venous specification and formation of secondary vessels. Conventional wisdom is that the majority of new vessels form by angiogenesis after early development. After early developmental stages, there is evidence for continued vasculogenesis mediated by circulating endothelial progenitor cells, which are thought to repair vascular damage and contribute to angiogenesis [19, 20]. Nonetheless, pathological models have indicated that de novo angioblast specification may occur in adult tissues. For instance, neuroblastoma stem cells have been shown to have the capacity to give rise to endothelial and these cultured cells are wholly derived from ectoderm [21]. Despite recent progress, the molecular and cellular mechanisms that regulate the specification and differentiation of endothelial lineage remain elusive. Given their diverse function and morphology, it is plausible that the endothelial lineage emerges from heterogeneous populations

of progenitors during development [22]. And by delineating novel transcriptional programs directing vasculogenesis and angiogenesis, therapeutics for a wide variety of diseases can be created.

Genetic and Molecular Mechanisms of Vascular Development

As previously mentioned specification and differentiation of the endothelial lineage is regulated by multiple arrays of signaling pathways and transcription factors. Many of these pathways play key roles during angiogenesis. Previous research has identified key signaling pathways that modulate the patterning and proliferation of endothelial cells, including Vascular Endothelial Growth Factor (VEGF)[23, 24], Fibroblast Growth Factor (FGF)[25, 26], Wnt[27], and Bone Morphogenetic Protein (BMP)[28], as well as essential transcription factors such as ETS transcription factor family member, *Etv2/ER71* and *FLI1* [29].

Molecular and cellular analyses have led to the characterization of many markers of arterial, venous and lymphatic endothelium [30]. There have been many genes characterized which mark only subsets of endothelial cells [30]. For instance, it is well established that *ephrinB2*, *notch1b*, and *tbx20* are preferentially expressed within arterial endothelial cells, while *ephB4*, *disabled2*, and *nr2f2* (*COUP-TFII* in mouse) are selectively expressed within venous endothelial cells during development [30, 31]. Even endothelial cells residing within the same vessel display high level of heterogeneity. For instance, a subset of endothelial cells within the dorsal aorta differentiate as a hemogenic endothelium and express hematopoietic stem cell markers *runx1* and *c-myb*, while retaining the molecular properties of endothelial cells [32-34]. In addition,

certain markers such as *sox17* appear to be expressed at varying levels in cells within the same vessel (Fig. 1.3). Therefore, multiple lines of evidence support the prevalent heterogeneity within the endothelial lineage.

Consistent with the observation that the developmental origin of the endothelial lineage is diverse, subtypes of endothelial cells appear to possess distinct molecular and cellular properties. Indeed, it has been shown that subtypes of endothelial cells distinctively respond to extracellular signaling. EG-VEGF was shown to promote proliferation of endocrine gland endothelium selectively over other types of endothelial cells [35]. It was further shown that this mitogen, EG-VEGF, elicited very little response from endothelial cells in other tissues, such as cornea or skeletal muscle, indicating that endothelial cells from different tissues may have distinct molecular identities [35]. We have recently reported that BMP2 signaling selectively activates venous endothelial cells without very little influence arterial endothelial cells [36]. This effect was shown to be important in multiple venous tissues such as caudal vein plexus and sub-intestinal vein [36]. While markers of arterial or venous identity have been well established, selective response to angiogenic cues is relatively new. Expression of genes in the Notch pathway [37] as well as a transcription factor, *hlx-1* [38], have been shown to determine tip versus stalk cell phenotype in the developing vasculature. Therefore, even transient changes in expression levels of genes within endothelial cells can greatly affect behavior and phenotype.

Taken together, the vertebrate endothelial lineage is comprised of a multiple populations of cells with multiple origins and different molecular

programs. Therefore, identification of additional factors that regulate specification and differentiation of the endothelial lineage will help to further study the genetic mechanisms of vascular development.

cloche and *groom of cloche*, two avascular zebrafish mutants

Zebrafish has been extensively used to study cardiovascular development and is an excellent model to delineate the cellular and molecular mechanisms that contribute to heterogeneity within the endothelial lineage. Since embryos are transparent[39] and begin circulation by 24 hours post fertilization (hpf)[40], the zebrafish allows for short completion of experiments. A high fecundity allows for the collection of data with a large sample size [41]. Additionally, the embryos are small enough that development can proceed in the absence of heartbeat, induced chemically or genetically [42]. Furthermore, zebrafish vascular development is remarkably similar to mammalian development. The stepwise timing of events such as vascular cord coalescence, arterio-venous specification, onset of circulation, intersegmental vessel angiogenesis, and lymphangiogenesis recapitulate that which is observed in mammalian systems [39].

Previous attempts have been made to harness the attributes of zebrafish as a model system to better understand development of higher vertebrate species. For instance, several forward genetic screens have identified many mutations with altered development of the endothelial lineage [43]. One mutation, *cloche* (*clo*), is particularly interesting. Homozygous *clo* mutant embryos lack *kdrl*$^{+}$ endothelial cells as well as *gata1*$^{+}$ or *gata2*$^{+}$ hematopoietic progenitors, supporting the notion of a hemangioblast [44]. Named *cloche*,

because of the cardiac morphology of mutant resembles a bell ("cloche" in French). Lineage tracing studies have determined that the increase in myocardial lineage is at the expense of most hematopoietic, endocardial and endothelial lineages, indicating common progenitors for these lineages in development [45]. Although the nature of the locus that is affected by *clo* mutation is currently unknown, it appears to be the one of the earliest genes involved in endothelial differentiation since over-expression of several known factors alleviate the phenotype of homozygous mutant embryos. Nevertheless, *clo* homozygotes display a dramatic early absence of *scl*$^{+}$, *gata1*$^{+}$, *pu.1*$^{+}$, and *kdrl*$^{+}$ lineages, leading to embryonic lethality at around 7dpf [46].

To identify additional factors involved in vascular development, a large scale forward genetic screen was performed using *Tg(kdrl:eGFP)*^{s843} transgenic zebrafish, which labels all endothelial cells with eGFP.[25] From the screen, we have identified a novel mutant, *groom of cloche* (*grc*), which lacks the majority of the endothelial lineage at early stage[47], which is reminiscent of previously isolated mutant, *cloche* (*clo*) that lacks both endothelial and hematopoietic lineages[44]. Additionally, we found that other mesodermal lineages are not perturbed using *in situ* hybridization. Using high-throughput genome and transcriptome sequencing, we determined that *grc*$^{-/-}$ embryos have a point mutation causing a leucine to proline amino acid change in the *etv2* gene, also known as *etsrp*/*er71*. Mutations in this gene with similar phenotypes have also been reported as it appears to function to specify the majority of endothelium from lateral plate mesoderm.[48] Although much of the early *kdrl*$^{+}$ lineage is

missing or delayed in these mutants, a crude vascular network does form in both *grc* and *clo* homozygotes. Despite the lack of endothelial cells at early stages, these avascular mutant embryos can generate endothelial cells at later stages[47], suggesting that distinct molecular mechanisms may be used to modulate the emergence of the endothelial lineage in these embryos.

Nevertheless, both mutants retain a small population of *kdrl*$^+$ progenitors which subsequently undergo vasculogenesis and angiogenesis, such as formation of intersegmental vessels. Additionally, *grc* are distinct from *clo* in that homozygotes have been raised to adulthood and are viable. I have hypothesized that the majority of *kdrl*$^+$ cells in both mutants are derived from tailbud and that *grc* is able to specify some angioblasts from the lateral plate mesoderm (Figure 1.1 Panel A). Using the *Tg(kdrl:EGFP)* transgenic line, we found that *kdrl*$^+$ cells appear in homozygous *grc* and *clo* embryos as early as 18.5 hpf (shown in Figure 1.1 panel C). While *kdrl*$^+$ cells found in homozygous *clo* embryos are clustered within the intermediate cell mass (ICM), which is located in the posterior region of the embryos, those found in homozygous *grc* embryos are also clustered in this region with sparse *kdrl*$^+$ cells along the entire body axis, indicating that some lateral plate-derived angioblasts are specified in *grc*. Interestingly, *kdrl*$^+$ cells in *grc* or *clo* homozygous embryos fail to express *cdh5* (*VE-Cadherin*), suggesting that these cells are not fully differentiated endothelial cells. Therefore, the *kdrl*$^+$ cells found in these embryos appear to be a unique population, and might be distinct in their molecular and cellular characteristics. Due to this apparent lack of majority of endothelial lineage in both mutants, we

hypothesized that the existing *kdrl*$^+$ cells are able to be specified despite their *clo* or *grc* genetic backgrounds. Furthermore, this apparent resiliency may indicate a unique transcriptional program or developmental origin.

As seen in **Figure 1.1 Panel B** (white arrows), GFP$^+$ cells arise in the caudal region of the embryo, posterior to the yolk-extension. Vasculature in these mutants is aberrant. This may be due to a developmental delay where *kdrl*$^+$ cells are specified at a later time and therefore miss their proper migratory cues *or* are intrinsically unable to pattern properly.

Research presented in this dissertation

The majority of this thesis is based upon a pilot experiment that involved the transcriptional profiling of *kdrl*$^+$ cells in the early mutant embryos to elucidate alternative mechanisms of vasculogenesis and/or angiogenesis. In Chapter 2, we performed Significance analysis of microarrays (SAM) [49] to reveal the molecular profile of avascular mutant *kdrl*$^+$ cells. We isolated *kdrl*+ cells using FACS sorting and profiled their transcriptome using microarray analyses and found that the relative levels of thousands of mRNAs in both mutants compared to wild-type was significantly different. Screening these lists for transcription factors, we identified 43 transcription factors that were greater than two-fold upregulated in avascular mutant *kdrl*$^+$ cells. Using morpholino-mediated knockdown, the function of one transcription factor, *SRY-related HMG Box 11b* (*sox11b*), was interrogated and found to be necessary for proper vascular patterning, particularly sprouting angiogenesis.

In Chapter 3, I focused on another validated transcription factor, *pax9*, which was found to preferentially affect avascular mutant secondary vessel morphogenesis. I characterized the novel mutation, *grc*, which lacks a majority of endothelial cells by evaluating the phenotype, the mode of action of *grc* and cloning of the genetic lesion. Using lineage tracing in early gastrula, I determined that much of the mesodermal lineage defaults to an unspecified mesodermal-subtype in the absence of *clo* or *etv2* function. Additionally, using tailbud lineage tracing found that the majority of *kdrl*$^{+}$ cells in these mutants are derived from the tailbud as opposed to lateral plate mesoderm.

Using multifaceted approaches, we validated a subset of transcription factors indicated to be upregulated by the array and found that two, *pax9* and *sox11b*, were involved in vascular morphogenesis. Taken together, the research presented in this dissertation includes multiple novel findings. Foremost, *kdrl*+ cells in *clo* or *grc* have a unique transcriptional profile. These endothelial cells are dependent on *pax9* for proper morphogenesis (summarized in **Figure1.3**). Much of the avascular mutant endothelial cells come from tailbud mesoderm as opposed to lateral plate mesoderm. Our model has allowed for the discovery of new genes involved in vascular development. Our results demonstrate that developmental ontogeny of the endothelial lineage is far more complex than previously thought. The research in this thesis expands our current understanding on how spatial, developmental and molecular heterogeneity within the endothelial lineage is a real phenomenon and is regulated during development. Considering that dysregulation of angiogenesis is frequently

associated with the onset and subsequent progression of various pathological conditions, including cancer, retinopathy, and diabetes, knowledge obtained from the thesis research present here may help us to develop anti- or pro-angiogenic therapies selectively targeting sub-populations of endothelial cells.

Figures:

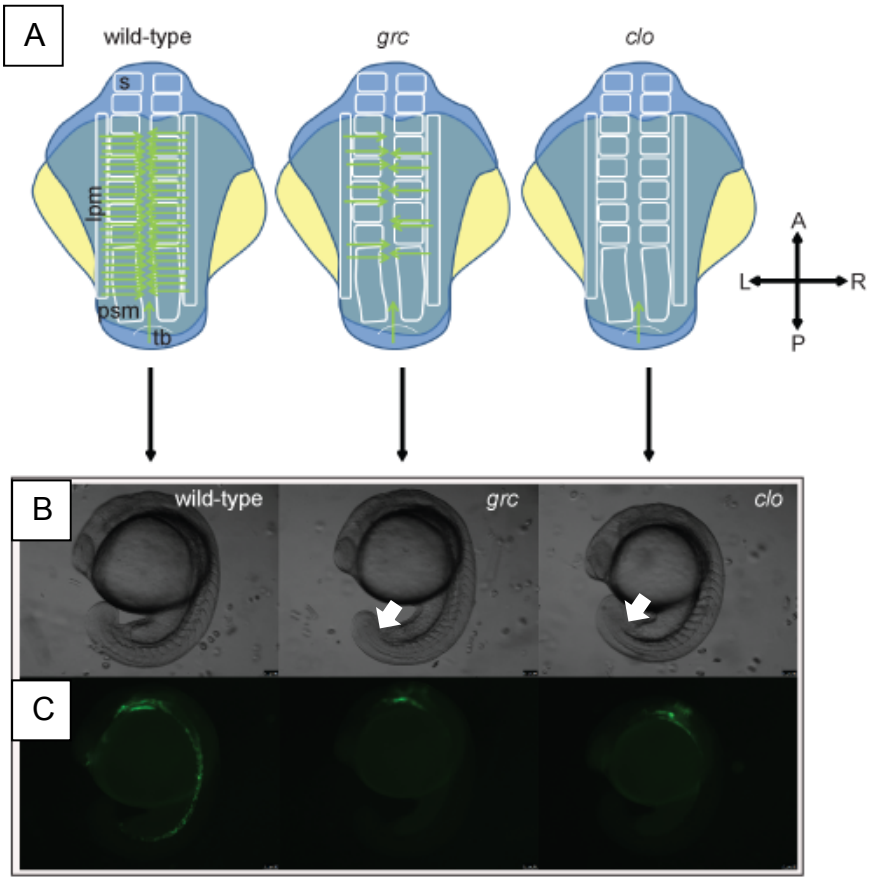

Fig. 1.1. Emergence of the endothelial lineage in zebrafish embryos.

(A) Schematic diagram illustrating the location of emerging endothelial cells in wild-type (left), grc/etv2 (middle), and clo (right) embryos. The top row is a depiction of a dorsal view of 12-15 somite embryos. Lateral plate mesoderm (lpm), Somite (s), Pre-somitic mesoderm (psm) and tailbud (tb) are all depicted in the wild-type embryo. Green arrows indicate angioblast migration into the midline. (B) Brightfield micrographs of 18.5 hpf wild-type (left), grc/etv2 (middle), and clo (right) embryos. (C) epifluorescent micrographs of 18.5 hpf wild-type

(left), grc/etv2 (middle), and clo (right) embryos in *Tg(kdrl:eGFP)* transgenic background. The only apparent *kdrl*$^{+}$ lineage in the avascular mutants is the pharyngeal endoderm at 18.5 hpf, though *kdrl*$^{+}$ cells are present in the midline (Data not shown).

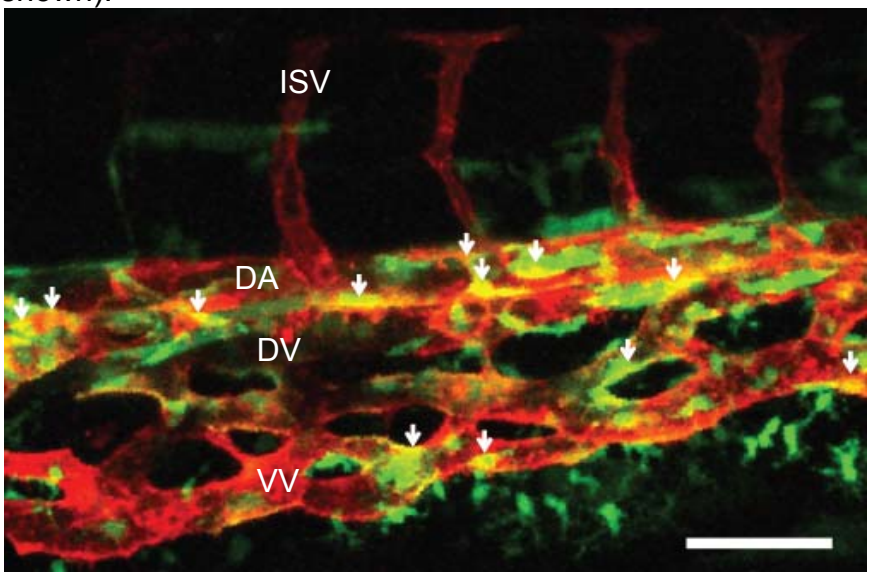

Fig. 1.2. An example of endothelial heterogeneity.

Flattened confocal z-stacks image series taken from the caudal vein plexus of a 72 hpf *Tg(sox17:eGFP;kdrl:mCherry)* embryo. Lateral view; anterior left and posterior right. Intersegmental vessels (ISV), dorsal aorta (DA), dorsal vein (DV), and ventral vein (VV) are labeled. White arrows indicate double positive cells. Scale bar= 30μM.

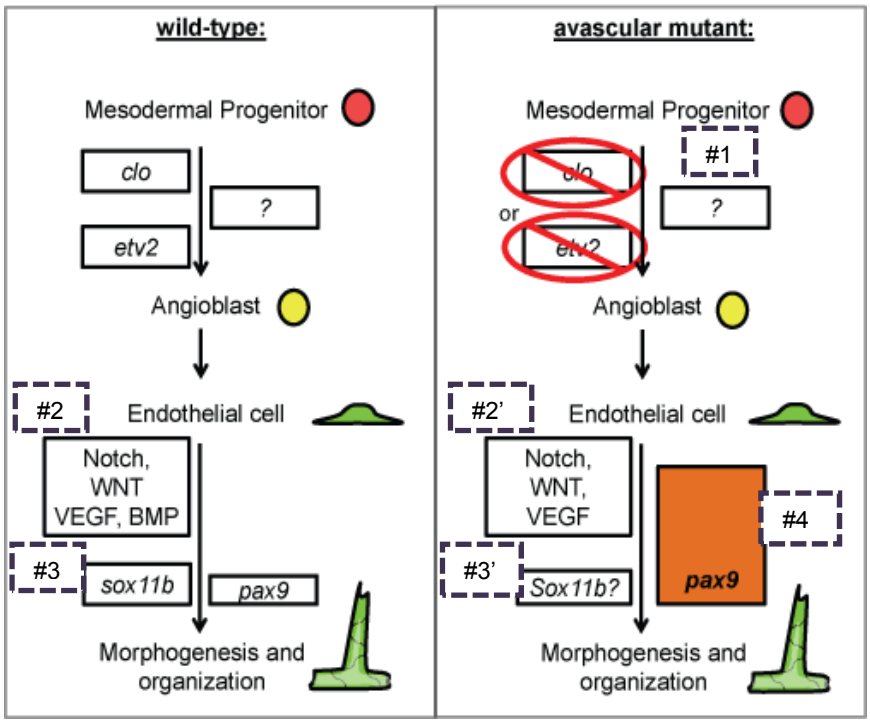

Fig. 1.3. Model incorporating data from this thesis.

Vasculogenesis and angiogenesis in wild-type (left) and avascular mutant (right) embryos during development. 1) In the absence of *clo* or *etv2*, alternative mechanism(s) may facilitate specification of angioblasts to compensate the initial deficit of the endothelial lineage. 2) While Notch, WNT and VEGF modulation all seemed to affect vascular morphogenesis in avascular mutants, BMP appears to be less important. 3) *sox11b* only affected wild-type vascular morphogenesis. 4) *pax9* is dispensable for wild-type angiogenesis, yet essential for avascular mutant angiogenesis.

REFERENCES

1. Carmeliet, P., **Angiogenesis in life, disease and medicine**. *Nature*, 2005. **438**(7070): p. 932-6.

2. Saha, M.S., E.A. Cox, and C.W. Sipe, **Mechanisms regulating the origins of the vertebrate vascular system**. *J Cell Biochem*, 2004. **93**(1): p. 46-56.

3. Rasmussen, T.L., et al., **ER71 directs mesodermal fate decisions during embryogenesis. Development**, 2011. **138**(21): p. 4801-12.

4. Visvader, J.E., Y. Fujiwara, and S.H. Orkin, **Unsuspected role for the T-cell leukemia protein SCL/tal-1 in vascular development**. *Genes Dev*, 1998. **12**(4): p. 473-9.

5. Sumanas, S. and S. Lin, **Ets1-related protein is a key regulator of vasculogenesis in zebrafish**. *PLoS Biol*, 2006. **4**(1): p. e10.

6. Jin, S.W., et al., **Cellular and molecular analyses of vascular tube and lumen formation in zebrafish**. *Development*, 2005. **132**(23): p. 5199-209.

7. Noden, D.M., **Interactions and fates of avian craniofacial mesenchyme**. *Development*, 1988. **103 Suppl**: p. 121-40.

8. Pardanaud, L., et al., **Two distinct endothelial lineages in ontogeny, one of them related to hemopoiesis**. *Development*, 1996. **122**(5): p. 1363-71.

9. Ferkowicz, M.J. and M.C. Yoder, **Blood island formation: longstanding observations and modern interpretations**. *Exp Hematol*, 2005. **33**(9): p. 1041-7.

10. Risau, W. and I. Flamme, **Vasculogenesis**. *Annu Rev Cell Dev Biol*, 1995. **11**: p. 73-91.

11. Caprioli, A., et al., **Hemangioblast commitment in the avian allantois: cellular and molecular aspects**. *Dev Biol*, 2001. **238**(1): p. 64-78.

12. Wilting, J., et al., **Angiogenic potential of the avian somite**. *Dev Dyn*, 1995. **202**(2): p. 165-71.

13. Demir, R., Y. Seval, and B. Huppertz, **Vasculogenesis and angiogenesis in the early human placenta**. *Acta Histochem*, 2007. **109**(4): p. 257-65.

14. Yamaguchi, T.P., et al., **flk-1, an flt-related receptor tyrosine kinase is an early marker for endothelial cell precursors**. *Development*, 1993. **118**(2): p. 489-98.

15. Noden, D.M., **Embryonic origins and assembly of blood vessels**. *Am Rev Respir Dis*, 1989. **140**(4): p. 1097-103.

16. Mills, K.R., D. Kruep, and M.S. Saha, **Elucidating the origins of the vascular system: a fate map of the vascular endothelial and red blood cell lineages in Xenopus laevis**. *Dev Biol*, 1999. **209**(2): p. 352-68.

17. Vogeli, K.M., et al., **A common progenitor for haematopoietic and endothelial lineages in the zebrafish gastrula**. *Nature*, 2006. **443**(7109): p. 337-9.

18. Martin, B.L. and D. Kimelman, **Canonical Wnt signaling dynamically controls multiple stem cell fate decisions during vertebrate body formation**. *Dev Cell*, 2012. **22**(1): p. 223-32.

19. Asahara, T., et al., **Isolation of putative progenitor endothelial cells for angiogenesis**. *Science*, 1997. **275**(5302): p. 964-7.

20. Drake, C.J., **Embryonic and adult vasculogenesis**. *Birth Defects Res C Embryo Today*, 2003. **69**(1): p. 73-82.

21. Pezzolo, A., et al., **Tumor origin of endothelial cells in human neuroblastoma**. *J Clin Oncol*, 2007. **25**(4): p. 376-83.

22. Liao, E.C., et al., **Hereditary spherocytosis in zebrafish riesling illustrates evolution of erythroid beta-spectrin structure, and function in red cell morphogenesis and membrane stability**. *Development*, 2000. **127**(23): p. 5123-32.

23. Leung, D.W., et al., **Vascular endothelial growth factor is a secreted angiogenic mitogen**. *Science*, 1989. **246**(4935): p. 1306-9.

24. Keck, P.J., et al., **Vascular permeability factor, an endothelial cell mitogen related to PDGF**. *Science*, 1989. **246**(4935): p. 1309-12.

25. Gospodarowicz, D., J. Cheng, and M. Lirette, **Bovine brain and pituitary fibroblast growth factors: comparison of their abilities to support the proliferation of human and bovine vascular endothelial cells**. *J Cell Biol*, 1983. **97**(6): p. 1677-85.

26. Abraham, J.A., et al., **Nucleotide sequence of a bovine clone encoding the angiogenic protein, basic fibroblast growth factor**. *Science*, 1986. **233**(4763): p. 545-8.

27. Ishikawa, T., et al., **Mouse Wnt receptor gene Fzd5 is essential for yolk sac and placental angiogenesis**. *Development*, 2001. **128**(1): p. 25-33.

28. Yamashita, H., et al., **Growth/differentiation factor-5 induces angiogenesis in vivo**. *Exp Cell Res*, 1997. **235**(1): p. 218-26.

29. Wernert, N., et al., **c-ets1 proto-oncogene is a transcription factor expressed in endothelial cells during tumor vascularization and other forms of angiogenesis in humans**. *Am J Pathol*, 1992. **140**(1): p. 119-27.

30. De Val, S. and B.L. Black, **Transcriptional control of endothelial cell development**. *Dev Cell*, 2009. **16**(2): p. 180-95.

31. Aranguren, X.L., et al., **Transcription factor COUP-TFII is indispensable for venous and lymphatic development in zebrafish and Xenopus laevis**. *Biochem Biophys Res Commun*, 2011. **410**(1): p. 121-6.

32. North, T., et al., **Cbfa2 is required for the formation of intra-aortic hematopoietic clusters**. *Development*, 1999. **126**(11): p. 2563-75.

33. North, T.E., et al., **Runx1 expression marks long-term repopulating hematopoietic stem cells in the midgestation mouse embryo**. *Immunity*, 2002. **16**(5): p. 661-72.

34. Bertrand, J.Y., et al., **CD41+ cmyb+ precursors colonize the zebrafish pronephros by a novel migration route to initiate adult hematopoiesis**. *Development*, 2008. **135**(10): p. 1853-62.

35. LeCouter, J., et al., **Identification of an angiogenic mitogen selective for endocrine gland endothelium**. *Nature*, 2001. **412**(6850): p. 877-84.

36. Wiley, D.M. and S.W. Jin, **Bone Morphogenetic Protein functions as a context-dependent angiogenic cue in vertebrates**. *Semin Cell Dev Biol*, 2011. **22**(9): p. 1012-8.

37. Hellstrom, M., et al., **Dll4 signalling through Notch1 regulates formation of tip cells during angiogenesis**. *Nature*, 2007. **445**(7129): p. 776-80.

38. Herbert, S.P., J.Y. Cheung, and D.Y. Stainier, **Determination of Endothelial Stalk versus Tip Cell Potential during Angiogenesis by H2.0-like Homeobox-1**. *Curr Biol*, 2012. **22**(19): p. 1789-94.

39. Lawson, N.D. and B.M. Weinstein, **In Vivo Imaging of Embryonic Vascular Development Using Transgenic Zebrafish**. *Dev Biol*, 2002. **248**(2): p. 307-318.

40. Winata, C.L., et al., **The role of vasculature and blood circulation in zebrafish swimbladder development**. *BMC Dev Biol*, 2010. **10**: p. 3.

41. Mullins, M.C., et al., **Large-scale mutagenesis in the zebrafish: in search of genes controlling development in a vertebrate**. *Curr Biol*, 1994. **4**(3): p. 189-202.

42. Isogai, S., et al., **Angiogenic network formation in the developing vertebrate trunk**. *Development*, 2003. **130**(21): p. 5281-90.

43. Stainier, D.Y., et al., **Mutations affecting the formation and function of the cardiovascular system in the zebrafish embryo**. *Development*, 1996. **123**: p. 285-92.

44. Stainier, D.Y., et al., **Cloche, an early acting zebrafish gene, is required by both the endothelial and hematopoietic lineages**. *Development*, 1995. **121**(10): p. 3141-50.

45. Schoenebeck, J.J., B.R. Keegan, and D. Yelon, **Vessel and blood specification override cardiac potential in anterior mesoderm**. *Dev Cell*, 2007. **13**(2): p. 254-67.

46. Thompson, M.A., et al., **The cloche and spadetail genes differentially affect hematopoiesis and vasculogenesis**. *Dev Biol*, 1998. **197**(2): p. 248-69.

47. Jin, S.W., et al., **A transgene-assisted genetic screen identifies essential regulators of vascular development in vertebrate embryos**. *Dev Biol*, 2007. **307**(1): p. 29-42.

48. Palencia-Desai, S., et al., **Vascular endothelial and endocardial progenitors differentiate as cardiomyocytes in the absence of Etsrp/Etv2 function**. *Development*, 2011. **138**(21): p. 4721-32.

49. Tusher, V.G., R. Tibshirani, and G. Chu, **Significance analysis of microarrays applied to the ionizing radiation response**. *Proc Natl Acad Sci U S A*, 2001. **98**(9): p. 5116-21.

CHAPTER 2

Mutant-Specific Gene Expression Profiling Identifies SRY-Related HMG Box 11b (*Sox11b*) as a Novel Regulator of Vascular Development in Zebrafish

Summary

Previous studies have identified two zebrafish mutants, *clo*che and groom of *clo*che, which lack the majority of the endothelial lineage at early developmental stages. However, at later stages, these avascular mutant embryos generate rudimentary vessels, indicating that they retain the ability to generate endothelial cells despite this initial lack of endothelial progenitors. To further investigate molecular mechanisms that allow the emergence of the endothelial lineage in these avascular mutant embryos, we analyzed the gene expression profile using microarray analysis on isolated endothelial cells. We find that the expression of the genes characteristic of other mesodermal lineages are substantially elevated in the *kdrl*$^{+}$ cells isolated from avascular mutant embryos. Subsequent validation and analyses of the microarray data identifies *Sox11b*, a zebrafish ortholog of SRY-related HMG box 11 (SOX11), which has not previously implicated in vascular development. We further define the function of *sox11b* during vascular development, and find that *Sox11b* function is essential for developmental angiogenesis in zebrafish embryos, specifically regulating sprouting angiogenesis. Taken together, our analyses illustrate a complex regulation of endothelial specification and differentiation during vertebrate development.

Introduction

Endothelial cells are a major component of the vascular system, which is essential for the development, growth, and survival of an individual. Failures in regulating the development of endothelial lineage contribute to a wide variety of pathological conditions, including cancer, psoriasis, arthritis, congenital or inherited diseases, as well as heart and brain ischemia, neurodegeneration, and osteoporosis [1]. During development, the endothelial lineage arises from mesodermal tissues. It has been reported that diverse mesodermal tissues including lateral plate mesoderm [2], blood islands within the yolk sac [3,4], allantois [5], somitic mesoderm [6], as well as placenta [7,8], can produce endothelial cells during development. Moreover, the entire mesoderm excluding notochord and prechordal mesoderm can serve as sources for endothelial cells [9], suggesting that angiogenic potential might be one of the intrinsic properties of the developing mesoderm. Subsequently, endothelial cells further differentiate as arterial, venous or lymphatic endothelial cells, each of which possesses unique molecular and cellular characteristics.

Specification and differentiation of the endothelial lineage are regulated by arrays of signaling pathways and transcription factors. Many pathways that regulate the emergence and organization of the endothelium have been characterized such as receptor tyrosine kinases [10,-13], G-protein signaling pathways [14], serine-threonine kinase [15], as well as transcription factors [16-17]. Overall, many of these pathways are preferentially required for the proper development of a subset of vasculature, such as cranial versus trunk or arterial versus venous endothelium. This is not surprising given the numerous developmental sources of endothelial

cells. One of the most striking examples is that of BMP2 signaling, which is preferentially required for venous endothelial development in zebrafish [18]. Similarly, Wnt signaling regulates the formation of the endothelial lineage within the tailbud mesoderm, without obvious effects on the lateral plate mesoderm [19]. Therefore, identification of additional factors that regulate specification and differentiation of the endothelial lineage will help us to further delineate the heterogeneity of endothelial cells.

From a forward genetic screen [20], we have isolated a mutant, named *groom of cloche* (*grc*), which lacks the majority of early *Tg(kdrl:eGFP)*$^{+}$ cells [21], which is reminiscent of another mutant, *clo*che (*clo*) that lack displays a severe deficiency of both hematopoietic and endothelial lineages [22]. Nevertheless, both mutant embryos recover [21]. This indicates that alternative mechanisms for the emergence of the endothelial lineage.

In this report, we performed microarray analysis using the endothelial cells isolated from late stage avascular mutant embryos and compared the expression profile of transcription factors with endothelial cells isolated from wild-type embryos. We find that the expression level of 43 transcription factors is significantly up-regulated in endothelial cells isolated from avascular mutant embryos. The majority of transcription factors we identified in our microarray have not been implicated in vascular development. We further analyze the function of one of these transcription factors, SRY-related HMG Box 11b (*Sox11b*), in endothelial differentiation and subsequent vascular patterning. We find that *Sox11b* is expressed in endothelial cells during development, and is essential for sprouting angiogenesis in zebrafish.

Our results demonstrate that developmental ontogeny of the endothelial lineage is far more complex than previously thought.

Experimental Methods

Zebrafish Husbandry

Zebrafish (Danio Rerio) embryos were raised as previously described [23]. The following transgenic and mutant fish lines were utilized: *Tg(kdrl:eGFP)*^{s843} [20], *clo*che (*clo*)^{s5} [22], *Cas*anova (*cas*)^{s4} [24], groom of *clo*che (*grc*)^{s635} [21].

Florescent Activated Cell Sorting (FACS) and RNA Isolation

18.5 hpf *Tg(kdrl:eGFP)*^{s843} embryos were dissociated in HBSS with 5% FBS and subsequently incubated with 100µg/ml Liberase solution (Roche) for 15 minutes at 37°C. Embryos were then triturated and the resulting suspension was pushed through a 40µM cell culture filter (BD Biosciences) and the reaction was stopped using 5mM EDTA, pH 8.0 in HBSS minus $Ca2^{+}$ and $Mg2^{+}$. Gates for flow cytometry were selected based on the Phycoerythrin versus FITC plot. Double sorts indicated an enrichment to >95% GFP^{+} cells. RNA was extracted from isolated cells using Trizol (Invitrogen) and the accompanying protocol. Multiple rounds of flow cytometry were performed and RNA for each biological replicate was pooled.

Microarray Analyses and quantitative RT-PCR

The WT ovation Pico Kit was used to amplify the RNA samples to satisfactory RNA integrity score (RIN) score [25]. Otherwise, gene expression profiling was performed as previously described [26] using an Agilent Zebrafish array version 2. Using the Statistical Analysis of Microarrays (SAM), the raw data for wild-type, *grc*,

clo and *cas* was analyzed. We disregarded genes whose expression was down-regulated in *cas*, which would represent genes expressed in pharyngeal endoderm. Genes highly significantly up-regulated (q=0, fold change > 2) in both *grc* and *clo* mutants were further analyzed.

For qRT-PCR, RNA was extracted using the QIagen RNeasy mini kit and accompanying protocol opting to add 300ng of carrier RNA to each sample. The iScript cDNA synthesis kit (Bio-Rad) was used to transcribe entire RNA extracts, immediately after RNA extraction. cDNA samples were then diluted to a volume of 300µl. Using 2X Power syber mastermix, 640nM of each primer, and 8µl of cDNA in a 25µl reaction, amplification of transcript amplicon was monitored on a Bio-Rad cfx96 system. Gene expression was normalized to either 18S rRNA or B-actin housekeeping genes. Melting curve analysis was performed on all reactions. Ct versus cDNA concentration plots were also used to determine that there was a linear ratio of amplification of housekeeping genes to gene-of-interest at a particular cDNA concentration. Data was analyzed using the $2^{-\Delta\Delta CT}$ method [27]. At least three biological replicates of three technical replicates were performed for each conditon. Primers used were:

18s rRNA (5'-CACTTGTCCCTCTAAGAAGTTGCA-3' and 5'-GGTTGATTCCGATAACGAACGA-3'), *sox11b* (5'-CGAGTTCCCGGACTATTGCA-3' and 5' TCTCCCGCGATCATCTCACT-3'), zfhx4 (5'-CTCCTTTGTGTGGGAAGCAT-3' and 5'-CCCTGAATGTGGAACAGCAT-3'), and klf5l (5'-AACCCGCAGTGAGAATCGCAAC-3' and

5'-ATCCATCTCCATCCGTGTCTGAGC-3').

***in situ* probe synthesis**

Probes were synthesized using the SP6/T7 DIG-UTP labeling kit (Roche) from linearized template. RNA was quantified, monitored by agarose gel electrophoresis for a singular product, diluted in in situ hybridization solution to 100ng/µl and stored at -20°C.

Morpholino knockdown of *sox11b*

Previously reported and validated *sox11b* morpholino (5'-CATGTTCAAACACACTTTTCCCTCT-3'), which blocks peptide synthesis, and control morpholino (5'-CCTCTTACCTCAGTTACAATTTATA-3') were used [28]. All embryos were injected with 4.6nL of injection mix containing 5µM HEPES, pH 7.6 and 10% Phenol red as a tracer.

Results

As previously reported, both *clo* and *grc* homozygous mutant embryos lack endothelial cells at 18 hpf [21,22] (data not shown). However, at 72 hpf, *kdrl*$^{+}$ cells were present in these avascular mutant embryos (Figure 1A-1C). Interestingly, counterstaining with DAPI in this experiment also showed that the midline region where are exclusively populated by *kdrl*$^{+}$ cells in wild-type embryos also contains a substantial number of *kdrl*- cells in avascular mutant embryos (Figure 1A yellow asterisks), alluding that vascular progenitors in these embryos may fail to undergo proper differentiation.

To better understand molecular mechanisms underlying the recovery of endothelial lineage, we analyzed the transcriptional profile of *kdrl*$^+$ cells in wild-type and avascular mutant embryos by microarray analyses (Figure 2A). Since kdrl, a zebrafish ortholog of Vascular Endothelial Growth Factor Receptor 2 (VEGFR2) [29], is also expressed in pharyngeal endoderm [20], it is possible that a significant portion of *kdrl*$^+$ cells isolated in avascular mutant embryos may represent non-endothelial lineage. Therefore, we used homozygous *cas* embryos wherein the entire presumptive endoderm fails to specify with little apparent effect on the vasculature [20]. Genes down-regulated in *kdrl*$^+$ cells isolated from homozygous *cas* mutant embryos were discarded prior to further analyses and validation.

We found that the expression level of endothelial-enriched genes were largely unaltered in *kdrl*$^+$ cells of homozygous *grc* mutant embryos when compared to those seen in wild-type. In contrast, the majority of these genes were down-regulated in the same population from homozygous *clo* mutant embryos (Figure 2A), suggesting that a locus affected by *grc* mutation may be only required in a subset of endothelial cells. A small subset of endothelial-enriched genes was markedly down-regulated in both homozygous *grc* and *clo* mutant embryos. For instance, we found that an arterial specific marker, tbx20 [30], as well as a putative zebrafish ortholog of mammalian Platelet Endothelial Cell Adhesion Molecule (PECAM), ENSDART00000084729, was significantly down-regulated in *kdrl*$^+$ cells isolated from both homozygous *grc* and *clo* mutant embryos (Figure 2A). Interestingly, we found that genes up-regulated (q=0) in all three mutants were found to be characteristic of

other mesodermal, non-endothelial lineages such as somite, blood, or kidney (Figure 2B). For instance, we found protein kinase c delta a (*prkcda*), which are expressed in blood and somitic lineages [31], and adenosine kinase a (*adka*), which are expressed in blood and pronephric lineages [32], was up-regulated in *kdrl*$^+$ cells from avascular mutant embryos. Taken together, our microarray data suggest that *kdrl*$^+$ cells found in avascular mutant embryos may retain more mesodermal characteristics than those from wild-type embryos.

To better understand molecular characteristics of the *kdrl*$^+$ cells in avascular mutant embryos, we analyzed the expression level of transcription factors in our microarray data (Figure 2C). We found that total of 43 transcription factors were up-regulated in *kdrl*$^+$ cells from avascular mutant embryos (Figure 2D) at q=0. Among these transcription factors, we further analyze the function of *sox11b*, a zebrafish ortholog of SRY-related HMG Box 11 (SOX11) [28], which is a member of SOXC subgroup [33]. Previously, it has been shown that *Sox11b* is essential for mediating retinal development and neuronal regeneration in zebrafish [28]. However, its role in endothelial cells and vascular development has not been investigated. Up-regulation of *sox11b* in *kdrl*$^+$ cells in avascular mutant embryos was confirmed by quantitative RT-PCR (Figure 3A).

During development, *sox11b* is highly expressed in multiple tissues including neurons, somites, and retina as previously proposed. In addition, approximately at 24 hpf, *sox11b* expression was detectable in developing posterior axial vessels in wild-type embryos (Figure 3B). A similar expression pattern was seen in avascular mutants (Data not shown). To analyze temporal changes in *sox11b* expression

within endothelial cells, *kdrl*$^{+}$ cells were isolated from wild-type embryos and quantitative RT-PCR was performed. We found that *sox11b* expression can be detected as early as 18 hpf, and the level of expression gradually increases until 72 hpf within endothelial cells, consistent with our in situ hybridization result (Figure 3C). Interestingly, the expression of *sox11b* appears to be induced by Bone Morphogenetic Protein (Bmp) signaling, as over-expression of Noggin3, an endogenous antagonist of Bmp signaling, led to a substantially decrease on the level of *sox11b* transcript level (Figure 3D). Considering that Bmp signaling functions as a context-dependent pro-angiogenic cue [18,34], it is possible that *Sox11b* may function as one of the effectors in this process.

To better assess the function of *Sox11b* during vascular development, we attenuated the activity of *Sox11b* by injecting morpholino (MO) anti-sense oligonucleotide as previously reported [35]. Embryos injected with *sox11b* MO displayed discernible defects in vascular development, compared to control MO injected embryo (Figure 4A). At 32-34 hpf, the length of intersegmental vessels, which sprout from the dorsal aorta at this stage [36], was substantially reduced in *sox11b* MO injected embryos (Figure 4B). While control MO injected embryos had an average length of 89.82±1.92μm (N=139 ISVs), *sox11b* MO injected embryos intersegmental vessels were significantly shorter, 82.67±2.46μm (N=156 ISVs, N=8 embryos; Figure 4B, 4C and E), indicating that the function of *Sox11b* is essential for the morphogenesis of sprouting intersegmental vessels during development. Since a mammalian ortholog of *Sox11b*, SOX11 is known to promote transcription of key cell cycle regulators including Cyclin-dependent kinase CDKN2B and Histones [37],

as well as arrays of Actin binding proteins which modulate cell motility [37], it is possible down-regulation of *Sox11b* by MO injection led to a decreased endothelial proliferation and/or migration.

Since intersegmental vessels at 24 hpf are arterial in nature [36], we investigated whether *sox11b* preferentially influences migration of arterial endothelial cells, by analyzing the effects of *sox11b* knock-down on sprouting angiogenesis of caudal vein plexus (CVP). Previously, we reported that the CVP undergoes morphogenetic changes starting at 30 hpf by forming extensive ventral sprouts [18]. In *sox11b* MO injected embryos, the number of angiogenic sprouts was drastically reduced compared to control MO injected embryos at 32 hpf (1.85±0.56 in *sox11b* MO injected embryos and 11.4 ±1.0 in control MO injected embryos; Figure 4A, white arrowheads and 4D). Morphologically, the CVP in *sox11b* MO injected embryos failed to undergo proper morphogenesis to generate the dorsal vein and the ventral vein as in wild-type embryos (Figure 4G), reflecting the attenuated sprouting angiogenesis in these embryos.

Conclusion

Our results indicate that *kdrl*$^+$ cells in avascular mutant embryos express a unique transcriptional profile that allow them to circumvent the initial failure of endothelial specification, which led to the formation of rudimentary vascular structure in these embryos. We found that a number of transcription factors were selectively up-regulated in the *kdrl*$^+$ cells of avascular mutant embryos, indicating that these transcription factors may guide an alternative mechanism to generate the endothelial lineage. We analyzed the function of one of the transcription factors isolated from

our microarray, *sox11b*, and found that *sox11b* plays an important role in early morphogenesis of the vasculature by mediating sprouting angiogenesis. Taken together, our data provides a compelling evidence of developmental heterogeneity of the endothelial lineage.

FIGURES:

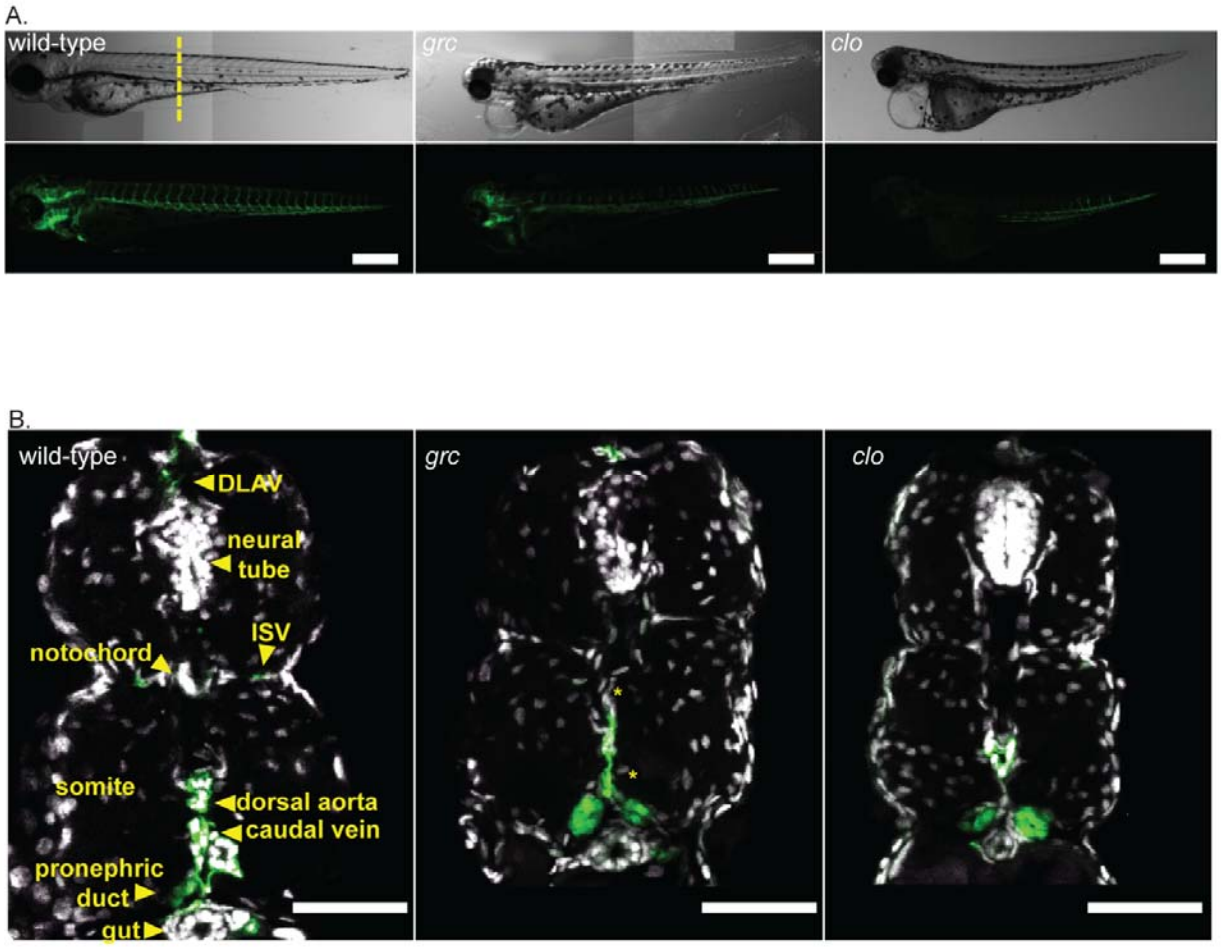

Figure 2.1: Avascular mutant embryos generate endothelial cells at later stages

(a) Gross morphology of 72 hpf wild-type (left), groom of *clo*che (*grc*) (middle), and *clo*che (*clo*) embryos in *Tg(kdrl:eGFP)* background. Both bright-field (top rows) and epifluorescent (bottom rows) images are shown. Scale bar=250μm. (b) Transverse section of 72 hpf embryos taken from the area marked by dashed line in (a). GFP^+ endothelial cells are shown in green and nuclei stained with DAPI are shown in white. Scale bar=50μm.

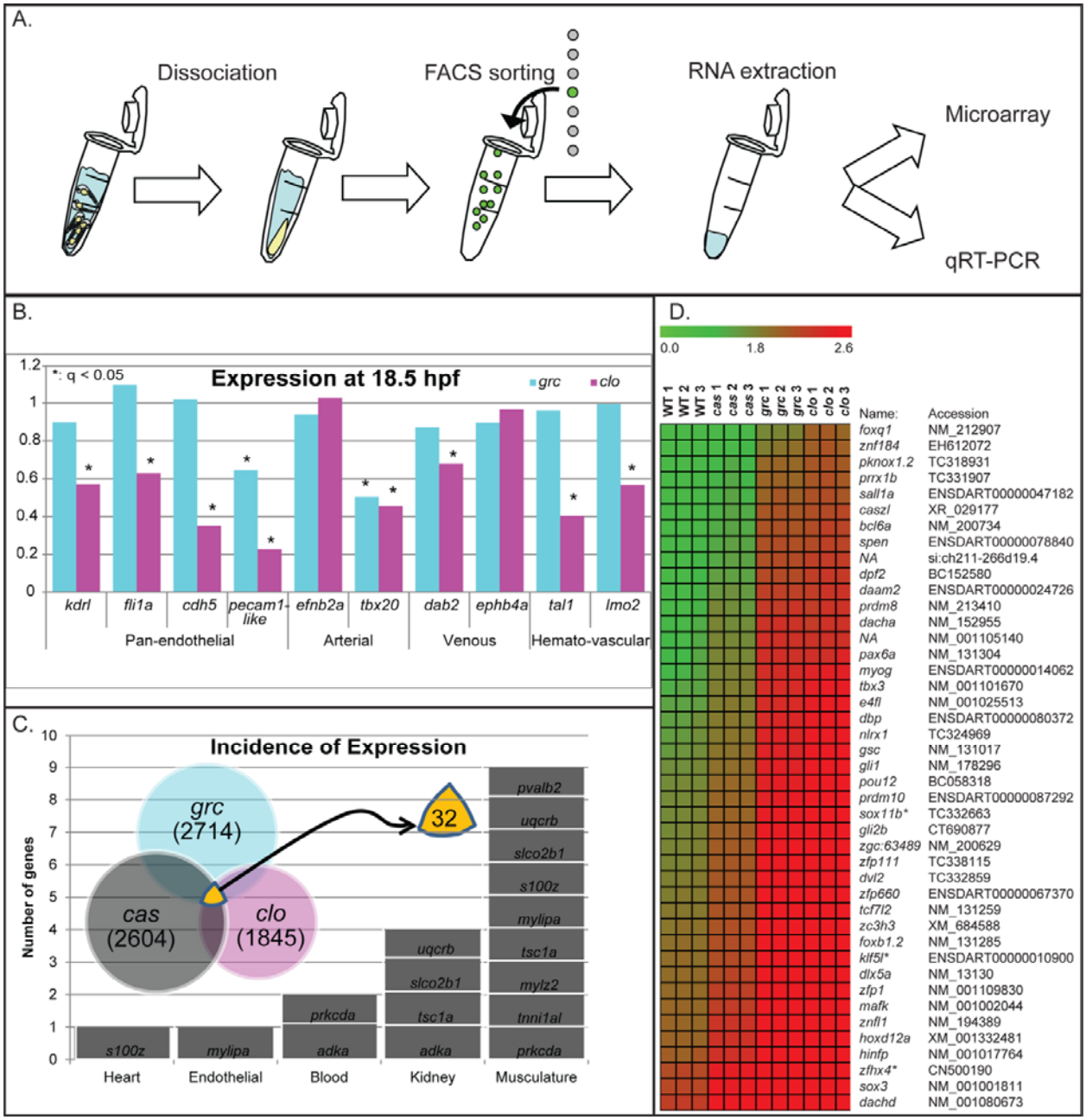

Figure 2.2: Expression profile of *kdrl*$^{+}$ cells isolated from avascular mutant embryos.

(a) Schematic diagram for molecular profiling. (b) Expression profile of known lineage specific markers in microarray (*: q<0.05). (c) Characteristics of genes which are up-regulated in endothelial cells in all three avascular mutant embryos. A total of 32 genes were shown to be up-regulated. (d) Expression profiles of putative transcription factors of which function have not previously implicated in the endothelial lineage. These genes were up in *grc* and *clo* (q=0), but not down-regulated in *cas*.

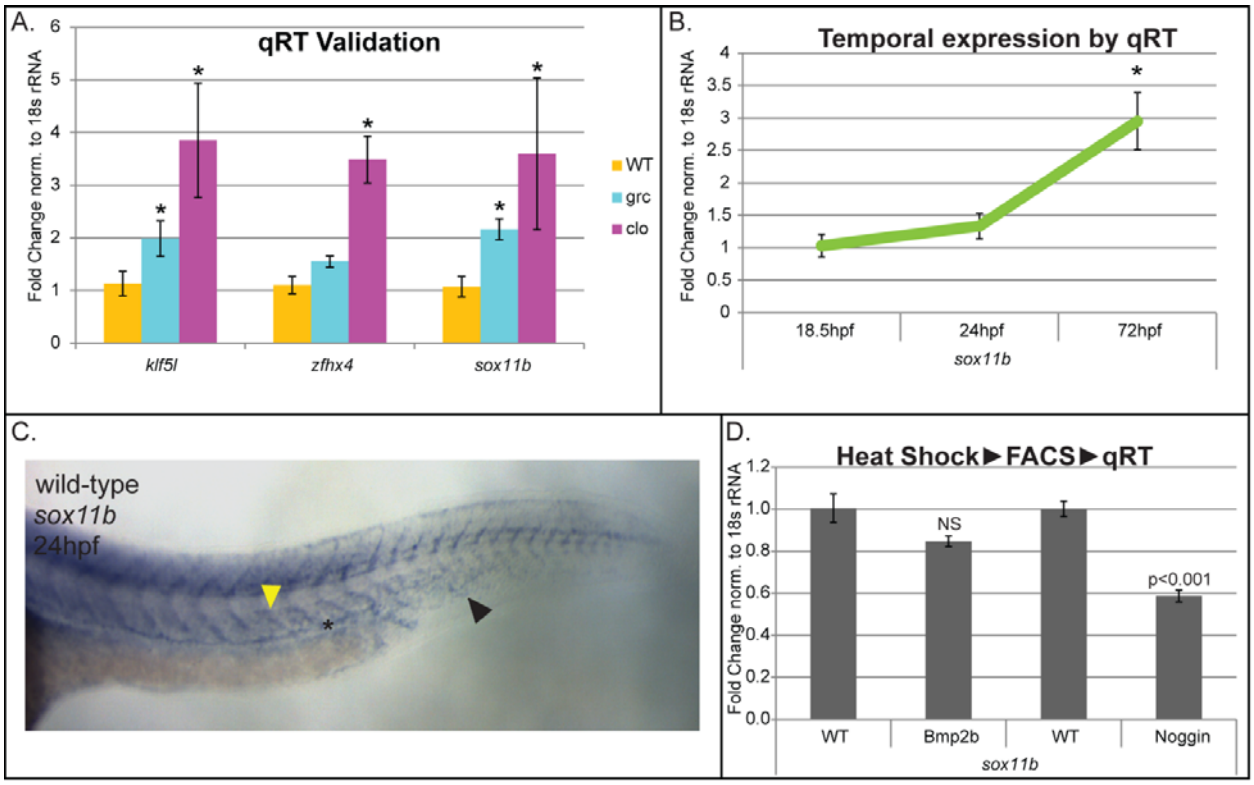

Figure 2.3: *sox11b* expression is elevated in *kdrl*$^{+}$ cells isolated from avascular mutant embryos.

(a) Quantitative RT-PCR analyses confirmed the up-regulated expression of *sox11b* in endothelial cells of avascular mutant embryos. Two additional transcription factor, klf5l and zfhx4, were used as positive controls. (b) Temporal expression change of *sox11b* expression in endothelial cells. (c) in situ hybridization of *sox11b* at 24 hpf wild-type embryo. In addition to neural tube and somite, axial vessels express *sox11b*. Anterior somite, axial vessel, and caudal vein are indicated by the yellow arrow, asterisk, and black arrow, respectively. (d) Effects of BMP signaling on *sox11b* expression. A decreased activity of BMP signaling significantly reduces the expression of *sox11b* in endothelial cells.

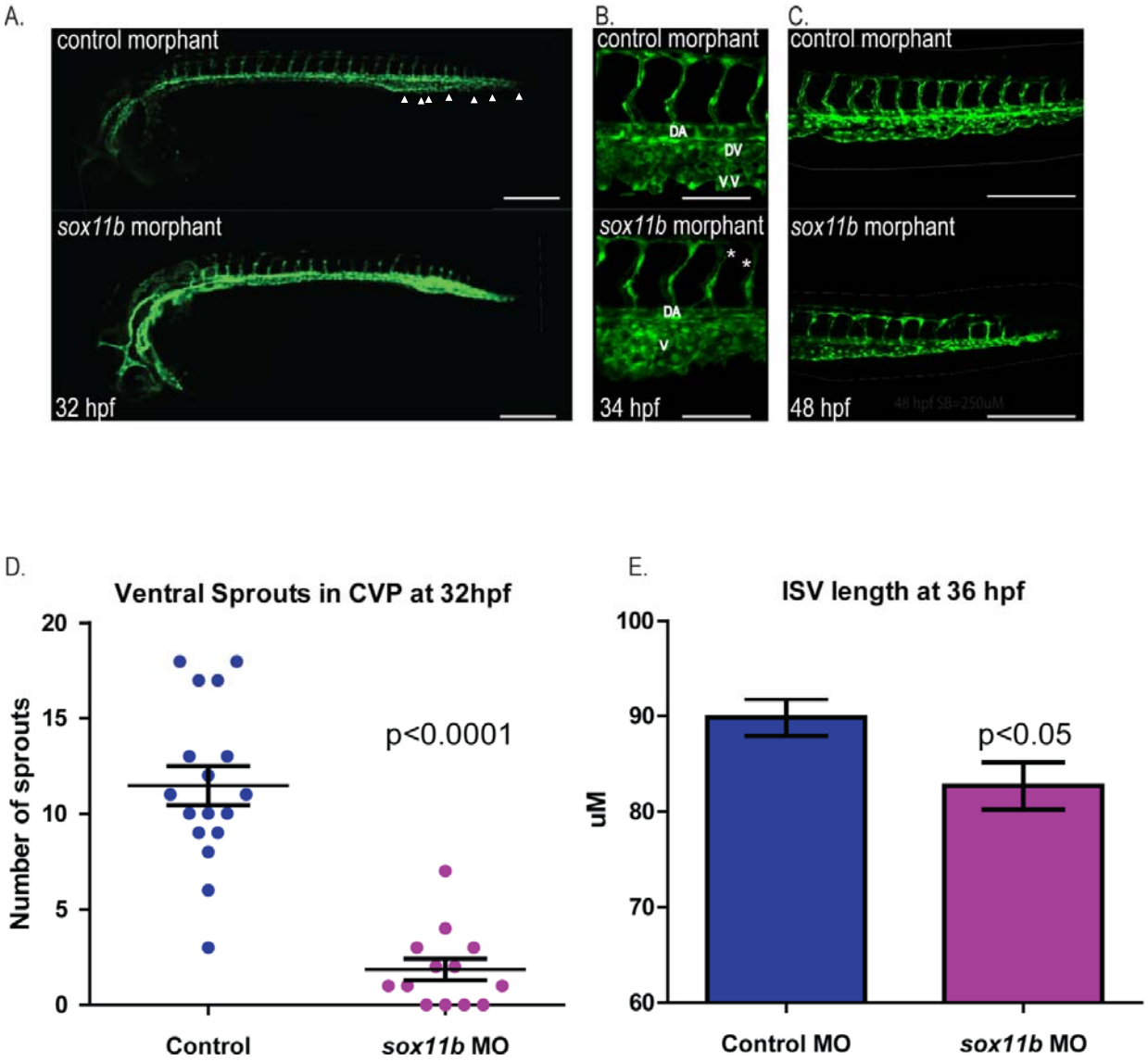

Figure 2.4: *sox11b* regulates sprouting angiogenesis during development.

(a) Epifluorescent micrographs of control (top) or *sox11b* (bottom) morpholino (MO) injected embryos. Trunk regions posterior to the end of yolk extension are shown. White arrowheads indicate ventral sprouts. Scale bar=250µm. (b) Intersegmental vessel and caudal vein defect in *sox11b* MO injected embryos at 34 hpf. Scale bar=100µm. (c) Truncation of ISVs and plexus defects at 48 hpf. Scale bar=250µm. (d) Decreased venous sprouting angiogenesis in the caudal vein plexus (CVP) of *sox11b* MO injected embryos at 32 hpf is quantified. (e) The effect of *sox11b* MO on the length of intersegmental vessels is quantified (N=139, N=10 embryos).

REFERENCES

1. P. Carmeliet: **Angiogenesis in life, disease and medicine**, *Nature* 2005, **438:**932-936.

2. L. Pardanaud, D. Luton, M. Prigent, L.M. Bourcheix, M. Catala, F. Dieterlen-Lievre: **Two distinct endothelial lineages in ontogeny, one of them related to hemopoiesis**, *Development* 1996, **122:**1363-1371.

3. M.J. Ferkowicz, M.C. Yoder: **Blood island formation: longstanding observations and modern interpretations**, *Exp Hematol* 2005, **33:**1041-1047.

4. W. Risau, I. Flamme: **Vasculogenesis**, *Annu Rev Cell Dev Biol* 1995, **11:**73-91.

5. A. Caprioli, K. Minko, C. Drevon, A. Eichmann, F. Dieterlen-Lievre, T. Jaffredo: **Hemangioblast commitment in the avian allantois: cellular and molecular aspects**, *Dev Biol* 2001, **238**:64-78.

6. J. Wilting, B. Brand-Saberi, R. Huang, Q. Zhi, G. Kontges, C.P. Ordahl, B. Christ: **Angiogenic potential of the avian somite**, *Dev Dyn* 1995, **202:**165-171.

7. R. Demir, Y. Seval, B. Huppertz: **Vasculogenesis and angiogenesis in the early human placenta**, *Acta Histochem* 2007, **109**:257-265.

8. T.P. Yamaguchi, D.J. Dumont, R.A. Conlon, M.L. Breitman, J. Rossant: **flk-1, an flt-related receptor tyrosine kinase is an early marker for endothelial cell precursors**, *Development* 1993, **118**:489-498.

9. D.M. Noden: **Embryonic origins and assembly of blood vessels**, *Am Rev Respir Dis* 1989, **140:**1097-1103.

10. D.W. Leung, G. Cachianes, W.J. Kuang, D.V. Goeddel, N. Ferrara: **Vascular endothelial growth factor is a secreted angiogenic mitogen**, *Science* 1989, **246:**1306-1309.

11. P.J. Keck, S.D. Hauser, G. Krivi, K. Sanzo, T. Warren, J. Feder, D.T. Connolly: **Vascular permeability factor, an endothelial cell mitogen related to PDGF**, *Science* 1989, **246:1**309-1312.

12. D. Gospodarowicz, J. Cheng, M. Lirette: **Bovine brain and pituitary fibroblast growth factors: comparison of their abilities to support the proliferation of human and bovine vascular endothelial cells**, *J Cell Biol* 1983, **97:**1677-1685.

13. J.A. Abraham, A. Mergia, J.L. Whang, A. Tumolo, J. Friedman, K.A. Hjerrild, D. Gospodarowicz, J.C. Fiddes: **Nucleotide sequence of a bovine *clo*ne encoding the angiogenic protein, basic fibroblast growth factor**, *Science* 1986, **233:**545-548.

14. T. Ishikawa, Y. Tamai, A.M. Zorn, H. Yoshida, M.F. Seldin, S. Nishikawa, M.M. Taketo: **Mouse Wnt receptor gene Fzd5 is essential for yolk sac and placental angiogenesis**, *Development* 2001, **128:**25-33.

15. H. Yamashita, A. Shimizu, M. Kato, H. Nishitoh, H. Ichijo, A. Hanyu, I. Morita, M. Kimura, F. Makishima, K. Miyazono: **Growth/differentiation factor-5 induces angiogenesis in vivo**, *Exp Cell Res* 1997, **235:**218-226.

16. N. Wernert, M.B. Raes, P. Lassalle, M.P. Dehouck, B. Gosselin, B. Vandenbunder, D. Stehelin: **c-ets1 proto-oncogene is a transcription factor expressed in endothelial cells during tumor vascularization and other forms of angiogenesis in humans**, *Am J Pathol* 1992, **140:**119-127.

17. J.E. Visvader, Y. Fujiwara, S.H. Orkin: **Unsuspected role for the T-cell leukemia protein SCL/tal-1 in vascular development**, *Genes Dev* 1998, **12:**473-479.

18. D.M. Wiley, S.W. Jin: **Bone Morphogenetic Protein functions as a context-dependent angiogenic cue in vertebrates**, *Semin Cell Dev Biol* 2011, **22:**1012-1018.

19. B.L. Martin, D. Kimelman: **Canonical Wnt signaling dynamically controls multiple stem cell fate decisions during vertebrate body formation**, *Dev Cell* 2012, **22:**223-232.

20. S.W. Jin, D. Beis, T. Mitchell, J.N. Chen, D.Y. Stainier: **Cellular and molecular analyses of vascular tube and lumen formation in zebrafish**, *Development* 2005, **132:**5199-5209.

21. S.W. Jin, W. Herzog, M.M. Santoro, T.S. Mitchell, J. Frantsve, B. Jungblut, D. Beis, I.C. Scott, L.A. D'Amico, E.A. Ober, H. Verkade, H.A. Field, N.C. Chi, A.M. Wehman, H. Baier, D.Y. Stainier: **A transgene-assisted genetic screen identifies essential regulators of vascular development in vertebrate embryos***, Dev Biol* 2007, **307:**29-42.

22. D.Y. Stainier, B.M. Weinstein, H.W. Detrich, 3rd, L.I. Zon, M.C. Fishman: ***Clo*che, an early acting zebrafish gene, is required by both the endothelial and hematopoietic lineages**, *Development* 1995, **121:**3141-3150.

23. M. Westerfield: **The Zebrafish Book; A Guide for the Laboratory Use of Zebrafish (Brachydanio rerio)** *University of Oregon Press*, Eugene., 1989.

24. J. Alexander, D.Y. Stainier, D. Yelon: **Screening mosaic F1 females for mutations affecting zebrafish heart induction and patterning**, *Dev Genet* 1998, **22:**288-299.

25. A. Schroeder, O. Mueller, S. Stocker, R. Salowsky, M. Leiber, M. Gassmann, S. Lightfoot, W. Menzel, M. Granzow, T. Ragg: **The RIN: an RNA integrity number for assigning integrity values to RNA measurements**, *BMC Mol Biol* 2006, **7**:3.

26. E.K. Lobenhofer, J.T. Auman, P.E. Blackshear, G.A. Boorman, P.R. Bushel, M.L. Cunningham, J.M. Fostel, K. Gerrish, A.N. Heinloth, R.D. Irwin, D.E. Malarkey, B.A. Merrick, S.O. Sieber, C.J. Tucker, S.M. Ward, R.E. Wilson, P. Hurban, R.W. Tennant, R.S. Paules: **Gene expression response in target organ and whole blood varies as a function of target organ injury phenotype***, Genome Biol* 2008, **9:**R100.

27. K.J. Livak, T.D. Schmittgen: **Analysis of relative gene expression data using real-time quantitative PCR and the 2(-Delta Delta C(T)) Method**, *Methods* 2001, **25**:402-408.

28. M.B. Veldman, M.A. Bemben, R.C. Thompson, D. Goldman: **Gene expression analysis of zebrafish retinal ganglion cells during optic nerve regeneration identifies KLF6a and KLF7a as important regulators of axon regeneration**, *Dev Biol* 2007, **312:**596-612.

29. J. Bussmann, N. Lawson, L. Zon, S. Schulte-Merker: **Zebrafish VEGF receptors: a guideline to nomenclature**, *PLoS Genet* 2008, **4:**e1000064.

30. D.G. Ahn, I. Ruvinsky, A.C. Oates, L.M. Silver, R.K. Ho: **tbx20, a new vertebrate T-box gene expressed in the cranial motor neurons and developing cardiovascular structures in zebrafish**, *Mech Dev* 2000, **95:**253-258.

31. S.A. Patten, R.K. Sihra, K.S. Dhami, C.A. Coutts, D.W. Ali: **Differential expression of PKC isoforms in developing zebrafish**, *Int J Dev Neurosci* 2007, **25:1**55-164.

32. B. Thisse, S. Pflumio, M. Fürthauer, B. Loppin, V. Heyer, A. Degrave, R. Woehl, A. Lux, T. Steffan, X.Q. Charbonnier, and C. Thisse: **Expression of the zebrafish genome during embryogenesis**, *ZFIN Direct Data Submission* 2001.

33. J. Bowles, G. Schepers, P. Koopman: **Phylogeny of the SOX family of developmental transcription factors based on sequence and structural indicators**, *Dev Biol* 2000, **227:**239-255.

34. J.D. Kim, H. Kang, B. Larrivee, M.Y. Lee, M. Mettlen, S.L. Schmid, B.L. Roman, Y. Qyang, A. Eichmann, S.W. Jin: **Context-dependent proangiogenic function of bone morphogenetic protein signaling is mediated by disabled homolog 2**, *Dev Cell* 2012, **23:**441-448.

35. A. Nasevicius, S.C. Ekker: **Effective targeted gene 'knockdown' in zebrafish**, *Nature Genetics* 2000, **26:**216-220.

36. S. Isogai, M. Horiguchi, B.M. Weinstein: **The vascular anatomy of the developing zebrafish: an atlas of embryonic and early larval development**, *Dev Biol* 2001, **230**:278-301.

37. X. Wang, S. Bjorklund, A.M. Wasik, A. Grandien, P. Andersson, E. Kimby, K. Dahlman-Wright, C. Zhao, B. Christensson, B. Sander: **Gene expression profiling and chromatin immunoprecipitation identify DBN1, SETMAR and HIG2 as direct targets of SOX11 in mantle cell lymphoma**, *PLoS One* 2010, **5:**e14085.

CHAPTER 3

A Paired Box Homeodomain Transcription Factor *pax9* as a Novel Regulator for the Migration of Endothelial Cells during Vascular Morphogenesis

Summary

Multiple populations of endothelial cells exist during development and into adulthood. Two avascular zebrafish mutants, *clo* and *grc*, which retain small populations of *kdrl*$^{+}$ cells and undergo vascular morphogenesis allow for the study of endothelium which is able to specify in the absence of *clo* or *etv2*. Using *clo* and *grc* as models for endothelial heterogeneity, we performed lineage tracing from shield stage and found an increase of *kdrl*$^{-}$ unspecified mesoderm, indicating that much of the mesoderm fated to become angioblasts fails to specify. Additionally, we determined that a large portion of early *kdrl*$^{+}$ cells in these mutants are specified from tailbud, as opposed to lateral plate mesoderm. Given the unique developmental source of endothelium in avascular mutants, we focused on a transcription factor previously indicated to be up-regulated in avascular mutant *kdrl*$^{+}$ cells, *pax9*. We found that *pax9* is highly enriched in developing zebrafish vasculature and controls vascular morphogenesis. We also found that *pax9* controls scratch closure in HUVEC cell culture, indicating that its role in vascular morphogenesis is likely conserved across vertebrates.

Highlights

- **Avascular mutants undergo endothelial specification at later stages.**
- **Tailbud mesoderm largely contributes to vascular recovery.**
- ***pax9* is up-regulated in avascular mutant *kdrl*$^{+}$ cells.**
- **Modulation of *pax9* controls vascular morphogenesis.**

Results and Discussion

In order to define alternative mechanisms of endothelial specification and organization, we decided to use avascular mutants as a model for endothelial heterogeneity. We have previously isolated an avascular mutant, *groom of cloches*^{635} (*grc*^{635}) from a large scale forward genetic screen [1]. At early stages, the vascular phenotype of *grc* is comparable to that of *cloche* (*clo*), an avascular mutant that lacks both endothelial and hematopoietic lineages (**Fig. 3.1A**) [2]. Homozygous *grc* mutant embryos completely lack the expression of endothelial specific markers including *kdrl*, *dab2*, and *cdh5* at early developmental stages, indicating that the endothelial lineage failed to be specified or not maintained (**Fig. 3.5**). However, approximately at 18 hours post-fertilization (hpf), a small group of *kdrl*$^{+}$ cells can be detected in the posterior region of homozygous *grc* mutant embryos, which subsequently expanded. At 72 hpf, a rudimentary vascular structure can be detected in the majority of homozygous grc mutant embryos (**Fig. 3.2A**), and a small fraction (less than 5 percent) of these embryos survive to the adulthood. Similarly, we found that homozygous *clo* mutant embryos do possess *kdrl*$^{+}$ cells at later stages (Fig. 3.2A), indicating that the function of *grc* and *clo* may be required only during

early development, or may regulate differentiation of subsets of the endothelial lineage.

To determine whether the mutations in *grc* or *clo* locus shift the ratio of different mesoderm-derived lineages, we first evaluated whether mutation in grc locus led to an expansion of other related mesodermal lineages by performing a lineage tracing using caged fluorescein-conjugated Dextran as previously reported (Fig. 3.1B) [3]. Approximately two cells within the developing gastrula were activated with an ultraviolet laser at 5.5 hours post fertilization (hpf) when cells are restricted to a single lineage [4], and at 24-26 hpf, the distribution of the descendants from uncaged cells were analyzed. Compared to the wild-type embryos, homozygous *grc* or *clo* mutant embryos contain significantly increased number of mesodermal descendents that do not belong to an identifiable lineage in the midline and tail of the embryo, which preferentially localizes to the posterior, caudal to the yolk extension (**Fig. 3.1D**). Based on this observation, it was tempting to speculate that the mesodermal cells capable of generating the endothelial lineage fail to undergo further differentiation in the absence of *grc* or *clo* function, and remain undifferentiated and incorporated into the tailbud mesoderm. Consistent with earlier fate mapping studies, we found that cells within the first five tiers of wild-type gastrula generate somite, endothelium, blood, and pronephros, in addition to a small number of undifferentiated cells in 30 hpf embryos (**Fig. 3.1C**). Compared to the wild-type embryos where mesodermal cells give rise to the endothelial and hematopoietic lineages (33% for endothelial lineage and 5% for hematopoietic lineage, respectively), homozygous *clo* embryos lack both endothelial and

hematopoietic lineages, reflecting previously reported defects (**Fig. 3.1D**) [2]. Similarly, homozygous *grc* embryos selectively lack the endothelial lineage (**Fig. 1D**). In both cases, we observed substantial increase in *kdrl*$^{-}$ mesodermal cells in the midline and tail of the vascular mutant embryos (33% in *clo* and 17% in *grc*) (**Fig. 3.1D**). Therefore, it appears that the progenitors for the endothelial lineage remain undifferentiated in these avascular mutant embryos.

To better understand the molecular mechanisms underlying the emergence of the endothelial lineage at later stage, we isolated the locus affected by *grc* mutation by whole genome sequencing. Sequencing analyses revealed that the *grc* mutation was significantly associated with Leu248 to Pro248 changes in *etv2*, also known as *etsrp*, which is an essential transcription factor for the endothelial lineage [5, 6] (**Fig. 3.6**). Previously, mutation in *etv2* causing a premature stop has been identified in zebrafish, and morpholino (MO) knock-down of *etv2* has shown to cause a drastic reduction in the number of endothelial cells [7]. The phenotype of homozygous *grc* mutant embryos was wholly consistent with these findings. Additionally, we found *etv2* morphants displayed severe intersegmental vessel growth deficiencies (Data not shown, N=21).

Considering that both homozygous *grc* and *clo* mutant embryos generate endothelial cells at later stages, it appears that these avascular mutant embryos retain the ability to generate the endothelial lineage. We noted that the majority of the *kdrl*+ cells in avascular mutants are located in the posterior of the embryo at 24 hpf (**Fig. 3.2A**). Since it has been reported that tailbud can contribute to the endothelial lineage in Wnt-dependent manner [8], we examined whether endothelial

cells found in later stages of avascular mutant embryos are derived from the tailbud by laser-activation of uncaged fluorescein-conjugated Dextran at 14 hpf. While approximately 63% percent of endothelial cells within the posterior region (posterior to the cloaca) of wild-type embryos were the descendents of tailbud mesoderm, virtually all *kdrl*$^{+}$ endothelial cells found in either homozygous grc or clo embryos were originated from the tailbud (93% in *clo* and 93% in *grc*) (**Fig. 3.2E**). The lower percentage in wild-type was expected as there is observable mixing of endothelial cells in intact vasculature. Therefore, it appears that the tailbud mesoderm is the predominant source of endothelial cells in homozygous *grc* and *clo* embryos and a significant source in wild-type. Taken together, our observation raised an intriguing possibility that the emergence of endothelial cells derived from the tailbud may not require the activity of either *etv2* or *clo*, alluding that the molecular mechanisms that induce the endothelial lineage from the tailbud and the lateral plate mesoderm are likely to be distinct.

To ascertain whether *kdrl*$^{+}$ cells from wild-type or avascular mutant embryos have differential transcriptional profiles, we previously performed microarray analyses (**Chapter 2**). Using flow cytometry, *kdrl*$^{+}$ cells from 18.5 hpf wild-type and avascular mutant embryos were isolated and mRNA was extracted. We found that the expression of related mesodermal lineage markers was significantly up-regulated in *kdrl*$^{+}$ cells from avascular mutant embryos (**Fig. 2.2C**), and further validated alteration in the expression level of four genes, including *pax9*, by quantitative RT-PCR (**Fig. 2.3A** and **Fig. 3.3A**). A paired box homeodomain transcription factor, *pax9*, was one of the genes whose expression was significantly

up-regulated in avascular mutant embryos. Although *pax9* has previously been implicated as the key transcription factor for odontogenesis [9, 10] and development of pharyngeal pouch-derived organs in mouse [11], its role in endothelial biology is largely unknown. To further delineate the role of *pax9* during vascular development, we first examined the expression pattern of *pax9* in wild-type and avascular mutant embryos. In flow sorted endothelial cells, consistent with the microarray data, the expression of *pax9* within endothelial cells appears to be substantially elevated in homozygous *grc* or *clo* embryos compared to wild-type embryos (**Fig. 3.3A**). Moreover, in wild-type, the expression of *pax9* became stronger in endothelial cells isolated from the later stage embryos, and is more pronounced in endothelial cells isolated from the trunk region (**Fig. 3.7**). In wild-type embryos, strong endothelial expression of *pax9* could be detected at 24 hpf. At 36 hpf, the expression is gradually restricted to the endothelial cells in the trunk and tail region, indicating its role in endothelial cells at later stages (**Fig. 3.3B**). In homozygous *grc* and *clo* mutant embryos, strong *pax9* expression was present in the midline vascular area (**Fig. 3.3C**).

To examine the function of *pax9* during vascular development, we attenuated the activity of *pax9* by morpholino (MO)-mediated knock down in wild-type embryos. While the number of *kdrl*$^{+}$ cells, as well as proliferation and apoptosis of endothelial cells were unaltered (**Fig. 3.8**), the complexity of the vascular network in *pax9* MO-injected embryos was drastically reduced compared to control MO-injected embryos (**Fig. 3.4A** and **B**). Interestingly, we did not find any obvious differences in the total number of endothelial cells from pax9 MO-injected or control MO-injected embryos

(**Fig. 3.4B, top left**). However, the number and average length of intersegmental vessels (ISVs), as well as the number of branch points were substantially reduced in *pax9* MO injected embryos, compared to control MO injected embryos (**Fig. 3.4B, Panels 2-4**), indicating that *pax9* may affect migration and morphogenesis of endothelial cells. Similarly, inhibition of *pax9* in homozygous *grc* or *clo* mutant embryos caused similar phenotype (**Fig. 3.4A** and **B**). To determine whether the effect of *pax9* on endothelial morphogenesis was cell autonomous, we performed classic transplantation experiments. A small number of cells from control or *pax9* MO-injected donors were transplanted to wild-type host at gastrula stages. While transplanted cells contributed to the endothelial lineage in all cases, we found that cells from *pax9* MO-injected donor in wild-type recipient were selectively excluded from secondary angiogenic vessels such as intersegmental vessels (**Fig. 3.3D** and **E**). Therefore, it appears that *pax9* cell-autonomously influences the migration of endothelial cells and does not regulate the specification and differentiation of the endothelial lineage.

Considering that inhibition of *pax9* attenuated the formation of ISVs, but did not affect cell proliferation, apoptosis, and differentiation of endothelial cells, it is possible that *pax9* may influence the migration of endothelial cells during development. Our observation that *kdrl*$^{+}$ cells in homozygous *grc* or *clo* mutant embryos are more migratory than wild-type (**Fig. 3.1A** and **B**), and express higher level of pax9, further support this idea. To explore this possibility in detail, we first examined the migratory behaviors of endothelial cells in 24 hpf zebrafish embryos by tracking the movement of individual endothelial nuclei for 6 hours. We found that

endothelial cells from the pax9 MO-injected embryos moved significantly less than control MO-injected embryos, which resulted in delay in ISV formation (**Fig. 4B., bottom left**). To further examine the effects of *pax9* in endothelial migration, we knock-down *pax9* in human umbilical vein endothelial cells (HUVECs) and perform migration assays. In the wound healing scratch assay, *pax9* siRNA-treated HUVECs showed substantially decreased migration compared to control siRNA-treated HUVECs (**Fig. 3.4C** and **D**), indicating that the function of *pax9* promoting endothelial migration is conserved among vertebrates.

Since it has been reported that Wnt signaling promotes the differentiation of skeletal muscle at the expense of endothelial cells in tailbud of zebrafish[8], it is tempting to speculate that Wnt signaling may inhibit *pax9* expression within tailbud mesoderm with angiogenic potential, thereby regulate differentiation of endothelial cells. To test this notion, we examined the effects of Wnt signaling on pax9 expression. In 6-bromoindirubin-3'-oxime (BIO)-treated embryos, which up-regulates Wnt activity [12], the expression of *pax9* was substantially decreased compared to DMSO-treated embryos (**Fig. 9**). Since manipulation of Vascular Endothelial Growth Factor (VEGF) and Bone Morphogenetic Protein (BMP) signaling did not alter the expression level of pax9 (**Fig. 3.9**), it appears that the effects of Wnt signaling on *pax9* expression may be specific. Taken together, our data show that *pax9* is novel regulator of endothelial cell migration during development of which function is evolutionarily conserved. Moreover, our data suggest that *pax9* may be a novel target in diverse human pathological conditions with vascular components.

Experimental Methods.

Zebrafish husbandry and morpholino injection.

Zebrafish (*d. rerio*) embryos were reared at 28.5°C and, when necessary, synchronized for short periods at 25°C or 32°C. Morpholinos were injected at the one or two-cell stage at a volume of 4.6nL using a picospritzer gas-pressure injector. All morpholinos were injected in 5mM HEPES and 0.05% Phenol Red. *Pax9* morpholino (Sequence: 5′-CCAAAGGCTGGCTCTAGTTATGCAG-3′) was injected at a concentration of 600μM. Efficacy of this splice-blocking morpholino was measured using RT-PCR (**Fig 3.10**).

Cloning of *grc.*

grc was isolated from a previously published forward genetic screen using the *Tg(kdrl:eGFP)* transgene [1]. Homozygous mutants were identified by the absence of GFP vasculature and the retention of GFP fluorescence in the endocardium and pharyngeal endoderm. Bulked segregant analysis was performed using simple sequence length polymorphism (SSLP) markers as previously described [13] and the genetic lesion was found to be located on Chromosome 16. Further SSLP mapping refined the region to approximately 30kB on Chromosome 16. Since this region contained a gap, we utilized High Throughput Sequencing (paired end Illumina Sequencing technology) of the transcriptome and genome of pooled homozygotes in order to define the missing sequence and determine the mutation underlying *grc* [14]. Initially runs-of-homozygosity were scored and found to agree with the previously indicated region on Chromosome 16. Only one single nucleotide polymorphism (SNP) was exclusively found in the *grc* sequence library. This

mutation was an A to G substitution which results in a leucine to proline amino acid change. This mutation was then confirmed using a derived cleavage of amplified polymorphisms (DCAPS) assay [15].

Validation of up-regulation of *pax9*.

For qRT-PCR, RNA was extracted using the QIagen RNeasy mini kit and accompanying protocol with carrier RNA. The iScript cDNA synthesis kit (Bio-Rad) was used to reverse transcribe entire RNA extracts, immediately after RNA extraction. cDNA samples were then diluted to a volume of 300µl. Using 2X Power syber mastermix (Applied Biosystems), 640nM of each primer, and 8µl of cDNA in a 25µl reaction, amplification of transcript amplicon was monitored on a Bio-Rad cfx96 system. Gene expression was normalized to either *18S rRNA* or *β-actin* housekeeping genes. Melting curve analysis was performed on all reactions. Ct versus cDNA concentration plots were also used to determine that there was a linear ratio of amplification of housekeeping genes to gene-of-interest at a particular cDNA concentration. Data was analyzed using the $2^{-\Delta\Delta cT}$ method [16]. At least three biological replicates of three technical replicates were performed for each condition.

Primers:

Name	Forward	Reverse
18S rRNA	cacttgtccctctaagaagttgca	ggttgattccgataacgaacga
β-actin	tggcccctagcacaatgaag	gcctccgatccagacagacagagtat
pax9	tcaagagcatgagtgccacacg	agtcatagagctgaagccaccag

Lineage tracing.

0.2% w/v (2ul of stock in 10ul injection mix) caged fluorescein dextran with phenol red and HEPES was injected at a 4.6nL volume at the one to two cell stage. For shield stage uncaging, embryos were mounted laterally in 3% methylcellulose in 30% Danieau in a glass bottom dish. A two-photon laser on a Zeiss 710 scope was used. The laser line was set to 735nM. The bleach function was set to 30 pulses. For tailbud uncaging, embryos were mounted in a glass-bottom dish in 1% low-melt agarose and exposed to UV light using the scan function of the DAPI channel on a Leica SP5. ROIs were selected accordingly. Embryos were observed at 24 hpf. Further fixing, sectioning and staining were performed using established protocols[17] and the following antibodies: chick anti-GFP (AB-CAM), goat anti-fluorescein (Invitrogen), donkey anti-goat 594 (Jackson Immunoresearch), donkey anti-chick 488 (Jackson Immunoresearch).

In situ hybridization.

In situ hybridization was performed following established protocols [18]. *pax9* probe was generated using agarose-gel purified PCR fragments (PCR Primers: “PAX9ISHF”, 5′-cgctatcacatccgtctcg-3′ and “PAX9ISHR”, 5′tgcttgttaccccacactga-3′), which were ligated into the PGEM-T easy vector *(Promega). Transformed colonies were selected and sequenced. The final amplified vector was linearized and transcribed using SP6 polymerase (Roche T7/SP6 DIG-UTP labeling kit). Transverse cryostat sectioning of *in situ* hybridized embryos was performed as described[19] and counterstained with Nuclear fast red.

Mitosis/Apoptosis assays.

The Roche *in situ* cell death detection kit was used with the associated protocol to detect apoptotic *kdrl*$^{+}$ cells in 250μM vibratome sections of zebrafish embryos. Rabbit anti-phospho histone H3 (Ser 10) antibody (Millipore) and Donkey anti-rabbit 568 (Invitrogen) secondary antibodies were used to stain mitotic *kdrl*$^{+}$ cells in vibratome sections.

Transplantation

Transplantation was performed as previously described [20]. Embryos were observed at 24 hpf and image on a Leica SP5 confocal microscope for cellular resolution.

HUVEC Cell culture and scratch assay

HUVECs were cultured on 0.1% gelatin-coated plates in complete endothelial cell growth media containing supplements (Lonza, CC-3162) and 100 unit/ml penicillin-streptomycin. Cells between passages 3 and 7 were used for analyses. HUVECs were transfected with Human PAX9 or nontargeted control siRNA (100nM, Dharmacon, Lafayette, CO, USA) using lipofactamine 2000 (Invitrogen, Carlsbad, CA, USA). Cells were used for assays at 48 hours after transfection. Expression level of PAX9 (Cell signaling; 8739, 1:1,000) were determined by Western blotting. HUVECs were transfected with the indicated siRNAs. At 32 hours after transfection, cells were serum-starved overnight. The cell monolayer was scratched with a 200 μl pipette tip to create a cell-free zone. Thereafter, cells were gently washed twice with the medium and incubated for 6h. The cells were imaged using inverted microscope.

The wound areas were measured by ImageJ, normalized and presented as the percentage of wound measured at time 0. At least seven fields were analyzed for each scratch and each sample was performed in duplicate. The closure distance was generated by averaging 4 measurements per picture at 0h and 6hr.

Figures:

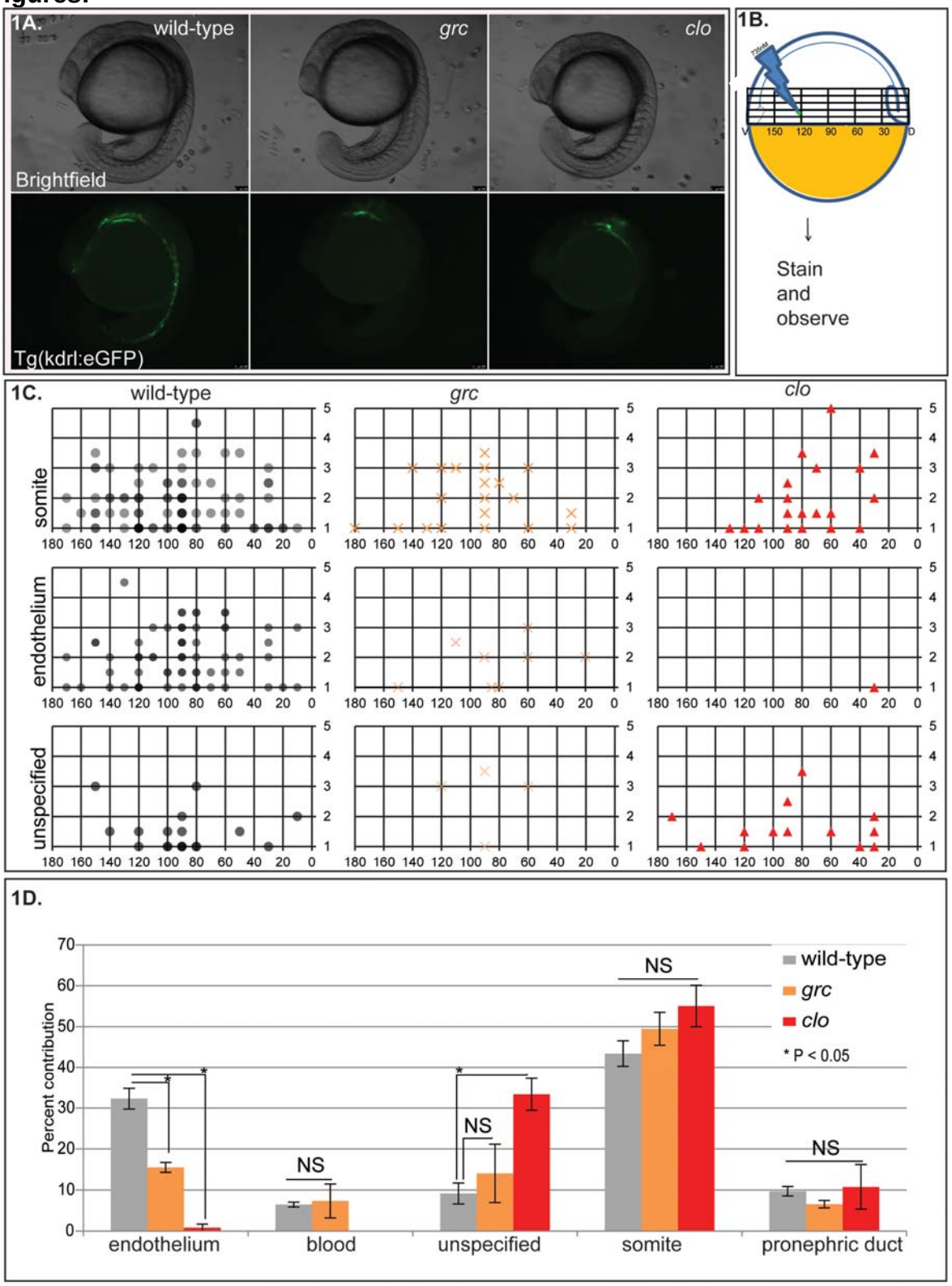
1A.
wild-type
grc
clo
Brightfield
Tg(kdrl:eGFP)
1B.
V
150
120
90
60
30
D
Stain
and
observe
1C.
wild-type
grc
clo
somite
endothelium
unspecified
180 160 140 120 100 80 60 40 20 0
1 2 3 4 5
1D.
Percent contribution
0 10 20 30 40 50 60 70
wild-type
grc
clo
* P < 0.05
NS
endothelium
blood
unspecified
somite
pronephric duct

Figure 3.1: Failure of the majority of endothelial cells to specify early on in avascular mutants.

(A) Wild-type, *grc*, and *clo* embryos at 18.5 hpf. (B) Schematic for shield-stage lineage tracing by caged-fluorescein dextran. (C) Spatial origin of somite, endothelium (*kdrl*$^{+}$), and unspecified cell-types in wild-type, *grc*, and *clo*. (D) Percentage of mesodermal cells giving rise to a particular lineage wild-type, *grc*, and *clo*. WT N=245, *grc* N=70, *clo* N=66 embryos.

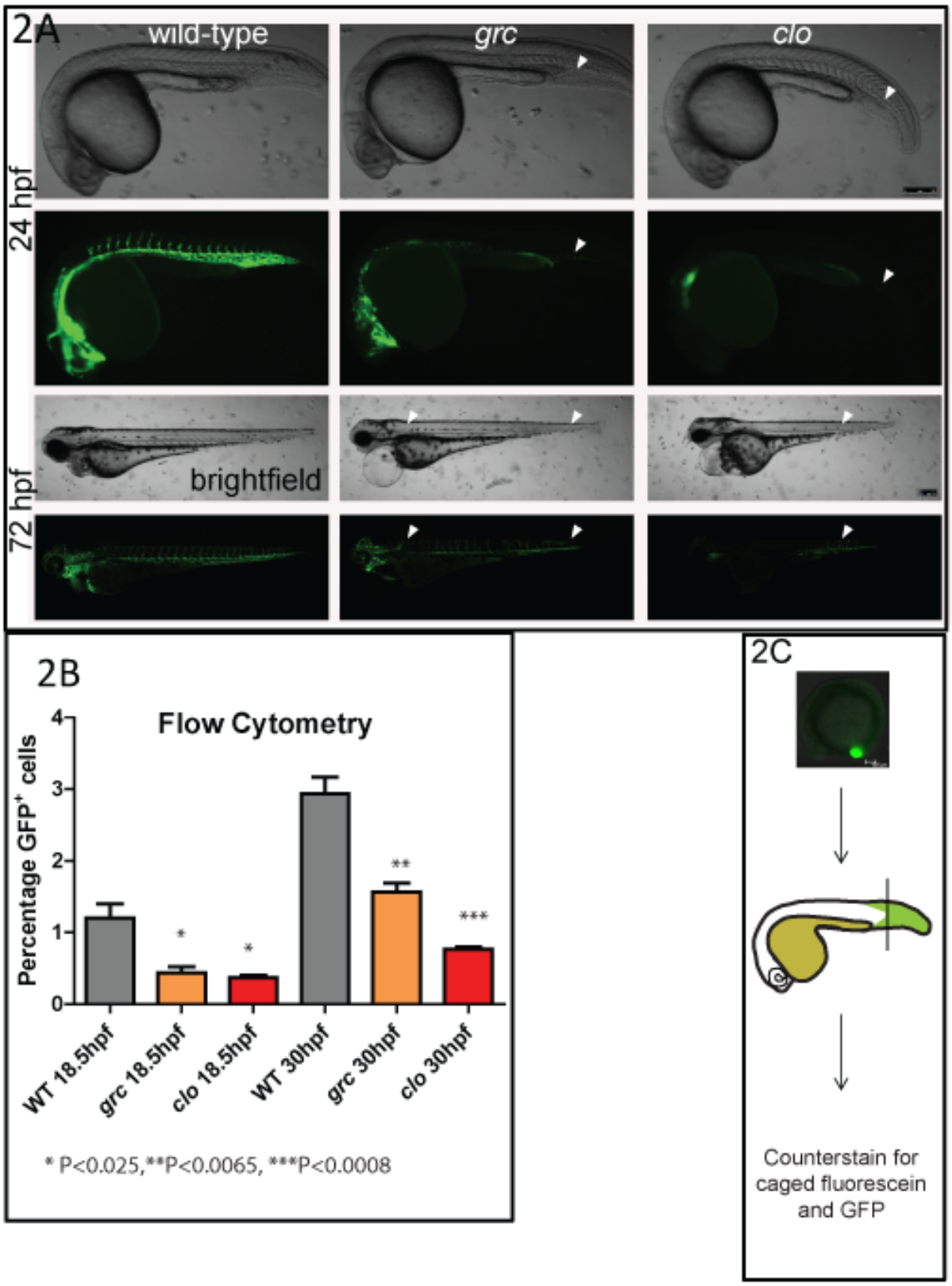
2A
wild-type
grc
clo
24 hpf
brightfield
72 hpf
2B
Flow Cytometry
Percentage GFP+ cells
0
1
2
3
4
*
*
**
***
WT 18.5hpf
grc 18.5hpf
clo 18.5hpf
WT 30hpf
grc 30hpf
clo 30hpf
* P<0.025,**P<0.0065, ***P<0.0008
2C
Counterstain for caged fluorescein and GFP

Figure 3.2 (cont.)

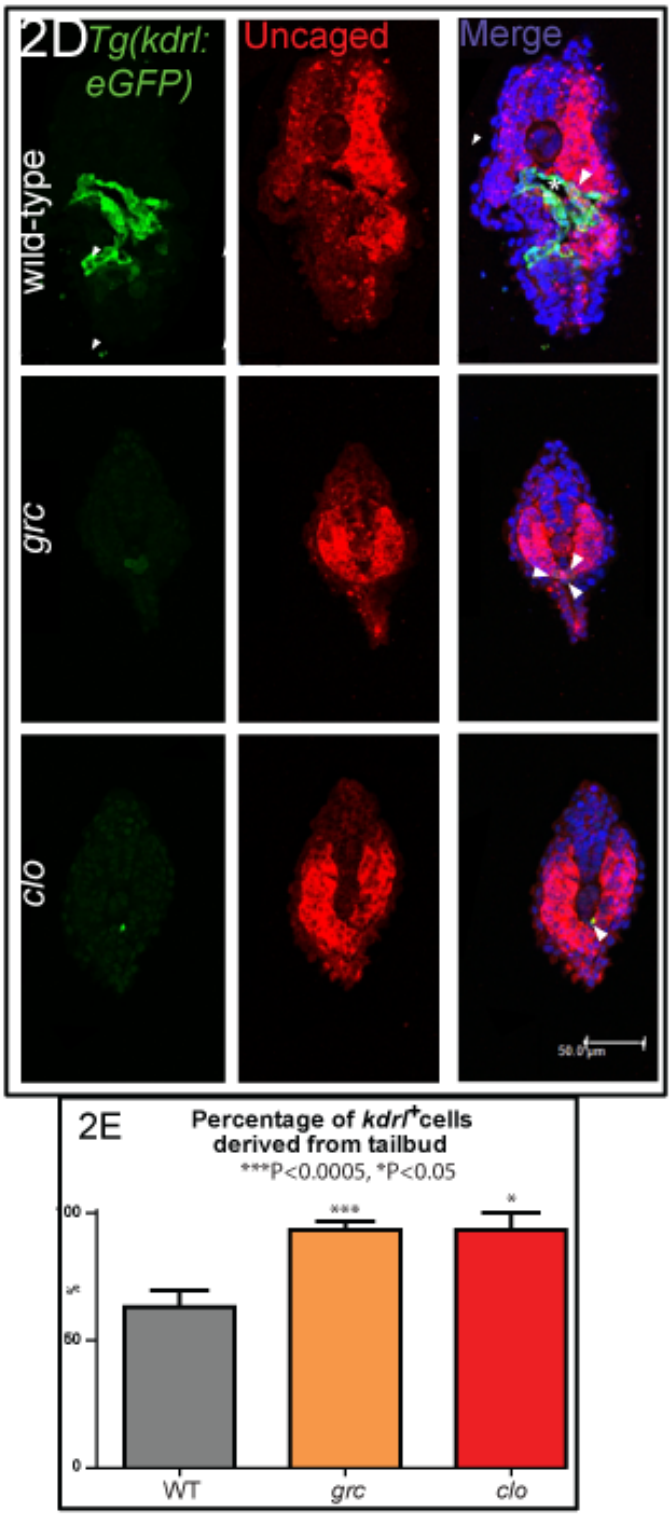

Figure 3.2: Recovery of the endothelial lineage via tailbud-dervied angioblasts.

(A) wild-type, *grc*, and *clo* embryos at 24 and 48 hpf respectively. White arrowheads indicate *kdrl*$^{+}$ cells. (B) Flow cytometry analysis of wild-type, *grc*, and *clo* at 18.5 hpf and 30 hpf. Three biological replicates consisting of 15 dissociated embryos were performed. (C) Schematic for tailbud lineage tracing at 12 somite stage. (D) Representative images of wild-type, *grc*, and *clo* transverse tail sections stained for GFP (green) and Uncaged fluorescein dextran (red), merged with DAPI (Blue), respectively. (E) Estimation of the percentage of *kdrl*$^{+}$ cells derived from tailbud. N=22,17, and 7 embryos for WT, *grc*, and *clo*, respectively

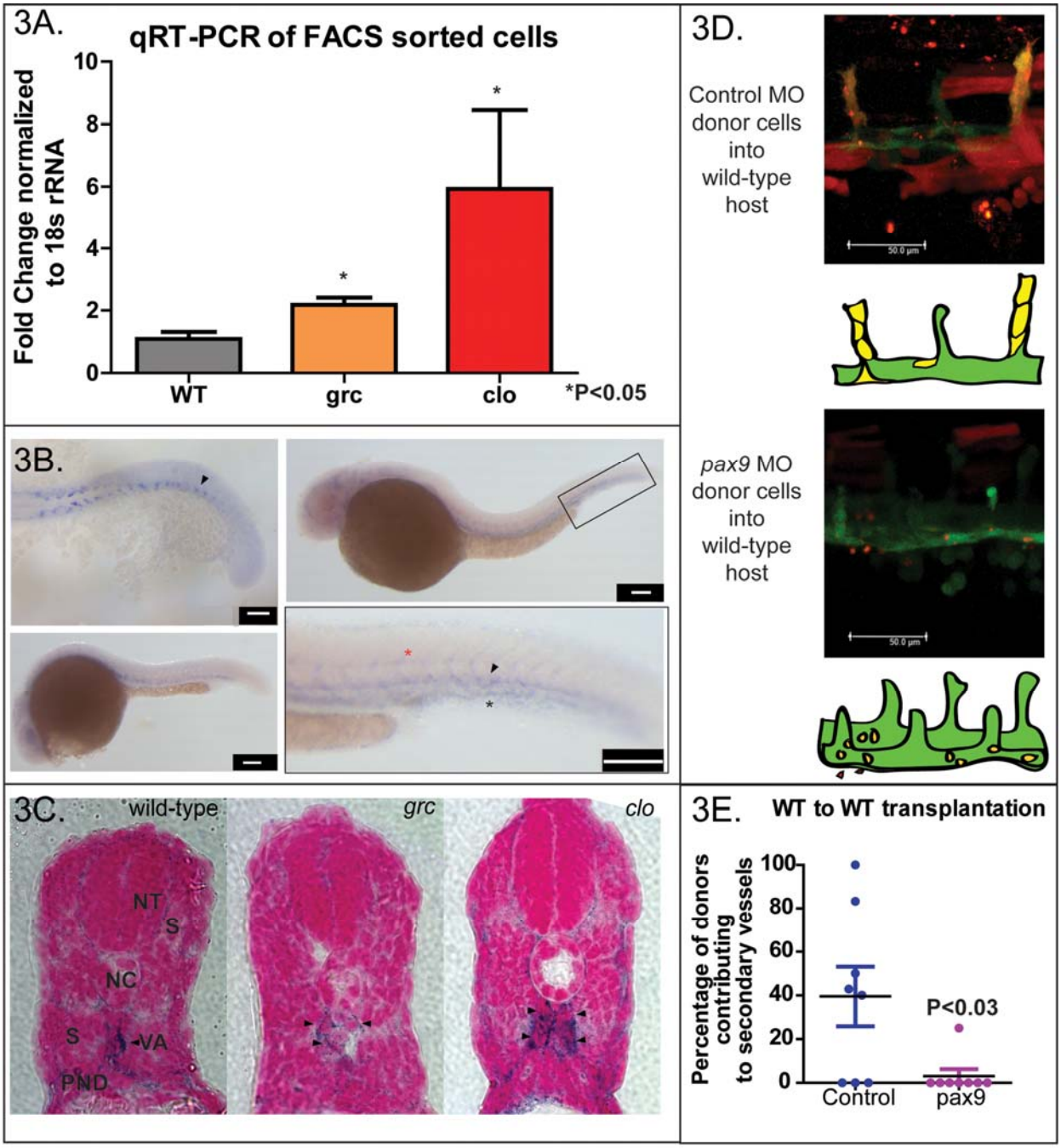

Figure 3.3: *pax9* expression in the vasculature and cell-autonomous function in vascular morphogenesis.

(A) qRT-PCR for *pax9* expression in FACS sorted cells at 18.5 hpf. Three biological replicates and three technical replicates were done. (B) *in situ* hybridization pattern of *pax9* at 18.5, 24 and 36 hpf (red asterisk indicates ISV, black arrow indicates dorsal aorta, black asterisk indicates caudal vein). (C)

Transverse sections of *in situ* hybridized embryos at 24 hpf (black arrows indicate expression in the vascular area (VA)). Images are 100μM wide. (D) Representative images for transplantation of control (top) or *pax9* morphant donor cells and schematics illustrating their contribution to different regions. (E) Quantification of wild-type *pax9* morphant to wild-type transplantation experiments (N=8 each). Scale bars = 50μm

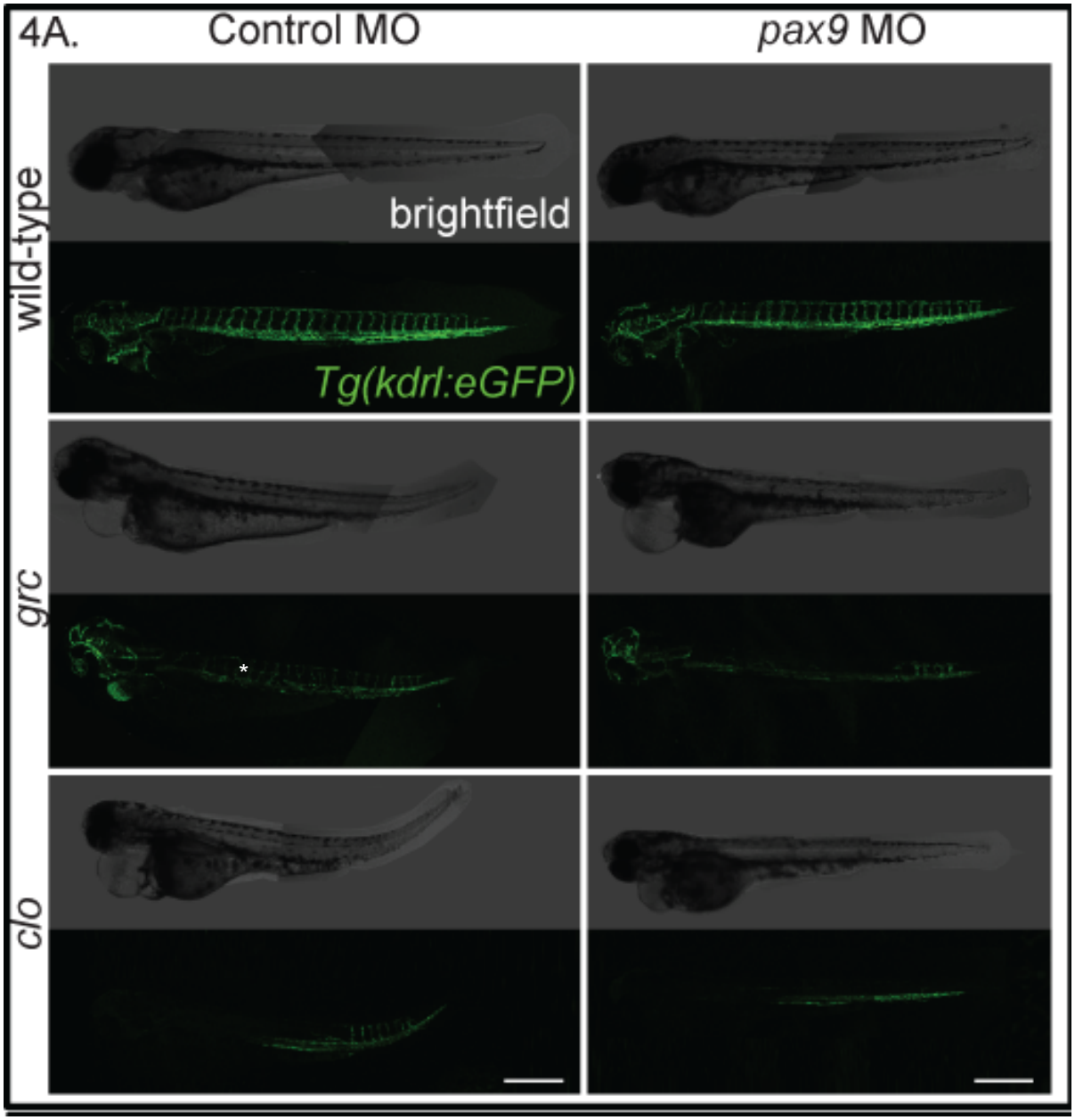
4A.
Control MO
pax9 MO
wild-type
brightfield
Tg(kdrl:eGFP)
grc
*
clo

Figure 3.4 (cont.)

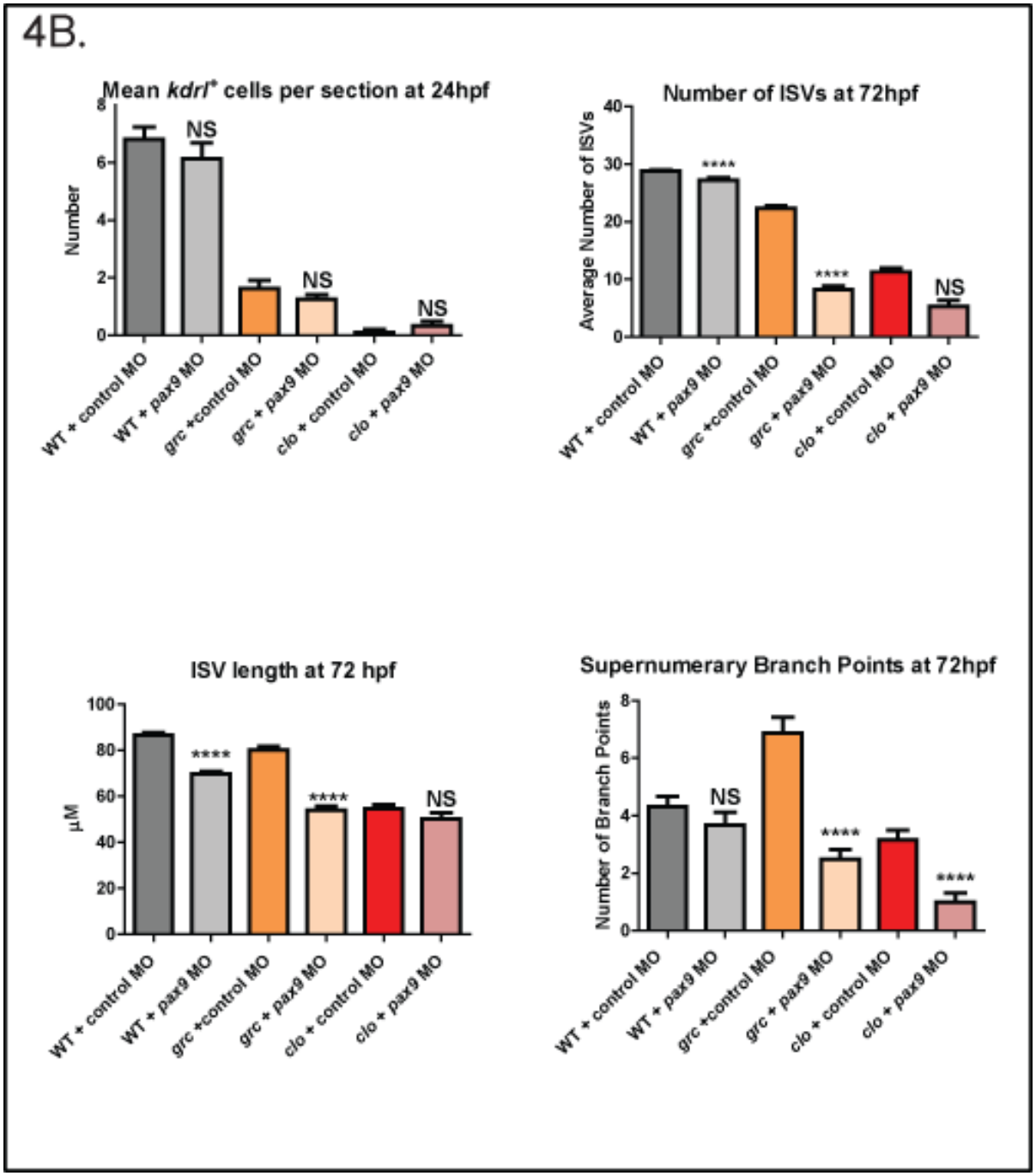

Figure 3.4 (cont.)

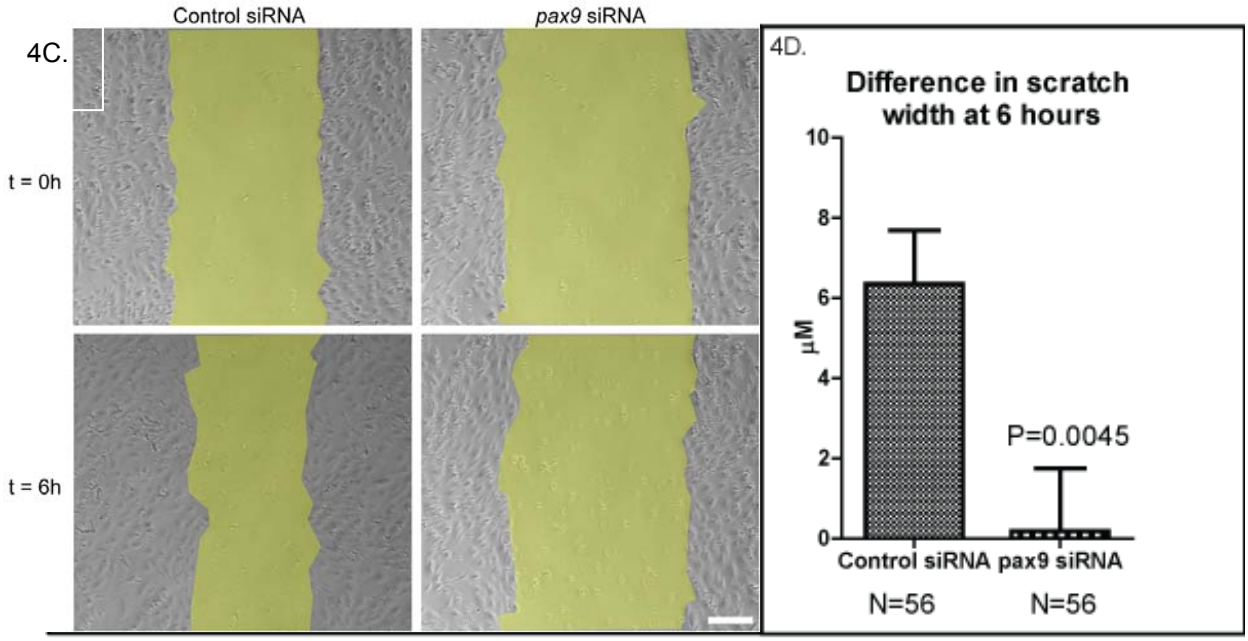

Figure 3.4: Conservation of the role of *pax9* in zebrafish and human endothelium.

(A) *pax9* morpholino severely reduces the number of ISVs, length, and branching morphogenesis in avascular mutants, while not decreasing the number of cells and (B) quantification. N=43, 50, and 25 for WT, *grc*, and *clo*, respectively. (C) Representative images from HUVEC cell scratch assay (scratch area highlighted in yellow) and (D) quantification. N=56 measurements, 14 regions per condition, 2 biological replicates. Scale bars in panels A and B are 250 µM and 20 µM, respectively.

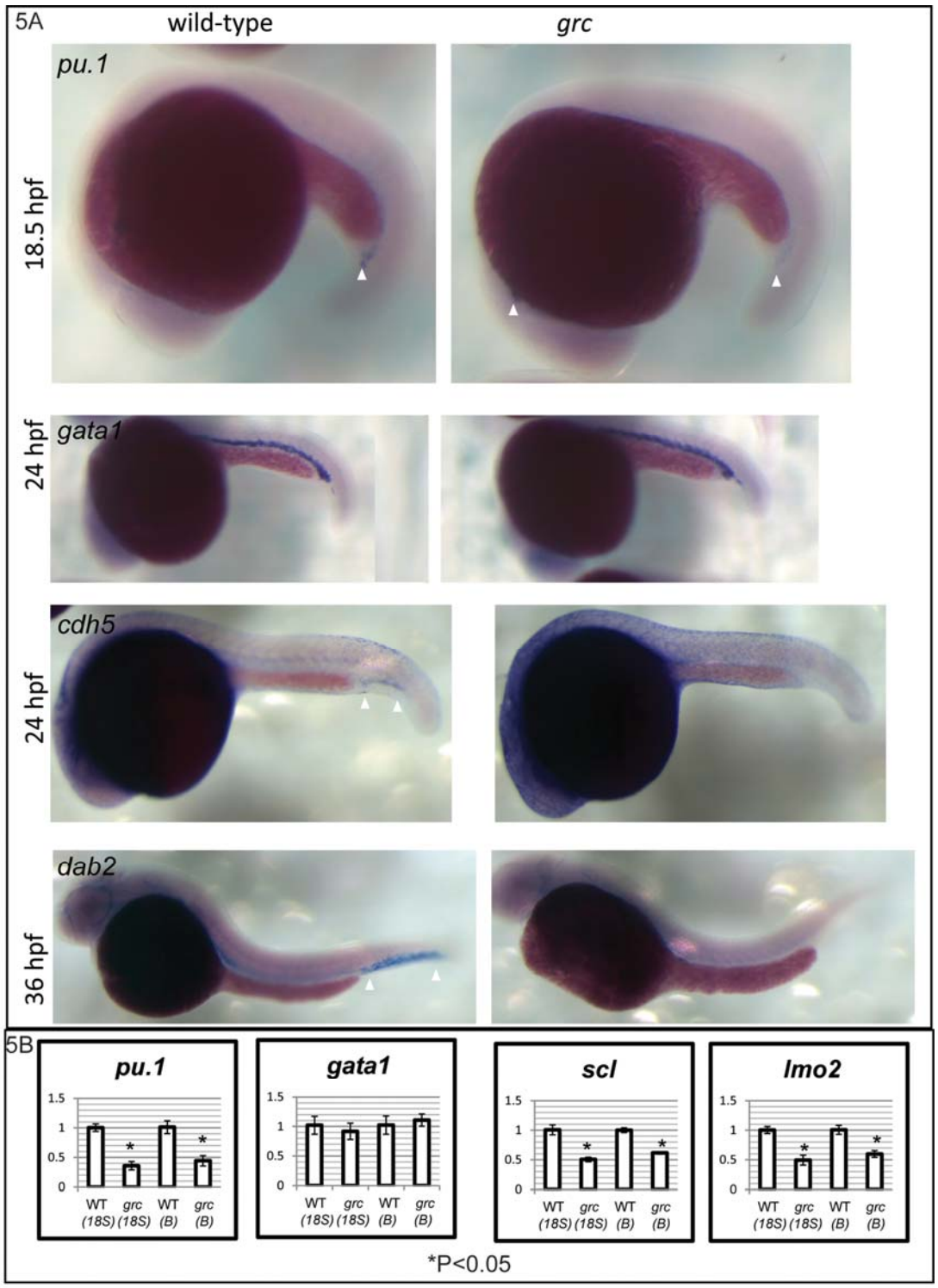
5A
wild-type
grc
pu.1
18.5 hpf
gata1
24 hpf
cdh5
24 hpf
dab2
36 hpf
5B
pu.1
gata1
scl
lmo2
1.5
1
0.5
0
WT (18S)
grc (18S)
WT (B)
grc (B)
*P<0.05

Figure 3.5: Phenotypic analysis: expression of hemato-vascular genes in *grc*.

(A) *in situ* hybridization shows *pu.1* expression in *grc* embryos is mildly changed in the posterior blood island, as was previously published.[5] *gata1* expression was not changed. *cdh5* expression was absent in *grc*. The venous marker, *dab2*, was absent in *grc* embryos. (N>5 embryos for each condition) (B) Whole embryo expression of *pu.1* and *gata1* confirmed the findings in panel A. Additionally *scl* and *lmo2* are down-regulated in *grc* embryos by qRT-PCR when normalized to *18S* rRNA or *β-actin*. Asterisk indicates a p-value of less than 0.05. Averages are the result of three biological replicates with three technical replicates each.

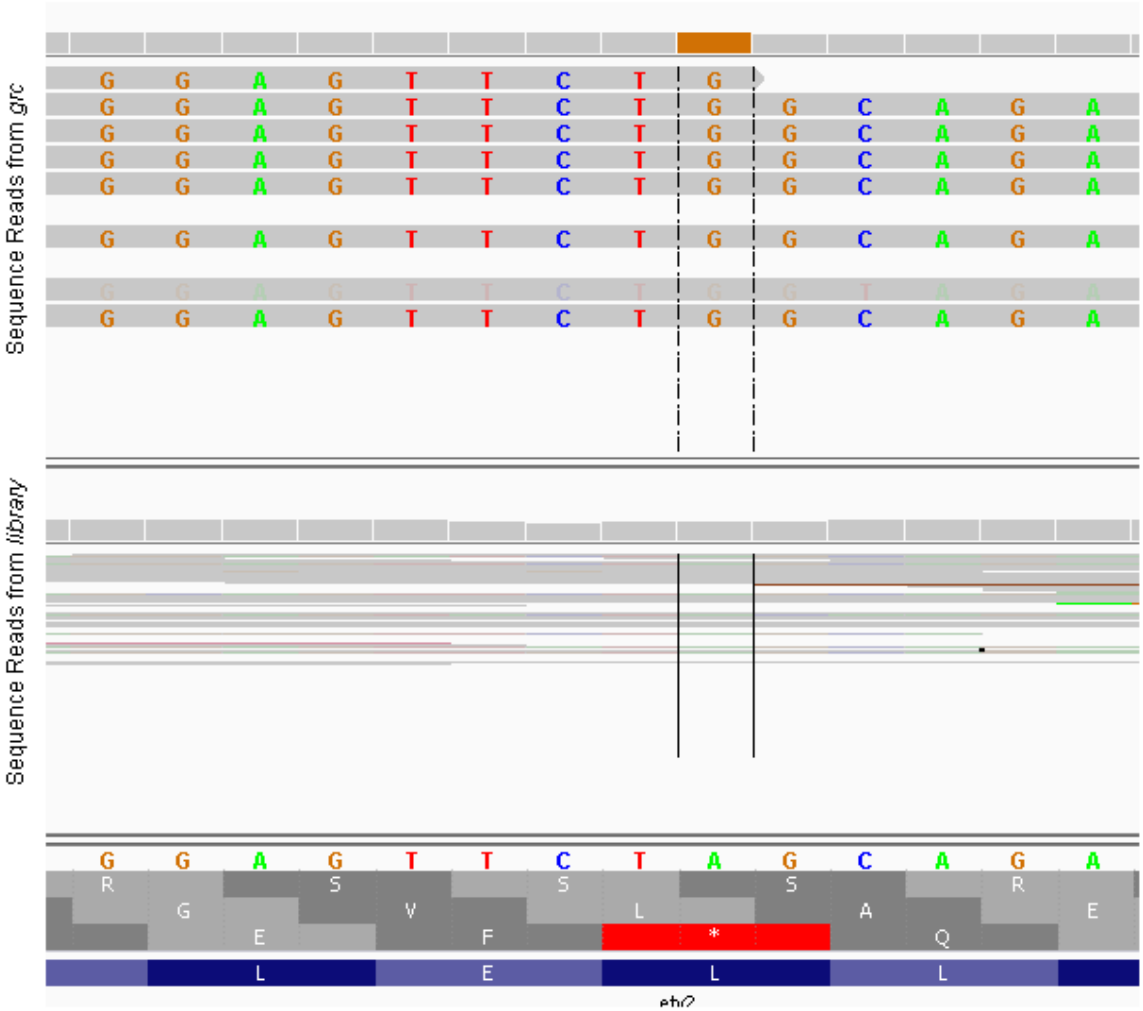

Figure 3.6: Cloning of *grc* mutation.

Using high-throughput transcriptome and genome sequencing with a large reference library, we isolated a single-nucleotide polymorphism not found in any other reference sequence. There were no other unreported SNPs in the run of homozygosity on Chromosome 16. The A to G substitution leads to a Leucine to Proline mutation in the Etv2 peptide. Using the program, Polyphen, this mutation was predicted to damage the overall protein structure.

Fig. 7

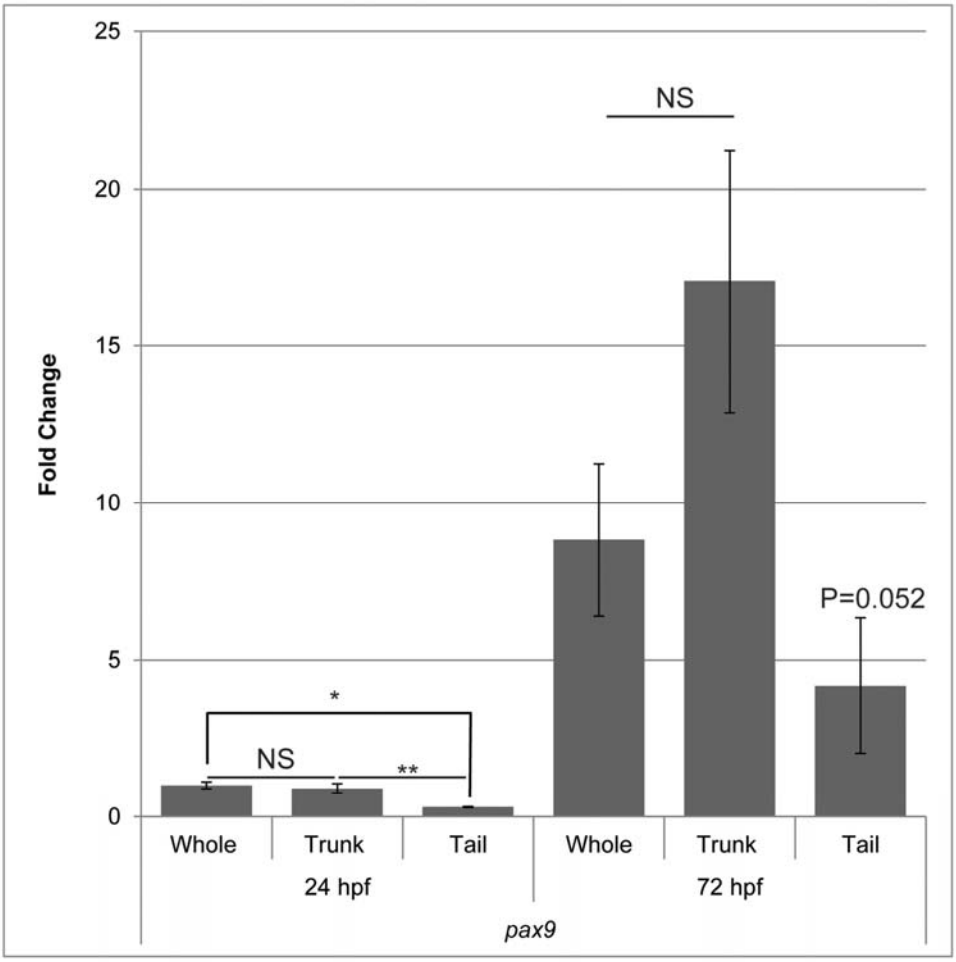

Figure 3.7: Expression profiling of *pax9* within endothelial cells.

qRT-PCR results showing that *pax9* is actually expressed at lower levels in the developing zebrafish tail vasculature in the tail compared to trunk, when normalized to 18S rRNA, at 24 and 72 hpf, respectively. Average of three biological replicates, three technical replicates. Error bars indicate SEM. P-value is from a two-tailed homoscedastic ttest.

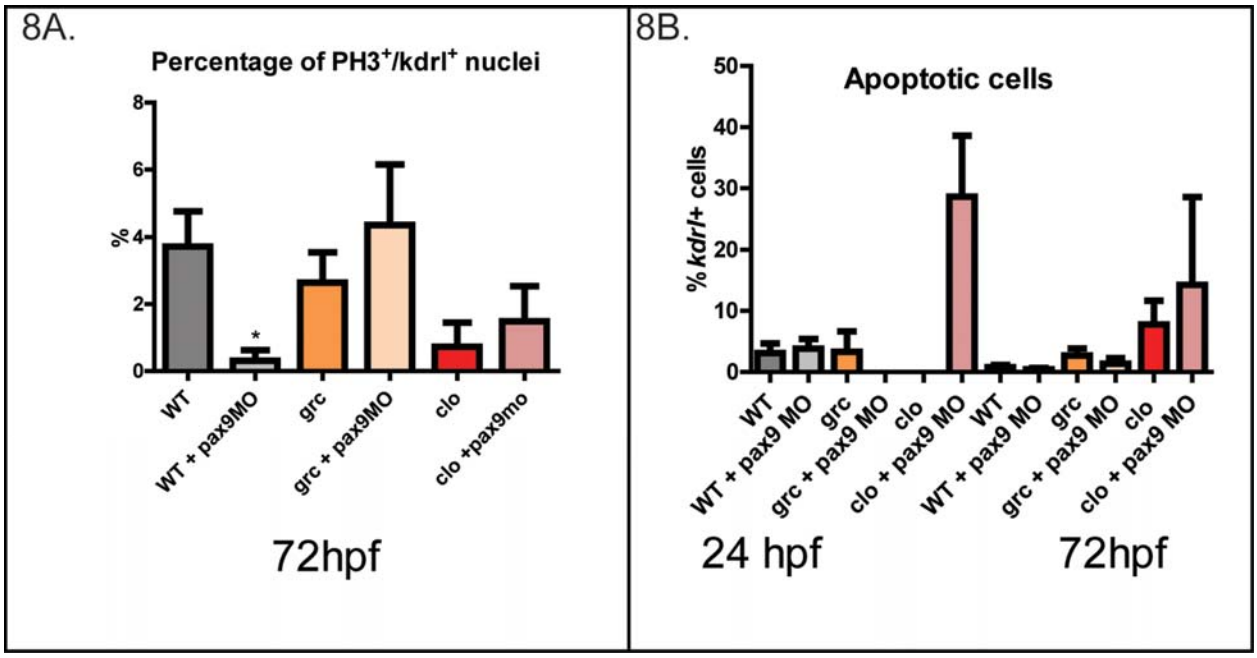

Figure 3.8: *pax9* does not affect vascular morphogenesis via apoptosis or proliferation in mutants.

(A) Phospho histone-H3 antibody staining in the developing vasculature did not reveal differences between mutant when *pax9* was knocked-down. *Pax9* down-regulation in wild-type did show a significant reduction in cell-cycle entry of about 4-fold. N > 23 samples for each condition. (B) No significant differences in apoptosis of kdrl+ cells was noted by TUNEL assay. Sample size for *clo* was low, but we noted a higher level of apoptosis in all tissues in homozygous *clo* embryos. Sample sizes for WT and *grc* at 24 hpf were N=60, N=18 respectively and at 72 hpf and N=96 N=32.

Fig. 9

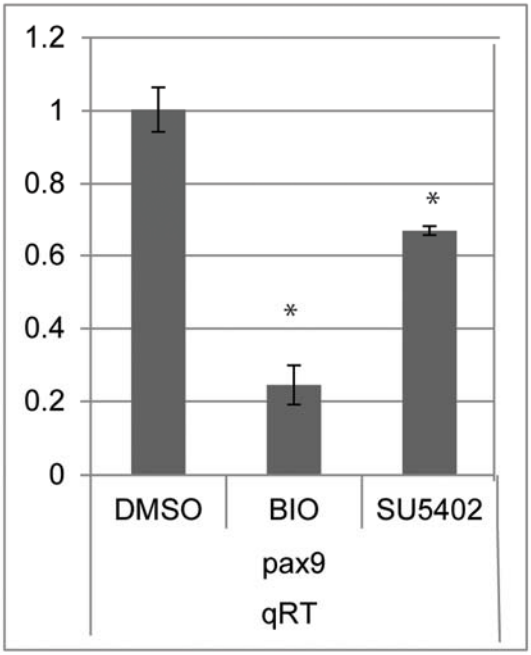

Figure 3.9: *pax9* expression is decreased by WNT agonist BIO within endothelial cells.

Agonism of WNT signaling by treatment with BIO from 20 hpf to 30 hpf reduced expression of *pax9* within endothelial cells by around five-fold. The FGF inhibitor, SU5402, also showed a significant decrease in expression of *pax9* by about one-third. Averages are of three biological replicates and three technical replicates each. Other drugs/treatments tested were Notch inhibitor (DAPT), BMPR2 inhibitor (DMH1), inducible BMP antagonist (*Tg(Hsp70l:Noggin3)*), and inducible BMP agonist (*Tg(Hsp70l:Bmp2b)*), which showed no effect. Treatment with VEGF inhibitor (SU5416) actually increased *pax9* expression by about two-fold within endothelial cells (Data Not Shown. 3 biological replicates, three technical replicates). Heat shock treatments were carried out at 26 hpf and all FACS sorts were carried out at 32 hpf.

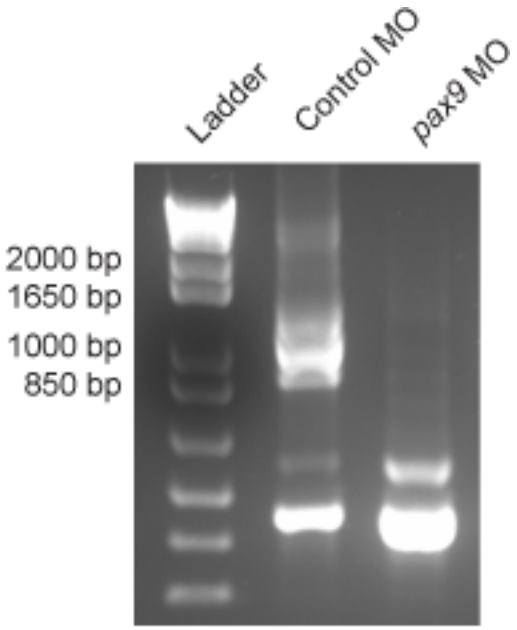

Figure 3.10: Efficacy of *pax9* splice-blocking morpholinos.

Agarose gel showing *Pax9* RT-PCR. The full coding sequence of pax9 was amplified from cDNA libraries from pools of control morpholinos injected embryos (lane 2) or *pax9* morpholino injected embryos (Lane 3) using primers recognizing the first and last coding exons. Lane 1 is Invitrogen 1kB plus ladder. Full-length *pax9* amplicon is 1205bp and a minor isoform of 1065bp is also seen (lane 2).

REFERENCES

1. Jin SW, Herzog W, Santoro MM, Mitchell TS, Frantsve J, Jungblut B, Beis D, Scott IC, D'Amico LA, Ober EA, et al: **A transgene-assisted genetic screen identifies essential regulators of vascular development in vertebrate embryos.** *Dev Biol* 2007, **307:**29-42.

2. Stainier DY, Weinstein BM, Detrich HW, 3rd, Zon LI, Fishman MC: **Cloche, an early acting zebrafish gene, is required by both the endothelial and hematopoietic lineages.** *Development* 1995, **121:**3141-3150.

3. Vogeli KM, Jin SW, Martin GR, Stainier DY: **A common progenitor for haematopoietic and endothelial lineages in the zebrafish gastrula.** *Nature* 2006, **443:**337-339.

4. Kimmel CB, Warga RM, Schilling TF: **Origin and organization of the zebrafish fate map.** *Development* 1990, **108:**581-594.

5. Sumanas S, Gomez G, Zhao Y, Park C, Choi K, Lin S: **Interplay among Etsrp/ER71, Scl, and Alk8 signaling controls endothelial and myeloid cell formation.** *Blood* 2008, **111:**4500-4510.

6. Rasmussen TL, Kweon J, Diekmann MA, Belema-Bedada F, Song Q, Bowlin K, Shi X, Ferdous A, Li T, Kyba M, et al: **ER71 directs mesodermal fate decisions during embryogenesis.** *Development* 2011, **138:**4801-4812.

7. Pham VN, Lawson ND, Mugford JW, Dye L, Castranova D, Lo B, Weinstein BM: **Combinatorial function of ETS transcription factors in the developing vasculature.** *Dev Biol* 2007, **303:**772-783.

8. Martin BL, Kimelman D: **Canonical Wnt signaling dynamically controls multiple stem cell fate decisions during vertebrate body formation.** *Dev Cell* 2012, **22:**223-232.

9. Neubuser A, Peters H, Balling R, Martin GR: **Antagonistic interactions between FGF and BMP signaling pathways: a mechanism for positioning the sites of tooth formation.** *Cell* 1997, **90:**247-255.

10. Vieira AR, Meira R, Modesto A, Murray JC: **MSX1, PAX9, and TGFA contribute to tooth agenesis in humans.** *J Dent Res* 2004, **83:**723-727.

11. Peters H, Neubuser A, Kratochwil K, Balling R: **Pax9-deficient mice lack pharyngeal pouch derivatives and teeth and exhibit craniofacial and limb abnormalities.** *Genes Dev* 1998, **12:**2735-2747.

12. Meijer L, Skaltsounis AL, Magiatis P, Polychronopoulos P, Knockaert M, Leost M, Ryan XP, Vonica CA, Brivanlou A, Dajani R, et al: **GSK-3-selective inhibitors derived from Tyrian purple indirubins.** *Chem Biol* 2003, **10:**1255-1266.

13. Postlethwait JH, Talbot WS: **Zebrafish genomics: from mutants to genes.** *Trends Genet* 1997, **13:**183-190.

14. Voz ML, Coppieters W, Manfroid I, Baudhuin A, Von Berg V, Charlier C, Meyer D, Driever W, Martial JA, Peers B: **Fast homozygosity mapping and identification of a zebrafish ENU-induced mutation by whole-genome sequencing.** *PLoS One* 2012, **7:**e34671.

15. Neff MM, Neff JD, Chory J, Pepper AE: **dCAPS, a simple technique for the genetic analysis of single nucleotide polymorphisms: experimental applications in Arabidopsis thaliana genetics.** *Plant J* 1998, **14:**387-392.

16. Livak KJ, Schmittgen TD: **Analysis of relative gene expression data using real-time quantitative PCR and the 2(-Delta Delta C(T)) Method.** *Methods* 2001, **25:**402-408.

17. Clanton JA, Shestopalov I, Chen JK, Gamse JT: **Lineage labeling of zebrafish cells with laser uncagable fluorescein dextran.** *J Vis Exp* 2011.

18. Thisse C, Thisse B: **High-resolution in situ hybridization to whole-mount zebrafish embryos.** *Nat Protoc* 2008, **3:**59-69.

19. Westerfield M: *The Zebrafish Book. A guide for the laboratory use of zebrafish (Danio rerio).* 4 edn. Eugene: Univ. of Oregon Press; 2000.

20. Kemp HA, Carmany-Rampey A, Moens C: **Generating Chimeric Zebrafish Embryos by Transplantation.** *J Vis Exp* 2009**:**e1394.

CHAPTER 4

Conclusions

This thesis elucidates an alternative developmental pathway that generates the endothelial lineage and illustrates the role of two genes, *pax9* and *sox11b*, in this process. My research is one of the first attempts that dissect the heterogeneous origin of the endothelial cells at molecular level. Therefore, findings of my thesis research represent important contributions to the field of vascular biology and will serve as building blocks for future studies into the role of these genes in endothelial biology. This discussion highlights the key points found in each chapter as well as discusses potential future endeavors which may prove to expand our knowledge of the mechanisms of vascular development.

Chapter 2

Key Points

1. Vascular development proceeds in the absence of *clo*/*etv2* function.
2. The *clo*/*grc* early *kdrl*$^{+}$ lineages have a unique transcriptional profile.
3. Modulation of *sox11b* levels by morpholino injection perturbs wild-type angiogenesis.

Conclusion

Together, the findings described in Chapter 2 of the first chapter suggest that vasculogenesis proceeds in mutant backgrounds which lack gene function necessary for the specification of the majority of the endothelial lineage. Furthermore, the novel transcriptional pathways functioning in mutant endothelial cells which are specified in these backgrounds is distinct from that in wild-type and definable.

Using transgenic avascular mutant zebrafish, we were able to highlight the earliest detectable emergence of the endothelial lineage in the attenuated mutant background. By microarray analyses, we were able to describe the transcriptional profile that is distinct in these cells. At initial review, many of the genes upregulated in early avascular mutant endothelium were characteristic of other mesodermal lineage, indicating a novel mechanism of differentiation and a unique identity from early wild-type endothelial cells.

Validation of the microarray by real-time qRT-PCR yielded at least four novel transcription factors upregulated in mutant angioblasts. Perturbation of *sox11b* by morpholino knockdown showed that this gene is necessary for proper vascular development. Furthermore, this morpholino experiment demonstrated that the transcriptional profile of avascular mutants could be used to elucidate new genes involved in vascular patterning that were not previously isolated by the study of wild-type animals.

Chapter 2 represents a validation of our attenuated model system. Further, it demonstrates that in the absence of *clo* or *etv2*, endothelial cells can

be specified. Additionally, endothelial cells specified despite this deficiency have a unique transcriptional profile that has allowed for the discovery of the involvement of *sox11b* in vascular morphogenesis.

Future Directions

The apparent delay in sprouting angiogenesis seen in *sox11b* morphants, while implicating this gene in vascular development, does not specify the mode of action of this gene. As such, I believe that by performing transplantation to determine if *sox11b* functions cell-autonomously or by cell-cell signaling, since *sox11b* is also expressed in the neighboring anterior somites. Our study did not rule out the possibility that *sox11b* expression in the surrounding somites provides signals that direct the vascular patterning of adjacent angioblasts and endothelial cells. Furthermore, cell-cycle analysis by phospho-histone H3 staining would be informative. Lastly, investigation into the two other validated genes, *zfhx4* and *klf5l* would reveal whether these genes have overlapping function. These analyses would greatly expand the role of these genes in the emergence of endothelial cells during avascular mutant development.

Given the expression in anterior somite, *sox11b* expression modulation might be acting to disrupt some signaling between these tissues. However, there are several indications that *sox11b* functions cell-autonomously. Firstly, *sox11b* is a transcription factor, which means it functions within the nucleus of the cell in which it is expressed. The microarray analyses and accompanying validation were measuring gene expression within *Tg(kdrl:eGFP)*$^{+}$ cells. By utilizing

isochronic blastula cell transplantation, it could be determined if *sox11b* morpholino has any measurable effect on endothelial cell behavior in a wild-type host environment.

Since previous reports have indicated that *sox11* has a role in cell-cycle progression [1-3], the phenotype seen in morphants could be due to a delay in proliferation of endothelial cells and subsequent recovery in a microenvironment lacking the necessary migratory cues. Because of this concern, I would suggest performing phospho-histone H3 staining to see if fewer endothelial cells are undergoing mitosis, at the 24 hpf time point. Additionally, flow cytometry analyses of the GFP^+ cells with propidium iodide staining would help to quantify cell cycle phase in control versus *sox11b* morphants.

Two additional genes were validated as up-regulated by qRT-PCR in the *kdrl*$^+$ lineage in early avascular mutant embryos, *klf5l* and *zfhx4.* These genes have not been implicated in vascular development and have little or no characterized role in other tissues. I would suggest morpholino-mediated knockdown of these genes to answer two questions. Of course, knockdown could show whether these genes play a role in vascular development at any time point. More importantly, this analysis would address whether these three genes function in a *similar* manner and by extension, belong to a functional class of transcription factors.

Chapter 3

Key Points

1. The mesodermal lineage defaults to unspecified fate in avascular mutants.
2. Avascular mutant *kdrl*+ cells are largely derived from tailbud during somitogenesis
3. *pax9* is expressed in the vasculature.
4. *pax9* cell-autonomously regulates vascular patterning preferentially in avascular mutant embryos.

Conclusions

Chapter 3 highlights a unique mechanism for the emergence of the endothelial lineage in avascular mutants and further interrogates the role of *pax9* in avascular mutant endothelial patterning. It was shown that much of the presumptive mesoderm in these mutants is unable to specify as *kdrl*$^+$ and therefore contributes to another lineage that remains unscored.

We had previously noted that much of the *kdrl*$^+$ lineage in avascular mutants first arises in the caudal region of the tail, a location largely derived for tailbud mesoderm. Using later stage lineage tracing, we showed that much of the endothelium in this region is derived from tailbud and that mutants displayed a higher percentage of tailbud mesoderm-derived endothelium. This finding highlights a unique developmental source for avascular mutant endothelium and therefore unique mechanisms may be involved in the biology of these cells.

We subsequently identified *pax9* as being upregulated in avascular mutant endothelials cells by qRT-PCR. Originally described for its role in odontogenesis, *pax9* has never been described as playing a role in vascular patterning. We found that *pax9* does, in fact, regulate proper vascular patterning to a large extent in mutants. Since *pax9* knockdown in wild-type embryos showed very little phenotype, avascular mutants allowed for the first-ever description of the role of this transcription factor in vascular patterning.

Taken together, Chapter 3 represents a remarkable discovery made possible through the use of an attenuated model system. We have described a unique developmental source for avascular mutant endothelium and a novel transcription factor regulating the morphogenesis of vasculature in these mutants. Furthermore, the putative role for *pax9* in vascular development in humans was highlighted by the use of HUVEC cell culture.

Future Directions

The role of *pax9* in odontogenesis has been well established [4]. *pax9* mediates mesenchymal progenitor aggregration to form tooth primordia. Given that we found that the FGF inhibitor does significantly down-regulate *pax9* mRNA, it is tempting to speculate that a similar signaling pathway functions to aggregate mesenchymal precursors to endothelial cells. Therefore, I propose the generation of a *Tg(pax9:eGFP)* transgenic fish for the study of FGF-regulation of *pax9* [5]. This transgenic line could be used for at least three purposes. First, direct measurement of transcription output of the pax9 promoter

after inducible heat-shock of the *Tg(hsp70l:DNFGFR)* line as well as treatment with the FGF inhibitor, SU5402 would help strengthen the argument that FGF is important in avascular mutant vascular patterning. Secondly, time-lapse microscopy of this transgenic in conjunction with *Tg(kdrl:mCherry)* at early stages could elucidate the source of avascular mutant *kdrl*$^{+}$ cells: directly from tailbud cells or through a somitic intermediate. Lastly, time-lapse at later stages in wild-type and mutants, could help delineate the angiogenic mechanism(s) *pax9* is important to, such as tip versus stalk cell phenoype. Given that transplanted *pax9* morphant donor cells preferentially localize to the axial vasculature, not the secondary vessels, at 24 hpf, I have reson to hypothesize that GFP might be up-regulated in tip cells.

Furthermore, during odontogenesis, *pax9* is known to interact genetically with another inhibitory transcription factor, *msx1* [6]. In order to determine whether this interaction happens in endothelial cells, several experiments are detailed below. First, expression levels of *msx1* should be quantified in FACS-sorted cells in comparison to other genes to establish that *msx1* is in fact expressed in endothelial cells. However, our microarray data did not indicate a change in this gene. *In situ* hybridization patterns for *msx1* in zebrafish have been published [7, 8]; its potential expression in vasculature should be more closely examined as well. Intriguingly, *msx1* is expressed in tailbud [7] and in regenerating tail-fin tissue [9], but largely missing from post-segmetation mesodermal tissues. Nevertheless, knockdown of *msx1* by morpholino should produce a similar phenotype in avascular mutants, barring any early

developmental function. Humans with familial hypodontia, have been shown to have mutations in *pax9* or *msx1*, indicating that both genes are not necessary early development [4]. Lastly, a yeast two-hybrid screen could potentially identify other interacting proteins and endothelial specific expression libraries are available.

Conclusion

Taken together, the research contained within this thesis indicates several novel findings. First, the transgenic avascular mutant model proved to be an effective method for the discovery of novel angiogenic genes. Second, we have implicated two new genes, *sox11b* and *pax9*, in the development of the vasculature. Third, we have shown that the majority of the avascular mutant *kdrl*$^{+}$ cells are derived from tailbud mesoderm. Fourth, we have shown that in the absence of *clo* or *etv2* presumptive angioblasts default to an unspecified fate. Overall, avascular mutant *kdrl*$^{+}$ cells have a unique transcriptional profile.

REFERENCES

1. Y.H. Chen, et al.: **Nuclear expression of sox11 is highly associated with mantle cell lymphoma but is independent of t(11;14)(q13;q32) in non-mantle cell B-cell neoplasms**. *Mod Pathol* 2010,. **23**(1):105-12.

2. W. Xu, and J.Y. Li: **SOX11 expression in mantle cell lymphoma.** *Leuk Lymphoma,* 2010. **51**(11):1962-7.

3. B.L. Larson, et al.: **Sox11 is expressed in early progenitor human multipotent stromal cells and decreases with extensive expansion of the cells**. *Tissue Eng Part A* 2010, **16**(11):3385-94.

4. M. Goldenberg, et al.: **Clinical, radiographic, and genetic evaluation of a novel form of autosomal-dominant oligodontia**. *J Dent Res* 2000, **79**(7):1469-75.

5. A. Neubuser, et al.: **Antagonistic interactions between FGF and BMP signaling pathways: a mechanism for positioning the sites of tooth formation**. *Cell* 1997, **90**(2): 247-55.

6. A.R. Vieira, et al.: **MSX1, PAX9, and TGFA contribute to tooth agenesis in humans**. *J Dent Res*, 2004. **83**(9):723-7.

7. B. Thisse, S. Pflumio, M. Fürthauer, B. Loppin, V. Heyer, A. Degrave, R. Woehl, A. Lux, T. Steffan, X.Q. Charbonnier and C. Thisse: **Expression of the zebrafish genome during embryogenesis**. *ZFIN Direct Data Submission* 2001, (http://zfin.org).

8. T. Kudoh, et al., **A gene expression screen in zebrafish embryogenesis**. *Genome Res*, 2001. **11**(12):1979-87.

9. N. Yoshinari, et al., **Gene expression and functional analysis of zebrafish larval fin fold regeneration**. *Dev Biol*, 2009. **325**(1): p. 71-81.

CHAPTER 5

Visualizing Vascular Networks in Zebrafish: An Introduction to Microangiography

Summary

Visualizing the circulatory pattern in developing embryos becomes an essential technique for the field of cardiovascular biology. In the zebrafish model system, there are currently several techniques available to visualize the circulatory pattern. Microangiography is a simple technique in which a fluorescent dye is injected directly into the Sinus Venosus and/or the Posterior Cardinal Vein, allowing for the rapid labeling and easy detection of patent vessels. Here, we compare microangiography to other vascular labeling techniques, describe the benefits and potential applications of microangiography, and give step by step instructions for microangiography.

Introduction.

The advent of transgenic animals has provided a unique opportunity to expand our current knowledge of vascular development using diverse vertebrate model systems. In the majority of cases, however, the use of transgenic animals is not well situated for assessing the function of vasculature. In zebrafish, multiple transgenic lines which express a specific fluorescent protein under an endothelial-specific promoter have been generated [1,7-12]. However, since the majority of

transgenic animals express the molecular tag in all endothelial cells, it is extremely difficult to rely on transgenic animals to examine whether a specific vessel is used for circulation. Analyzing circulating red blood cells using high power bright-field or video microscopes is adequate to obtain such information, but requires significant time and effort [13]. Microangiography can offer a simple yet sophisticated alternativeto visual observation under high power bright-field microscopes. By labeling all patent vessels used for circulation, microangiography significantly reduces the time required for the observation of the circulatory pattern [1]. Furthermore, in combination with various transgenic animals that express fluorescent proteins in a tissue-specific manner, one can carry out more sophisticated analyses of the vascular system by using microangiography.

Application of Microangiography.

Microangiography may be used in any scenario where the vascular system needs to be visualized. For instance, microangiography can be used to determine the patency of developing vessels [1,14]. In addition, it can be readily used to assess the vascular integrity since any vascular leakage leading to extravasation of plasma will be labeled with injected dye [15,16]. Since microangiography can be used at any developmental period, this technique can be combined with morpholino-injected, chemical-treated, or even surgically altered embryos, in addition to various mutant embryos [17,18]. Once injected into the blood stream, dye can stay within the vasculature for a few days. Therefore, microangiography can either precede or follow these treatments. However, because the injected dye is passively spread within the vascular lumen, microangiography will

not always reveal dynamic morphology of endothelial cells such as filopodial extensions in the migrating tip cell. In addition, microangiography is not an efficient technique to use in mutants without blood flow [19]. Even with the limitations, microangiography is an extremely useful technique to rapidly visualize patent vessels.

Microangiography: General Considerations and Experimental Design

When attempting an experiment using microangiography, it is useful to keep in mind that a number of factors will determine the experimental outcomes. We have enumerated the most important factors to consider before the experimental design.

1. **Developmental Stage of Embryos.** Dye can be injected into Sinus Venosus (SV) and/or Posterior Cardinal Vein (PCV) (**Fig. 1**). Depending on the age of the embryo, the method of injection will vary slightly. For the best results, we recommend trying both sites first and determine whether SV or PCV yields better outcomes.

2. **Condition of the Embryos.** Microangiography can be combined with various experimental procedures as aforementioned. However, if microangiography is performed in embryos that are previously treated with small chemicals or morpholino, any developmental delay or morphological abnormality that might potentially impede microangiography should be carefully examined.

3. **Intended Method of Observation**. Embryos that are injected with dye can be analyzed by various methods. If the injected embryos will be analyzed after fixation, sufficient time must be allowed for the dye to completely perfuse the entire vascular system. This can be monitored on a fluorescent microscope. Alternatively, if the embryos are to be observed in vivo, attention should be paid to minimize any interference to the cardiac function.

MATERIALS.

1. **Microinjector**. A microinjector is used to perfuse the vascular system of the embryos with a defined amount of dye. Based on the mechanism used to deliver the dye into the embryos, there are two main types of microinjectors widely used for the microinjection. Hydraulic microinjectors, such as the Nanoject (from Drummond Scientific) require oil to fill the injection needle. Pneumatic microinjectors, such as Picospritzer (from Parker) or Femtojet (from Eppendorf) use compressed air, rather than oil, to push out dye into the embryos.

2. **Micromanipulator**. Although one can hold the injection needle with hand, using a micromanipulator to modulate the microinjector provides better control of the delivery of dye. Normally, the micromanipulator can be mounted onto a stand, which allows the microinjector to approach the embryos at a 45° angle. Some stand-alone systems (i.e., Femtojet) do not need an external micromanipulator.

3. **Needle Puller**. The shape of needle is one of the most critical factors that affect the outcome of the microangiography. Traditionally, the needle puller makes the injection needle by heating the glass capillary tube with the Tungsten fi lament and pulling with a defined force. The parameters that determine the force that applies to the heated needle needs to be empirically determined. The new lines of needle pullers, however, use a CO_2 laser to heat up the glass capillary, providing more precise control.

4. **Injection Molds**. There are several prefabricated plastic molds available, which can create a series of grooves in which the embryos settle if placed on top of melted agarose. These molds allow the injection to large quantity of embryos quickly. Alternatively, by gluing capillary tubes or slide glass to the bottom of a Petri dish and pouring the agarose on top of the tubes, a homemade injection mold can be made. Both work equally well and are reusable (Fig. 1).

Solutions and Dyes.

1. Embryo Medium: 1.0 mL Hank's Stock #1 (8.0 g NaCl, 0.4 g KCl in 100 mL H_2O),0.1 mL Hank's Stock #2 (0.358 g Na_2HPO_4 Anhydrous, 0.60 g KH_2PO_4 in 100 mL H_2O), 1.0 mL Hank's Stock #4 (0.72 g $CaCl_2$ in 50 mL H2O), 1.0 mL Hank's Stock #5 (1.23 g $MgSO_4 \times 7H_2O$ in 50 mL H_2O), 1.0 mL fresh Hank's Stock #6 (0.35 g $NaHCO_3$ in 10 mL H_2O), and 95.9 mL double distilled water. Alternatively, use 1.5 mL stock salts (i.e., Instant Ocean) added to 1 L distilled water to achieve 60 µg/mL final concentration.

2. HEPES: 10 mM HEPES, pH 7.6 is added to the injection mix (5 mM final concentration). HEPES will buffer the injection mix to physiological pH.

3. Dye: Dextran-conjugated fluorophores are easy to use and effective. Alternatively, fluorescent microspheres such as Quantum dot can be used. Based on the fluorophores, these dyes have a wide range of excitation and emission spectra, allowing the user more flexibility.

Method.

1. Use a pair of forceps to remove the chorion. Alternatively, a short pulse of Pronase treatment can be used to dechorionate large numbers of embryos [20]. Removal of the chorion will allow for more efficient penetration of the injection needle into embryos.

2. Prepare the injection mold by adding 3% methylcellulose onto the petri dish. Methylcellulose immobilizes the embryos within the well and allows for easy repositioning, while the well itself acts as a backstop (**Fig. 1**).

3. Place embryos into wells using a glass Pasteur pipette. Avoid adding excessive embryo medium while transferring the embryos since this will dilute the Tricaine.

4. Add a layer of 40 μL/mL Tricaine in embryo media on top of the 3% methylcellulose. The most critical aspect of zebrafish cardinal vein dye injection is the concentration of Tricaine. Soaking the embryos in a solution of 40 μL/mL Tricaine in embryo medium will allow for the immobilization of the embryo without immediately stopping the heart.

5. Prepare the microinjector. A standard microcapillary tube pulled and cut to 5–10 nm is sufficient for this method. Additional grinding or sharpening of the needles is not necessary. The injection needle should be filled with dye mix. Turn

and dial the micromanipulator such that the needle is close to the first embryo (**Fig. 2**).

6. For 24–72 hpf embryos, inject the dye to the PCV plexus. For older embryos, one can inject directly into the SV, through the pericardium. We normally inject 4.6 nL of dye mixture into 24 hpf embryos. Injecting both areas on the same embryo will ensure rapid perfusion of the dye (see Note 1). By gently moving the needle in a circular motion, one can “drill” through external tissues that may be difficult to penetrate (see Note 2). If embryos will not be immediately imaged, after injecting ~20 embryos, draw them up using a glass Pasteur pipette and put them into fresh media. If the heart stops, dye will typically take longer to disseminate, thus, washing out the anesthetic with embryo media can speed perfusion. Zebrafish embryos are typically reared at 28.5°C, but we find that recovery and imaging work well, if not better, at room temperature.

7. For imaging the result of microangiography, wait at least 10 min for perfusion to complete. We often inject on a brightfield microscope (see Note 3), but injections may be performed on a fluorescence microscope to determine immediately if the dye has been perfused (see Notes 4 and 5).

8. Alternatively, embryos can be fixed for later observation since Dextran-conjugated probes can be fixed. After injection and perfusion, embryos are washed once with PBS and put into 1 mL of 4% PFA in PBS and incubated overnight at 4°C. Once fixed, embryos can be stored in methanol at for −20°C for several weeks. Either sectioned or whole embryos can be analyzed by confocal microscopy after fixation (see Note 6) (Fig. 3).

9. Concluding Remarks.

Microangiography is a relatively simple, yet powerful technique to visualize patent vessels. It also provides a powerful way to analyze vascular development and maintenance in combination with the increasing number of available transgenic lines. For instance, using endothelial specific transgenic lines, one can easily distinguish lumenized vessels within the developing vascular network. Furthermore, in combination with transgenic lines that label adjacent tissue, one can analyze the functional relationship between the vascular network and neighboring tissues. In addition, microangiography can be extremely useful to detect the subtle changes of the circulatory pattern since it can rapidly visualize the patent vessels. By selectively labeling those vessels used for circulation, microangiography can provide information on the functionality of specific vessels, which cannot be achieved by analyzing endothelial specific transgenic lines. With the advent of chemical biology and powerful imaging techniques, the potential application of microangiography is ever increasing.

Notes.

1. Embryos may be injected at multiple sites to ensure rapid perfusion of dye.

2. Embryos may also be injected in the Common Cardinal Vein which is located below the Sinus Venosus before 4 days post-fertilization.

3. Dextran-conjugated dyes, particularly Rhodamine, can be detected using the bright-field scope. Therefore, it is possible to monitor the perfusion effi cacy immediately after the dye injection.

4. We have observed that embryos may survive a significant and acute puncture wound. Take the time to empirically determine how much trauma the embryos can withstand.

5. Similarly, determine the proper needle diameter: thinner takes less force to penetrate tissues but may flex too much with mature tissues while thicker needles create more trauma.

6. Any unused Dextran-conjugated dye may be frozen at −20°C and reused for longer than 6 months.

FIGURES:

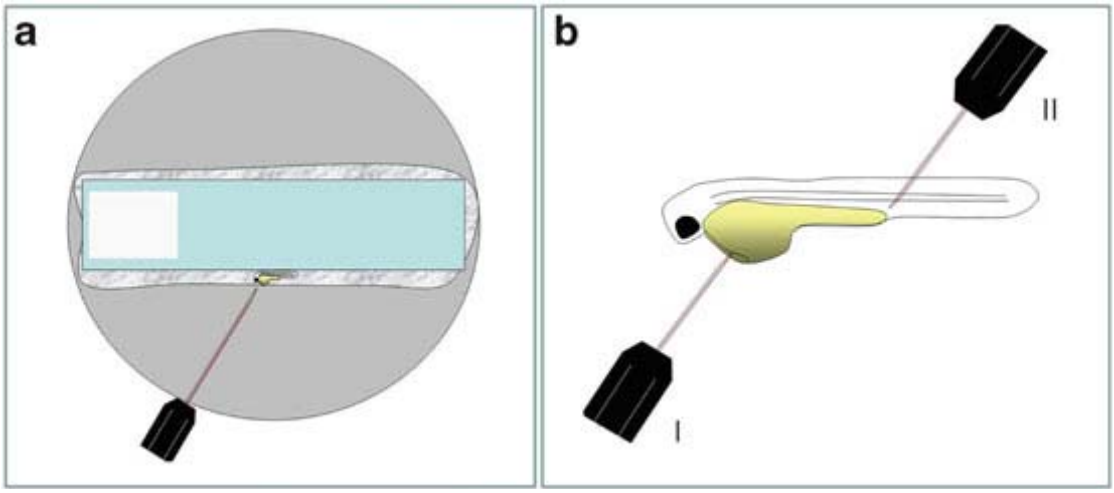

Figure 5.1: Schematic drawings of microangiography.

(a) An anesthetized embryo will be lined up against slide glass within the petri dish. (b) Dye can be injected into either the sinus venosus (I) or the posterior cardinal vein (PCV) of the embryo.

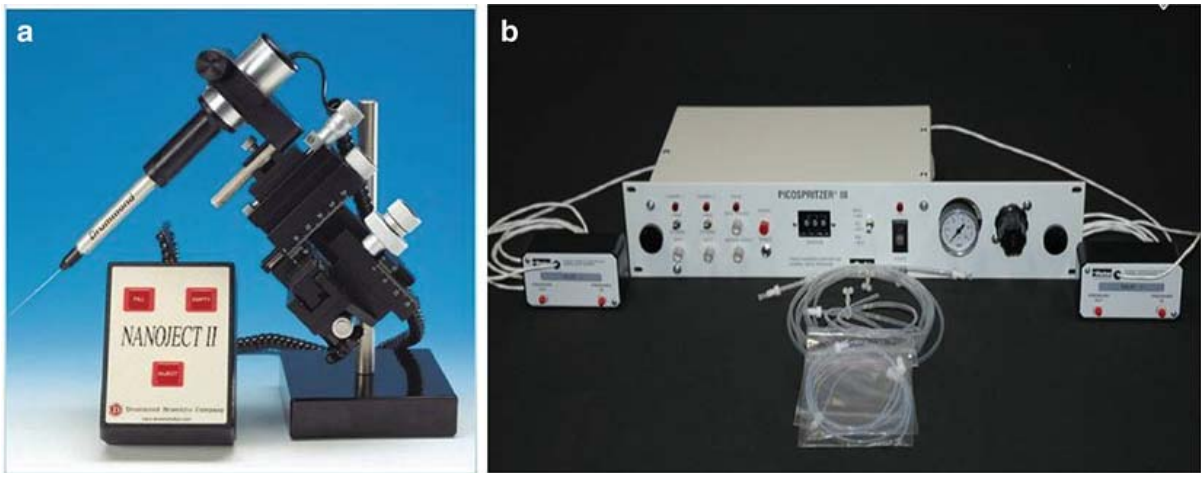

Figure 5.2: Commonly used microinjectors for microangiography.

Both hydraulic and pneumatic microinjectors can be used to deliver dye into the embryos to visualize vascular network. An example of a hydraulic microinjector (a) and a pneumatic microinjector (b) are shown.

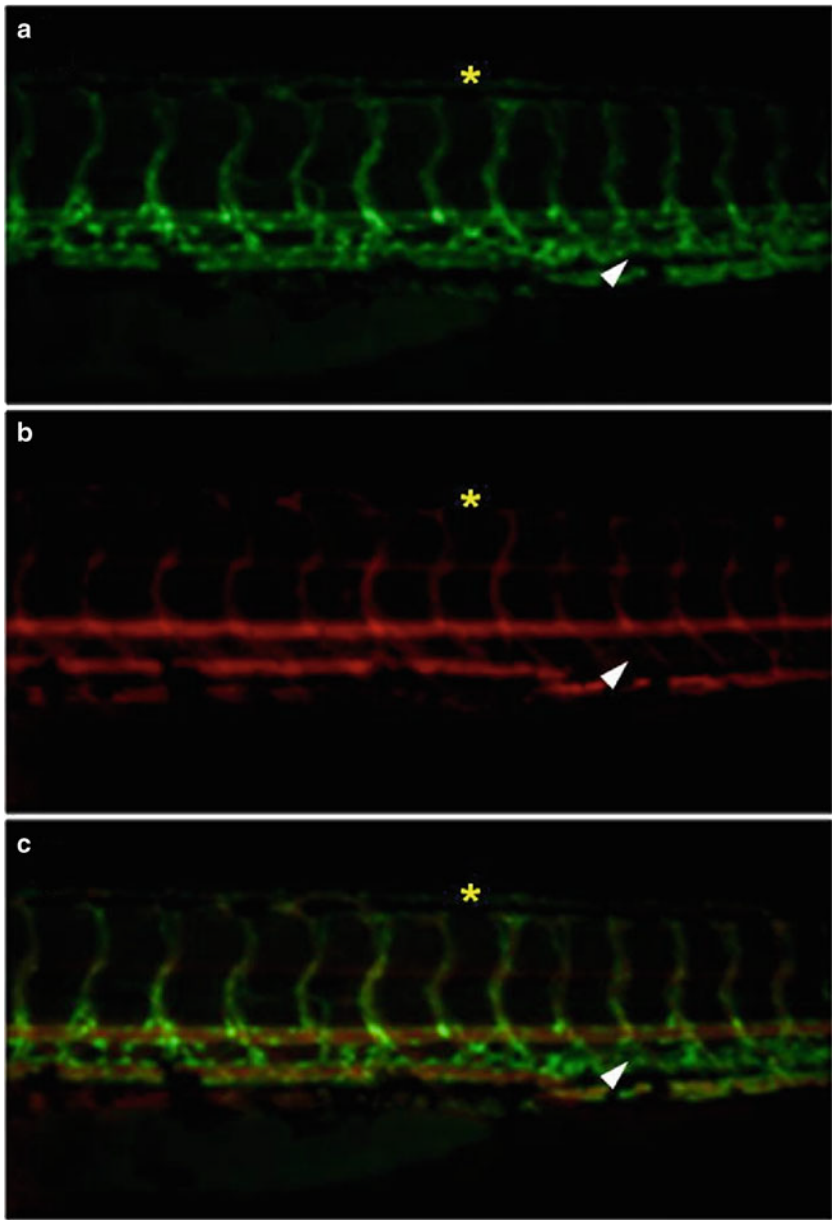

Fig. 5.3. An exemplary result of microangiography.

The trunk region of a 60 hpf embryo after the microangiography. (**a**) All the vascular network is visualized by *Tg*(*kdrl*:*EGFP*), which expresses EGFP under an endothelial specific promoter, *kdrl*. (**b**) Microangiography of the same embryo. (**c**) Merged image. Notice microangiography is only visualizing vessels actively used for circulation. For instance, the dorsal vein (*white arrowhead*) which constricts and shrinks to become the hematopoietic niche, or the dorsal longitudinal anastomotic vessel (*yellow asterisk*) which is not patent yet are not labeled with microangiography.

REFERENCES

1. S. Isogai, M. Horiguchi and B. M. Weinstein: **The vascular anatomy of the developing zebrafish: an atlas of embryonic and early larval development**, *Dev Biol* 2001, **230**:278–301.

2. N. D. Lawson and B. M. Weinstein: **Arteries and veins: making a difference with zebrafish**, *Nat Rev Genet* 2002, **3**:674–682.

3. R. K. Lee, D. Y. Stainier, B. M. Weinstein and M. C. Fishman: **Cardiovascular development in the zebrafish Endocardial progenitors are sequestered within the heartfield**, *Development* 1994, **120**:3361–3366.

4. D. Y. Stainier, B. Fouquet, J. N. Chen, K. S. Warren, B. M. Weinstein, S. E. Meiler, M. A. Mohideen, S. C. Neuhauss, L. Solnica-Krezel, A. F. Schier, F. Zwartkruis, D. L. Stemple, J. Malicki, W. Driever, and M. C. Fishman: **Mutations affecting themformation and function of the cardiovascular system in the zebrafish embryo**, *Development* 1996, **123**:285–292.

5. M. R. Swift and B. M. Weinstein: **Arterial-venous specifi cation during development**, *Circ Res* 2009, **104**:576–588.

6. D. Y. Stainier, R. K. Lee and M. C. Fishman:**Cardiovascular development in the zebrafish Myocardial fate map and heart tube formation**, *Development* 1993, **119**:31–40.

7. N. C. Chi, R. M. Shaw, B. Jungblut, J. Huisken, T. Ferrer, R. Arnaout, I. Scott, D. Beis, T. Xiao, H. Baier, L. Y. Jan, M. Tristani-Firouzi and D. Y. Stainier: **Genetic and physiologic dissection of the vertebrate cardiac conduction system**, *PLoS Biol* 2008, **6**:e109.

8. J. Choi, L. Dong, J. Ahn, D. Dao, M. Hammerschmidt and J. N. Chen: **FoxH1 negatively modulates flk1 gene expressionand vascular formation in zebrafish***, Dev Biol* 2007, **304**:735–744.

9. S. W. Jin, D. Beis, T. Mitchell, J. N. Chen and D. Y. Stainier: **Cellular and molecular analyses of vascular tube and lumen formation in zebrafish**, *Development* 2005, **132**:5199–5209.

10. N. D. Lawson and B. M. Weinstein: **In vivo imaging of embryonic vascular development using transgenic zebrafi sh**, *Dev Biol* 2002, **248**:307–318.

11. T. Motoike, S. Loughna, E. Perens, B. L. Roman, W. Liao, T. C. Chau, C. D. Richardson, T. Kawate, J. Kuno, B. M. Weinstein, D. Y. Stainier and T. N.

Sato: **Universal GFP reporter for the study of vascular development**, *Genesis* 2000, **28**:75–81.

12. B. L. Roman, V. N. Pham, N. D. Lawson, M. Kulik, S. Childs, A. C. Lekven, D. M. Garrity, R. T. Moon, M. C. Fishman, R. J. Lechleider, and B. M. Weinstein: **Disruption of acvrl1 increases endothelial cell number in zebrafish cranial vessels**, *Development* 2002, **129**:3009–3019.

13. T. Schwerte, D. Uberbacher and B. Pelster: **Non-invasive imaging of blood cell concentration and blood distribution in zebrafish Danio rerio incubated in hypoxic conditions in vivo**, *J Exp Biol* 2003, **206**:1299–1307.

14. M. Kamei, W. B. Saunders, K. J. Bayless, L. Dye, G. E. Davis and B. M. Weinstein: **Endothelial tubes assemble from intracellular vacuoles in vivo**, *Nature* 2006, **442:**453–456.

15. D. A. Buchner, F. Su, J. S. Yamaoka, M. Kamei, J. A. Shavit, L. K. Barthel, B. McGee, J. D. Amigo, S. Kim, A. W. Hanosh, P. Jagadeeswaran, D. Goldman, N. D. Lawson, P. A. Raymond, B. M. Weinstein, D. Ginsburg and S. E. Lyons: **pak2a mutations cause cerebral hemorrhage in redhead zebrafish**, *Proc Natl Acad Sci U S A* 2007, **104**:13996–14001.

16. J. Liu, S. D. Fraser, P. W. Faloon, E. L. Rollins, J. Vom Berg, O. Starovic-Subota, A. L. Laliberte, J. N. Chen, F. C. Serluca and S. J. Childs: **A betaPix Pak2a signaling pathway regulates cerebral vascular stability in zebrafish**, *Proc Natl Acad Sci U S A* 2007, **104**:13990–13995.

17. B. M. Hogan, F. L. Bos, J. Bussmann, M. Witte, N. C. Chi, H. J. Duckers, and S. Schulte-Merker: **Ccbe1 is required for embryonic lymphangiogenesis and venous sprouting**, *Nat Genet* 2009, **41**:396–398.

18. S. Nicoli, C. Standley, P. Walker, A. Hurlstone, K. E. Fogarty and N. D. Lawson: **MicroRNA-mediated integration of haemodynamics and Vegf signalling during angiogenesis**, *Nature* 2010, **464**:1196–1200.

19. T. P. Zhong, M. Rosenberg, M. A. Mohideen, B. Weinstein and M. C. Fishman: **gridlock, an HLH gene required for assembly of the aorta in zebrafish**, *Science* 2000, **287**:1820–1824.

20. M. Westerfield: **The zebrafish book, A Guide for the laboratory use of zebrafish (Danio rerio)**, (2000) **4th Ed**. University of Oregon.

CHAPTER 6

LRP1-Dependent Endocytic Mechanism Governs the Signaling Output of the Bmp System in Endothelial Cells and in Angiogenesis

Summary

Previous studies have identified the Bmp signaling pathway as a major modulator of venous angiogenesis. There is a multitude of well-characterized activators, inhibitors, and modulators of the BMP signaling pathway. One such molecule is Bmper, which, depending on context, can act as both an inhibitor and an activator. Using biochemical methods it was shown that Bmper functionally interacts with the LDL receptor-related protein 1, LRP1. Here we have shown that LRP1 gene function is necessary for proper vascular development, particularly those processes that are mediated by Bmp signaling. Using zebrafish transplantation, I showed that knockdown of LRP1 in donor cells excluded them from the venous vascular front during cardinal vein plexus development.

Introduction

Bone morphogenetic proteins (Bmps) are essential for embryonic vascular development, as illustrated by many severe, inherited vascular diseases associated with disrupted Bmp signaling [1]. One facet of regulation of Bmp signaling is provided by extracellular molecules that “fine-tune” Bmp signaling by modulating (usually inhibiting) Bmp’s interaction with surface receptors and subsequent downstream signaling events

[2]. Of these extracellular modulators of Bmp signaling, Bmper (Bmp-binding endothelial cell precursor derived regulator, the vertebrate ortholog for crossveinless-2 in *Drosophila*) is a critical determinant of endothelial functions such as differentiation, migration, and angiogenesis [3–6]. Bmper can both promote and inhibit Bmp activity [6,7], confounding the development of a working model to explain how Bmper impacts Bmp signaling. However, we recently found that Bmper modulates Bmp4 activity via a concentration dependent, endocytic trap-and–sink mechanism, with low levels of Bmper promoting and high levels inhibiting Bmp4 signaling, thereby accounting for the biphasic nature of Bmper's regulation of Bmp4 activity [7]. Our previous data suggested that endocytosis of the Bmper/Bmp4 complex may be critical in determining the inhibitory effect of Bmper on Bmp4 function. However, gaps remained in understanding how activation and inhibition of Bmp4 signaling by Bmper were coupled and the mechanism by which the Bmper/Bmp4 complex was endocytosed.

Here we report that LRP1 (LDL receptor-related protein 1) is a novel endocytic receptor for Bmper and a coreceptor of Bmp4 that is essential for mediating Bmp4 signaling. A requisite role for LRP1 in zebrafish angiogenesis is observed in that knockdown of *lrp1* decreases Smad1/5/8 activity and abnormal cardiovascular development. Together, these data demonstrate that LRP1 regulates Bmp4-mediated endothelial function and vascular development in vivo and is therefore a bone fide component of the Bmp signaling pathway.

Methods

Generation of Cell Lines

For stable mouse endothelial cell (MEC) cell line construction, MECs were transduced with *LRP1* or control shRNA lentiviral particles, and positive colonies were screened with puromycin and evaluated by Western blot analysis.

Chemical Cross-Linking in Intact Cells, Immunoblotting, Immunoprecipitation, and Ligand Blotting

Bmper-treated MECs were crosslinked with dithiobis(succinimidylproprionate) for immunoprecipitation and matrix-assisted laser desorption/ionization-time of flight analysis. Immunoblotting, immunoprecipitation, and ligand blotting were performed following our previous protocols [7, 8].

Fluorescence Energy Transfer Experiments

Experiments were performed following a previously published protocol [9]. Donor, acceptor, and fluorescence energy transfer images were acquired sequentially using fixed excitation and emission filters, and image processing was performed.

In Vitro Matrigel Tubulogenesis Assay

Endothelial cell tube formation was analyzed with the Matrigelbased tube formation assay [10].

Morpholino Injections and Zebrafish Analysis

Morpholino oligonucleotides (MOs) were produced by Gene Tools (Philomath, OR). All MOs were injected into 1 to 4 cell stage embryos as previously described. 11 Zebrafish (*Danio rerio*) vascular development was analyzed following previously published methods [12]. Please see the expanded Methods section, available in the

online-only Data Supplement for details regarding reagents, cell culture, immunoblotting, ligand blotting, immunofluorescence, and statistical analysis.

Transplantation Assay

Tg(kdrl:eGFP)^{S843} embryos were injected with either control or LRP1 morpholino/tracking dye mix at the one cell stage and allowed to develop to between sphere and germ ring stage. Donors and recipients were manually dechorionated at the 16 cell stage and allowed to develop in 30% Danieau solution at 28.5°C. Transplantations were performed under 40 to 60X magnification using a Hamilton syringe with a micrometer drive and micromanipulator in a standard petri dish containing a bed of 3% agarose in 30% Danieau with 150 individual embryo wells (Mold available from Adaptive Science Tools) at room temperature Donor cells were targeted to the presumptive mesendoderm at the ventral margin. Embryos were allowed to recover for one hour post-transplantation at room temperature and then washed three times with 10% Danieau solution and placed at 28.5'C. Representative images were taken using the whole mount immunohistochemistry. Briefly, chick anti-GFP primary antibody from Abcam and donkey anti-chick-488 secondary from Jackson Immunoresearch were used to boost GFP signal after storing embryos in methanol.

Results

LRP1 Associates With Bmper in MECs

Previously we demonstrated that endocytosis of the Bmper/Bmp4 complex is critical for Bmper-mediated Bmp4 signaling [7]. However, the mechanism governing this endocytosis remained unclear. Hypothesizing that Bmper may interact with a

partner to achieve endocytosis, we used matrix-assisted laser desorption/ionization-time of flight mass spectrometry as an inductive unbiased method of identifying Bmper-associated proteins in MECs. LRP1, a well-defined endocytic receptor, associated with Bmper in MECs (Figure 6.1A; Online Figure 6.7A). Confocal imaging of Bmper-treated MECs revealed that Bmper and LRP1 colocalize on the plasma membrane and in intracellular vesicles (Figure 6.1B). Immunoprecipitating for LRP1 and immunoblotting for Bmper (or the reverse, or Bmper ELISA) demonstrated that full-length Bmper associates with LRP1 in MEC lysates (Figure 6.1C, 6.7B and 6.7C), confirming our matrix-assisted laser desorption/ionization-time of flight and immunofluorescence data. Notably, this association was not affected by the addition of Bmps (Figure 6.7D and 6.7E). Because Bmp4 may bind Bmper through its amino-terminal domain [7,13], its inability to disrupt the LRP1/Bmper association suggested that LRP1 may bind a different domain of Bmper and carboxyl-terminal domain (CTD) fragments of Bmper associated with LRP1 (Figure 6.1C, 6.7D), indicating that Bmper may form a ternary complex with LRP1 and Bmp4 through respective associations with its CTD and amino-terminal domain. Consistent with this hypothesis, lysates of Bmp4-treated MECs immunoprecipitated with an anti-LRP1 antibody revealed the presence of LRP1/Bmp4 heterocomplexes (Online Figure 6.7F).

Like other members of the LDL receptor family, LRP1 is a heterodimer composed of a 515-kDa α chain possessing 4 extracellular ligand binding domains (LBDs) and an 85-kDa membrane-anchored β chain [14]. Ligand blotting analysis with full-length LRP1 revealed that Bmper associates with both the α and β chains of LRP1 (Figure 6.1D). To determine which LBD of LRP1 is required for binding to Bmper, cells were transfected

with membrane-containing mini-LRP1 receptors (mLRP1-415; Figure 6.1E, left panel) and analyzed via ligand blotting. LBDIII/IV exhibited the strongest association with Bmper, whereas LBDII had only a weak association and LBDI did not associate with Bmper at all (Figure 6.1E, right top panel), consistent with what is found with other LRP1 ligands such as RAP1 [15]. However, Bmper also binds to the β chain of LRP1, making Bmper unique among other known LRP1 ligands. The significance of Bmper binding to LRP1's β chain remains unknown; however, internalized CTD fragments of Bmper may bind LRP1 and modulate its association with scaffold proteins that participate in LRP1-dependent signaling mechanisms [16]. Together, these data identify that LRP1, a recognized endocytic receptor, associates with Bmper in MECs and therefore could be responsible for endocytosis of Bmper/Bmp4 complexes.

LRP1 Is Required for Physiological Bmper Internalization

Previously, we found that Bmper undergoes endocytosis via an unknown mechanism that modulates downstream Bmp4 signaling [7]. Given our observation of a direct interaction between Bmper and the endocytic receptor-LRP1, we hypothesized that LRP1 may act as an endocytic receptor for Bmper and examined cell lysates from LRP1-knockdown (or control) MECs treated with Bmper. The level of internalized Bmper in control MECs increased over time, peaking at 60 minutes and subsequently decreased, probably due to degradative processing, as previously demonstrated7 (Figure 6.2A and 6.2B). LRP1-knockdown MECs also demonstrated a time-dependent increase in Bmper internalization; however, internalization was substantially less than in control MECs (Figure 6.2B). When cells were treated with increasing doses of Bmper, the presence of cytoplasmic Bmper in control MECs increased, an effect that was

significantly decreased in LRP1-knockdown cells (Figure 6.2C and 6.2D). Similar results were observed in mouse embryonic fibroblasts (Figure 6.8A– 6.8D). These data suggest that the majority, but not all, of Bmper is via an LRP1-dependent mechanism and we further explored the role that LRP1 plays in Bmper/Bmp4 endocytosis.

We used confocal microscopy to investigate whether LRP1 is involved in the previously reported internalization and transport of Bmper to endosomes [7]. Following Bmper internalization, both LRP1 and Bmper were detected in a subset of vesicles expressing EEA-1 and Rab-7 (endosome markers; Figure 6.8E and 6.8F). LRP1-knockdown MECs contained far fewer Bmper-containing EEA-1 and Rab-7 positive endosomal vesicles compared to control MECs (Figure 6.2E). Similar results were found in LRP1 null mouse embryonic fibroblasts (Figure 6.8G). Further subcellular fractionation experiments confirmed this localization (Figure 6.8H). These data collectively indicate that LRP1 influences the endosomal localization of Bmper and acts as an endocytic receptor for Bmper. We have previously shown that Bmper is internalized in a complex together with Bmp4 and Bmp receptors and that endocytosis of this holocomplex is critical for modulating Bmp4 signaling [7]. Therefore, we next investigated whether the interaction between LRP1 and Bmp receptors could influence Bmp4-dependent Smad1/5/8 signaling in endothelial cells.

LRP1 Is Associated With Bmp Receptor Type IB/Activin-Like Kinase Receptor 6

LRP1 functions as a coreceptor for ligands such as transforming growth factor-β and NMDA [17,18]. Given our data demonstrating that LRP1 is an endocytic receptor for Bmper, we hypothesized that LRP1 may act as a coreceptor of Bmp receptors.

There are multiple Bmps (Bmp2, 4, and 6) and Bmp type I receptors (activin-like kinase receptor [ALK]1, 2, 3, and 6) in MECs and specific siRNA knockdown of ALK2, 3, and 6 (but not ALK1) inhibited Bmp4-induced Smad1/5/8 phosphorylation (Figure 6.8IA–IIIC). Given that our previous data identified ALK6 as a Bmp4 type I receptor that mediates Bmp-dependent endothelial migration and angiogenesis [10], we used ALK6 as a representative Bmp type I receptor in the following experiments. Fluorescence energy transfer imaging analysis demonstrated the close proximity of cyan fluorescent protein-tagged ALK6 (Figure 6.3A) and yellow fluorescent protein-tagged mLRP2 in cytoplasmic vesicles and plasma membranes of transfected cells (Figure 6.3B), indicating that LRP1 and ALK6 could physically interact in cells. Coimmunoprecipitation of lysates from cells transfected with a wild-type ALK6 plasmid (ALK6-WT; Figure 6.3A) and each mLRP construct (Figure 6.1E) confirmed this association (Figure 6.3C). Additionally, when cells were transfected with a LRP1β construct (Figure 6.3A), the LRP1 and ALK6 association persisted (Figure 6.3D), indicating that this association likely occurs through the LRP1β chain. Because Bmper could bind to this region of LRP1 (Figure 6.1D), this interesting observation suggests that both Bmper and Bmps influence LRP1 signaling, thereby initiating cross-talk between the LRP1 and Bmp signaling pathways.

To determine the domains of ALK6 involved in the interaction with LRP1, ALK6 deletion mutants were constructed (Figure 6.3A). Both ALK6-CTD and ALK6-protein kinase domain coimmunoprecipitated with mLRP2, indicating that the cytoplasmic region of ALK6 is required for the association of ALK6 with mLRP2 (Figure 6.3E). However, the association of mLRP2 with ALK6-CTD and protein kinase domain was decreased in comparison to mLRP2 binding to ALK6-WT, suggesting that CTD of ALK6

is required but not sufficient for the association with mLRP2. Similar results were observed with the interaction of ALK6 and mLRP4 (Figure 6.8ID). Collectively, we conclude that the intracellular domains and possible membrane region of ALK6 are required for the association with LRP1. Because the protein kinase domain of ALK6 is critical for downstream Bmp-mediated Smad1/5/8 phosphorylation [19], next we tested whether the ALK6 and LRP1 interaction was involved in Bmp4-regulated Smad1/5/8 signaling induced by Bmper.

Endocytosis of the Bmper/Bmp4 Complex Is Required for Both Stimulatory and Inhibitory Regulation of Bmp4 Signaling by Bmper

We previously demonstrated that endocytosis of the Bmper/Bmp4 complex is required for the inhibitory effect of Bmper on Bmp4 signaling [7], but whether endocytosis of the Bmper/Bmp4 complex is also required more generally for Bmper-dependent Bmp4 signaling regulation remained unclear. Therefore, we used 3 endocytosis inhibitors—chlorpromazine, chloroquine (CQ), and bafilomycin A1—in MECs and evaluated the subsequent effect on Bmp4-dependent phosphorylation of Smad1/5/8. Treatment of MECs with Bmp4 alone or in the presence of substoichiometric concentrations of Bmper increased Smad1/5/8 phosphorylation (Figure 6.4A, lanes 2, 4, 12, and 14; Figure 6.10A), consistent with our previous observations that substoichiometric ratios of Bmper to Bmp4 enhances Bmper-dependent Bmp4 signaling [7]. However, when cells were pretreated with chlorpromazine to prevent clathrin-mediated endocytosis, the level of Smad1/5/8 phosphorylation induced by either Bmp4 alone or Bmp4 plus Bmper in substoichiometric concentrations was substantially decreased (Figure 6.4A, lanes 7 and

9; Figure 6.10B), indicating that Bmper-mediated enhancement of Bmp4 signaling requires endocytosis of the Bmper/Bmp4 complex. Next we investigated whether Rab4-mediated rapid recycling is required for Bmper's promoting effect on Smad1/5/8 phosphorylation. Rab4 siRNA knockdown resulted in a significant decrease in Smad1/5/8 phosphorylation induced by Bmp4 alone or Bmp4 plus Bmper in substoichiometric concentrations (Figure 6.4B, Figure 6.10C). This suggests that the Rab4-mediated rapid recycling route is required for both Bmp4 activity and the promoting effect of Bmper at stoichiometric concentrations. This observation, combined with our previous data demonstrating that endocytosis is also necessary for the inhibition of Bmp4 signaling caused by suprastoichiometric concentrations of Bmper in the Bmper/Bmp4 complex [7], indicates that endocytosis is required for all aspects of Bmper-mediated regulation of Bmp4 signaling.

We next examined the effect that CQ and bafilomycin A1 had on Bmper-mediated Bmp4 signaling. Treatment of cells with CQ did not affect the ability of Bmp4 alone or Bmp4 plus Bmper in substoichiometric concentrations to induce Bmp4-mediated Smad1/5/8 phosphorylation (Figure 6.4A, lanes 17 and 19; Figure 6.10D). However, CQ treatment relieved the inhibitory effect of Bmp4 in the presence of suprastoichiometric concentrations of Bmper, resulting in augmented Smad1/5/8 phosphorylation (Figure 6.4A, compare lanes 15 and 20). A similar effect on Smad1/5/8 phosphorylation was obtained with bafilomycin A1 pretreatment (Figure 6.10E). Because CQ and bafilomycin A1 prevent endosomal acidification and inhibit endosome fusion and lysosomal degradation, our data suggest that the inhibition of Bmp signaling by suprastoichiometric concentrations of Bmper involves the lysosomal degradation of

the Bmper/Bmp4/Bmp receptor (BMPR) complex, and not simply endocytosis of the signaling complex as previously thought [7]. Collectively, these data demonstrate that endocytosis is a crucial process linked to Bmper's ability to both activate and inhibit Bmp4 signaling. In addition, the inhibitory effect of suprastoichiometric concentrations of Bmper on Bmp4 signaling may involve the lysosomal degradation of the Bmper/Bmp4 signaling complex.

LRP1 Is Required for Bmper/Bmp4-Dependent Signaling

We next examined the role that LRP1 plays in Bmper-dependent Bmp4 signaling. Following treatment with Bmp4 and Bmper, Smad1/5/8 phosphorylation was evaluated in LRP1-knockdown MECs. Not surprisingly, LRP1-knockdown inhibited Bmper and Bmp4 internalization in these cells (Figure 6.4C) and decreased Smad1/5/8 phosphorylation induced by Bmp4 alone and by Bmp4 plus Bmper in substoichiometric concentrations (Figure 6.4C, lanes 7, 9; Figure 6.10F), supporting that endocytosis is required for Bmper-dependent enhancement of Bmp4 signaling. Interestingly, LRP1-knockdown in MECs relieved the inhibitory effect of suprastoichiometric concentrations of Bmper on Bmp4-dependent Smad1/5/8 phosphorylation (Figure 6.4C, lane 10), proving that LRP1 mediates the inhibitory effect of suprastoichiometric concentrations of Bmper on Bmp4 signaling. These data demonstrate the pivotal role that LRP1 plays in Bmper-mediated Bmp4 signaling and support the theory that endocytosis of the Bmper/Bmp4 complex is essential for both the stimulatory and inhibitory actions that Bmper exerts on Bmp4 signaling.

To activate Bmp signaling, BMPRI/II heterodimers must form before Smad1/5/8 phosphorylation occurs [20]. Having established that LRP1 is required for Bmper-

dependent regulation of Bmp4 signaling, we tested the involvement of LRP1 in the regulation of ALK6/BMPRII heterodimerization. ALK6/BMPRII heterodimers were detected in control MECs under basal conditions (Figure 6.4D, lane 1) with the level increasing steadily with the addition of Bmp4, or Bmp4 plus substoichiometric concentrations of Bmper (Figure 6.4D, lanes 2 and 4; Figure 6.10G). In contrast, when cells were treated with Bmper alone or suprastoichiometric ratios of Bmper to Bmp4, the level of ALK6/BMPRII heterodimerization was similar to that seen under basal conditions (Figure 6.4D, lane 5). Surprisingly, in LRP1-knockdown MECs, the decrease of LRP1 protein level resulted in a greater abundance of ALK6/BMPRII heterodimers in the basal state (Figure 6.4D, comparing lane 6 to lane 1), suggesting that LRP1 competes with BMPRII for association with ALK6. In contrast, when LRP1-knockdown MECs were treated with Bmp4, Bmper, or Bmp4 and both low and high concentrations of Bmper, ALK6/BMPRII heterodimers were decreased in abundance (Figure 6.4D, lanes 7–10, compared to lane 6). These data suggest that LRP1 regulates the interaction of ALK6 with BMPRII under both basal and stimulated conditions—blocking the association of the receptors in the absence of Bmp4 or Bmper and promoting receptor interaction once stimulation with Bmp4 and/or Bmper at substoichiometric concentrations occurs. Other Bmp type II receptors (eg, activin receptor type II) showed different behavior in response to LRP1 (Figure 6.10H). In addition, the binding of ALK6 and BMPRII was similar but not the same in mouse embryonic fibroblasts (Figure 6.10I). Because exogenous mLRPs and ALK6 were associated in HEK293 cells (Figure 6.3), we wanted to know whether they form a complex in MECs and, if so, how Bmper/Bmp4 affect this association. Immunoprecipitation assays using MEC lysates confirmed that

ALK6 and LRP1 were associated in MECs. Whereas their interaction was inhibited by Bmp4, it was increased by treatment with Bmper alone, or Bmp4 and Bmper at both sub- and suprastoichiometric concentrations (Figure 6.4E, Figure 6.10J), suggesting that the LRP1 and ALK6 association is dynamically regulated by Bmp4 and Bmper, which may explain the differential effects of Bmper at sub- or suprastoichiometric concentrations on Smad1/5/8 activation.

LRP1 Regulates Bmper/Bmp4-Dependent Endothelial Migration and Angiogenesis

Our data demonstrating that LRP1 is required for the Bmper-mediated Bmp4 signaling module suggests that LRP1 could influence physiological outcomes of Bmper-mediated Bmp4 signaling such as endothelial migration and angiogenesis. In Boyden chamber migration assays, both Bmp4 and Bmper enhanced endothelial migration in MECs whereas a Bmp4 neutralizing antibody blocked Bmp4-induced cell migration (Figure 6.10K and IVL), consistent with previous reports [3,21]. However, LRP1 knockdown in MECs completely inhibited migration induced by Bmp4, Bmper alone, or Bmp4 plus a substoichiometric concentration of Bmper. Furthermore, LRP1 knockdown in MECs relieved the inhibition on cell migration caused by the combined treatment of Bmp4 plus suprastoichiometric concentrations of Bmper, consistent with our finding that the inhibition of Smad1/5/8 phosphorylation induced by high concentrations of Bmper was also relieved in the absence of LRP1 (Figure 6.4C). To study the role of LRP1 in angiogenesis, we performed an in vitro Matrigel tubulogenesis assay. Similar to the effects on endothelial migration, LRP1 knockdown in MECs blocked tube formation induced by Bmp4, Bmper, or the cotreatment of Bmp4 plus Bmper at the substoichiometric concentrations (Figure 6.4F). However, LRP1-knockdown MECs

demonstrated increased tube formation on the treatment of Bmp4 and Bmper at suprastoichiometric concentrations (Figure 6.4F). These data establish that the biochemical model we constructed through in vitro analysis holds true in a physiologically relevant cellular setting, demonstrating that LRP1 is a critical determinant of Bmper-mediated Bmp4 signaling events.

LRP1 Is Necessary for Cardiovascular Development in Zebrafish

The fact that Bmper/Bmp signaling pathways are essential for vascular development in zebrafish [5,12], along with our observations of a clear reliance of Bmper-mediated Bmp4 signaling on LRP1, prompted us to test whether LRP1 may also play an important role in Bmp4-dependent cardiovascular development. The spatiotemporal expression of *lrp1* during zebrafish embryonic development was examined. Weak *lrp1a* expression was observed at 12 hours post fertilization (hpf), whereas a stronger, symmetrical expression signal could be detected at the lateral dorsal aorta at 24 hpf and other vascular structures at later time points (Figure 6.5A, Figure 6.11A). Interestingly, the expression pattern of *lrp1a* closely paralleled that of *bmper* [5], in that *lrp1a* was expressed in structures that have Bmp and vasculogenic activity, such as lateral dorsal aorta and dorsal longitudinal anastomotic vessel.

To determine the importance of *lrp1a* in vasculogenesis, we used *lrp1a*-specific MOs to knock down *lrp1a* during zebrafish embryonic development. *lrp1a* knockdown efficiently decreased embryonic levels of *lrp1a* RNA as determined by RT-PCR (Figure 6.11B) and resulted in an abnormal vascular phenotype, illustrated by delayed dorsal and intersegmental vessel formation, fewer vascular branches within the caudal vein plexus, and a large swollen vascular lumen with ectopically-placed Kdr^+ cells (Figure

6.5B), which have also been described for *bmper* morphants [5]. Additionally, *lrp1a* morphants demonstrated disrupted blood flow and a slower or stopped heart beat (dsRed images in Figure 6.11C). Increased doses of *lrp1a* MOs resulted in a higher percentage of affected embryos (increasing from 75%–100%) at 24 hpf. This dose-dependent effect of the *lrp1a* MO was specific to the knockdown of *lrp1a* RNA and not due to activation of the p53-dependent cell death pathway [22] (Figure 6.11C–VF, Movies I–III). Knockdown of the second *lrp1* gene (*lrp1b*, ENSDART00000088208, chr. 23), either alone or with *lrp1a* resulted in a similar vascular phenotype, suggesting that the *lrp1* genes possess redundant functions (Figure 6.11G).

Next, we investigated whether the vascular defect of *lrp1* morphant fish is cell-autonomous by performing cell transplantation assays. Control or *lrp1* MO-injected donor cells were transplanted into wild-type recipient embryos. We observed that both control and *lrp1* MO-injected cells contributed to blood, endothelial structures (dorsal aorta, cardinal vein, caudal vein plexus, and intersegmental vessel) and other structures (somite, notochord, etc.) similarly (data not shown), suggesting that *lrp1* MO did not affect cell differentiation during development. *lrp1* MO-injected cells were excluded from the tip cell position within venous network located in the caudal vein plexus and participated in fewer ventral sprouting events (Figure 6.5C and 6.5D, Figure 6.11H). However, there was no obvious defect in the injected cell's ability to contribute to the tip cell within the intersegmental vessel, which is predominantly arterial in nature at this developmental stage. Bmp signaling was recently reported to regulate the ventral sprouting from the axial vein [12]. This finding, together with our data, suggests that

LRP1, similar to Bmp, regulates vein development in a cell-autonomous fashion. The cardiovascular defects observed in LRP1 morphant fish might be due to nonautonomous effects of LRP1 and reflect the autonomous requirement of LRP1 in venous endothelial function.

Bmper knockdown in zebrafish leads to diminished levels of Smad1/5/8 phosphorylation and a dorsalized phenotype consisting of defects in hematopoiesis and vascular patterning, reflecting the role that Bmper-mediated Bmp signaling plays during embryo gastrulation and vascular development [23,5]. Because the pattern of *lrp1a* in the developing zebrafish embryo mirrors that of *bmper*, we examined the effect of *lrp1a* knockdown on Bmper-mediated Bmp signaling in *lrp1a* MO-injected *Tg*(*kdrl:EGFP*)^{s843} fish using immunohistochemical localization of Smad1/5/8 phosphorylation. In wild-type fish, LRP1 expression was localized to the dorsal aorta, caudal vein, and caudal artery, whereas the expression of LRP1 protein was significantly reduced in *lrp1a* morphant fish (Figure 6.5E). In wild-type fish, the signal for phosphorylated Smad1/5/8 was mainly localized to the dorsal longitudinal anastomotic vessel, dorsal aorta, caudal artery, and some at intersegmental vessel and caudal vein (Figure 6.5F). In contrast, *lrp1a*knockdown decreased Smad1/5/8 phosphorylation in these regions (Figure 6.5F), indicating that LRP1, similar to Bmper, is required for Bmp-dependent events in vascular development

Discussion

The data presented in this report is a continuation of our previous work designed to elucidate the molecular mechanisms involved in Bmper regulation of Bmp signaling.

Here we present data supporting a model in which LRP1 acts as an endocytic receptor for Bmper, facilitating the formation and internalization of the Bmp4/BMPR signaling complex. Receptor endocytosis plays a critical role not only in the control of receptor protein levels at the cell surface and in the regulation of signaling pathways [24]. Similar to the case of endocytosis of transforming growth factor-β and epidermal growth factor [24], we believe that, in the case of Bmp4 signaling, clathrin-coated pits and early endosomes are signaling compartments, whereas late endosomes and lysosomes are sites where signaling is eventually blocked. Furthermore, our data support a model in which the magnitude and rate of LRP1-dependent endocytosis and the association of LRP1 and Bmp receptors, regulated by the Bmper:Bmp4 stoichiometric ratio, are critical factors determining the endocytic route of the Bmp4 signaling complex.

Previous studies have demonstrated that regulators of Bmp signaling modulate Bmp signaling using a spatial gradient effect that covers the distance of many cells [25]. In contrast, our data suggest that the mechanism for Bmper's regulation of Bmp4 signaling operates at the single cell level and involves a negative feedback loop within the same cell. For example, when Bmp4 is released it is bound by extracellular Bmper that initially is substoichiometric. Bmp4 together with Bmper binds to BMPRs and is subsequently endocytosed and recycled via an LRP1-dependent mechanism, which promotes the activation of Bmp4 signaling. Bmp signaling results in a plethora of cellular responses, including upregulation of Bmper expression [26]. As Bmp4 signaling continues, more Bmper is released into the extracellular environment until the intercellular concentration of Bmper eventually exceeds that of Bmp4. When this happens, the endocytosed Bmper/Bmp4/ALK6 complex is routed to lysosomes where it

is degraded, thereby resulting in inhibition of Bmp4 signaling. In this way, each cell involved in the Bmp4 signaling event responds in a tightly controlled manner.

Although the focus of this report has been the effect of LRP1 on Bmp4 signaling, it is entirely possible that Bmper/Bmp4 may also have an effect on LRP1 signaling. More than 40 ligands have been identified for LRP1, encompassing multiple cellular functions such as the regulation of lipid metabolism, cell migration, blood-brain barrier integrity, and neuronal homeostasis [14]. Our observation that both Bmper and ALK6 bind to the α chain of LRP1, which is responsible for ligand uncoupling [14], raises the interesting possibility that Bmper and Bmps may influence the signaling mechanisms carried out by LRP1. This is an intriguing thought, especially given the evidence that LRP1 regulates atherosclerosis via modulation of PDGF and transforming growth factor-receptor functions [14]. A potential interaction or competition between previously identified LRP1 signaling pathways and Bmp-mediated pathways remains a topic of future research.

We have demonstrated that LRP1, through its effect on Bmp signaling, is essential for cardiovascular development in zebrafish. The expression pattern of *lrp1* in developing embryos is remarkable for several reasons. *lrp1* is expressed in regions known for their high Bmper/Bmp activity and areas of known vasculogenesis [5]. This pattern places *lrp1* at a time and location in which it could interact with Bmper and therefore mediate Bmper/Bmp signaling. This observation is confirmed by the similar phenotype of *lrp1-* and *bmper* deficient fish. Knockdown of either *lrp1* or *bmper* leads to a similar abnormality in vascular development, such as the compromised caudal vein plexus and aberrant intersegmental vessels. However, *bmper* morphants also exhibit a

reducednumber of *gata1* expressing hematopoietic precursor cells and circulating blood cells [5]. Whereas these cell types were distributed in a disorganized pattern in *lrp1* morphants, the actual cell number remained similar to wild-type embryos. The subtle differences in the expression pattern and knockdown phenotype of LRP1, compared to Bmper, could be attributed to the activation of LRP1 by its other ligands.

Collectively, our data suggest that LRP1 plays a requisite role in Bmper-mediated regulation of Bmp4 signaling byacting as an endocytic receptor for Bmper and mediating the endocytosis of the Bmper/Bmp4/BMPR complex. Based on these observations, we propose the following working model to explain the role of LRP1 in the regulation of Bmper- mediated Bmp4 signaling (Figure 6.6). In the absence of ligand, ALK6 and LRP1 are associated, blocking the assembly of an active BMPRII/ALK6 complex (Figure 6.6A, left). However, in the presence of Bmp4 (Figure 6.6A, middle), ALK6 dissociates from LRP1 and heterodimerizes with BMRPII. The receptor complex is then endocytosed via clathrin-coated pits in an LRP1-independent manner and sequestered within endosomes where Bmp4-dependent Smad1/5/8 activation occurs [20]. When the concentration of Bmper is substoichiometric, Bmper/LRP1 forms a transient holocomplex with Bmp4/ALK6/BMPRII (Figure 6.6B), promoting the Rab4-dependent endocytic fast recycling and therefore enhancing downstream signaling (Figure 6.6D). The signaling reaction continues to completion, possibly by termination of Smad1/5/8 phosphorylation via phosphatase activation. We speculate that, at the completion of the signaling reaction, the various components of the Bmper/Bmp4 signaling complex are recycled back to the cell membrane (Figure 6.6D, red route), where they would be available for future signaling events. This pathway would explain

the ability of substoichiometric concentrations of Bmper to activate Bmp4 signaling. When the concentration of Bmper is suprastoichiometric, the association of LRP1 with ALK6 increases, but that of ALK6 with BMPRII decreases (Figure 6.6C). The LRP1-dependent endocytosis of a transient Bmper/Bmp4/ALK6/LRP1 holocomplex leads to the degradation of the Bmper/Bmp4 signaling complex and early termination of Bmp4 signaling activity (Figure 6.6E, green route). We therefore propose that the different components of the transient Bmp4/Bmper receptor holocomplex may be the determining factor in deciding which endocytic sorting routes are used in the presence of sub- versus suprastoichiometric concentrations of Bmper. Bmper was recently reported to preferentially regulate Bmp9/ALK1 signaling in endothelial cells [27]. Whether LRP1 is required for Bmper-modulated Bmp9/ALK1 signaling and how Bmp9 regulates Bmp4/Bmper/BMPR/LRP1 complex formation needs future investigation. Moreover, the mechanisms behind the receptor dependent endocytic sorting described remain unknown. The different components of the transient holocomplex may recruit different scaffolding proteins, thereby influencing the intracellular route of receptor complex processing. Alternatively, intracellular routing of the Bmper/Bmp4 signaling complex may be regulated by posttranslational modification of LRP1, which may occur differentially depending on which components comprise the Bmper/Bmp4 receptor complex. For example, LRP1 contains an NPxY motif in its cytoplasmic tail that lies proximal to the plasma membrane. This NPxY motif is a sorting nexin 17-binding motif that help sort LRP1-contained endosomes during the receptor recycling process. If this motif is mutated, LRP1-containing endosomes cannot be recycled and become targets of lysosomal degradation [28]. LRP1 endocytosis can also be regulated by a cAMP-

dependent protein kinase A-mediated serine phosphorylation on its cytoplasmic tail [29]. It is possible that the different Bmper/Bmp4 receptor complexes formed in the presence of high and low concentrations of Bmper may influence either the phosphorylation of the LRP1 cytoplasmic tail or the recruitment of endosome sorting proteins such as sorting nexin 17, which in turn may result in differential intracellular sorting routes. Although additional work is needed to fully elucidate the exact mechanism for the different sorting processes by which LRP1 regulates Bmper/Bmp4 signaling, LRP1-dependent endocytosis is clearly critical for all aspects of Bmper-mediated Bmp4 signaling, and the stoichiometric ratio of Bmper to Bmp4 is a key to determine whether Bmp signaling is activated or inhibited.

FIGURES:

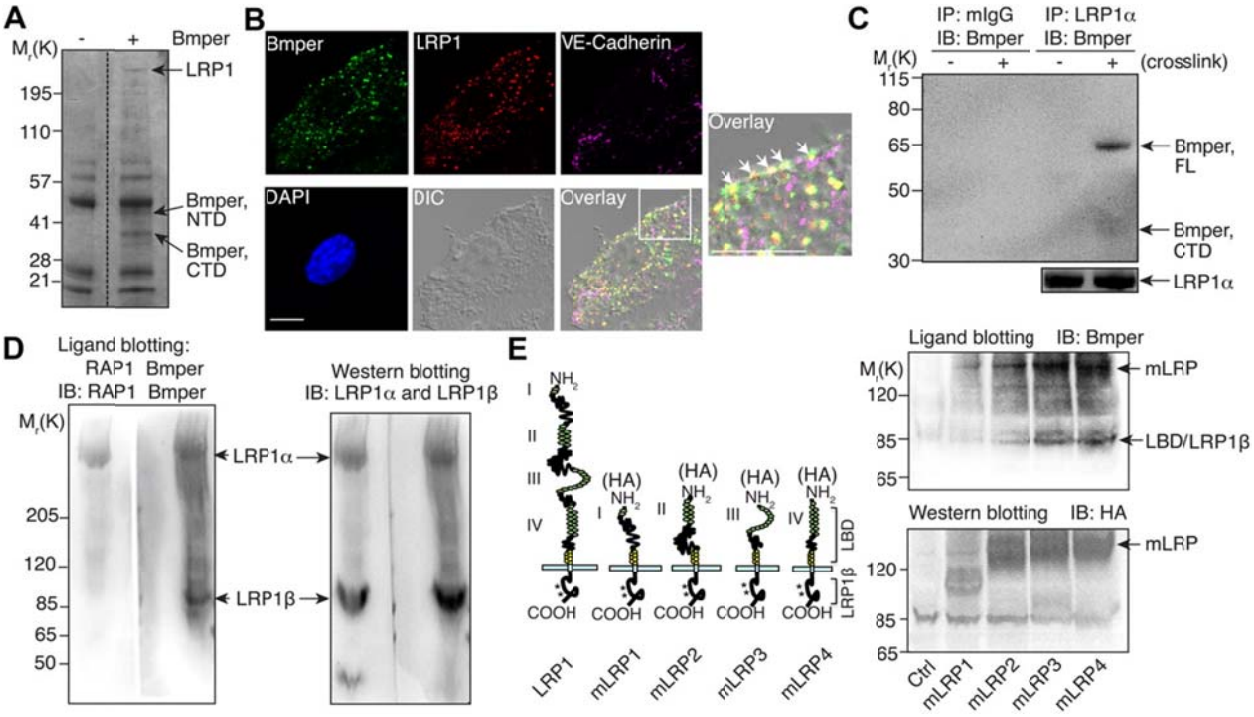

Figure 6.1: LDL receptor-related protein 1 (LRP1) associates with bone morphogenetic protein endothelial cell precursor-derived regulator (Bmper).

(A) Lysates of Bmper-treated mouse endothelial cells (MECs) were immunoprecipitated with an anti-Bmper antibody and stained with Coomassie blue to identify proteins. (B) Bmper-treated MECs (5 nmol/L for 1 min) were stained with anti-Bmper and LRP1 antibodies and examined using confocal imaging. Scale bar: 10 µm. (C) Lysates of MECs were immunoprecipitated with anti-LRP1 antibody or mouse control IgG and analyzed by Western blotting with a biotinylated anti-Bmper antibody. (D) Nondenatured lysates of MECs were analyzed for ligand blotting. The membrane was incubated with recombinant Bmper and immunoblotted with anti-Bmper antibody (left). LRP1 and RAP1 interaction[8] is included as a positive control. (E) Nondenatured lysates of HEK 293 cells transfected with mLRP1–4 were analyzed for ligand blotting with an anti-Bmper antibody (right top). Right bottom is included as a loading control. Left side is a schematic representation of LRP1 and each mLRP1–4 construct. NTD indicates amino-terminal domain; CTD, carboxyl-terminal domain; VE, vascular endothelial; LBD, ligand binding domains; DAPI, 4,6-diamidino-2-phenylindole; DIC, differential interference contrast.

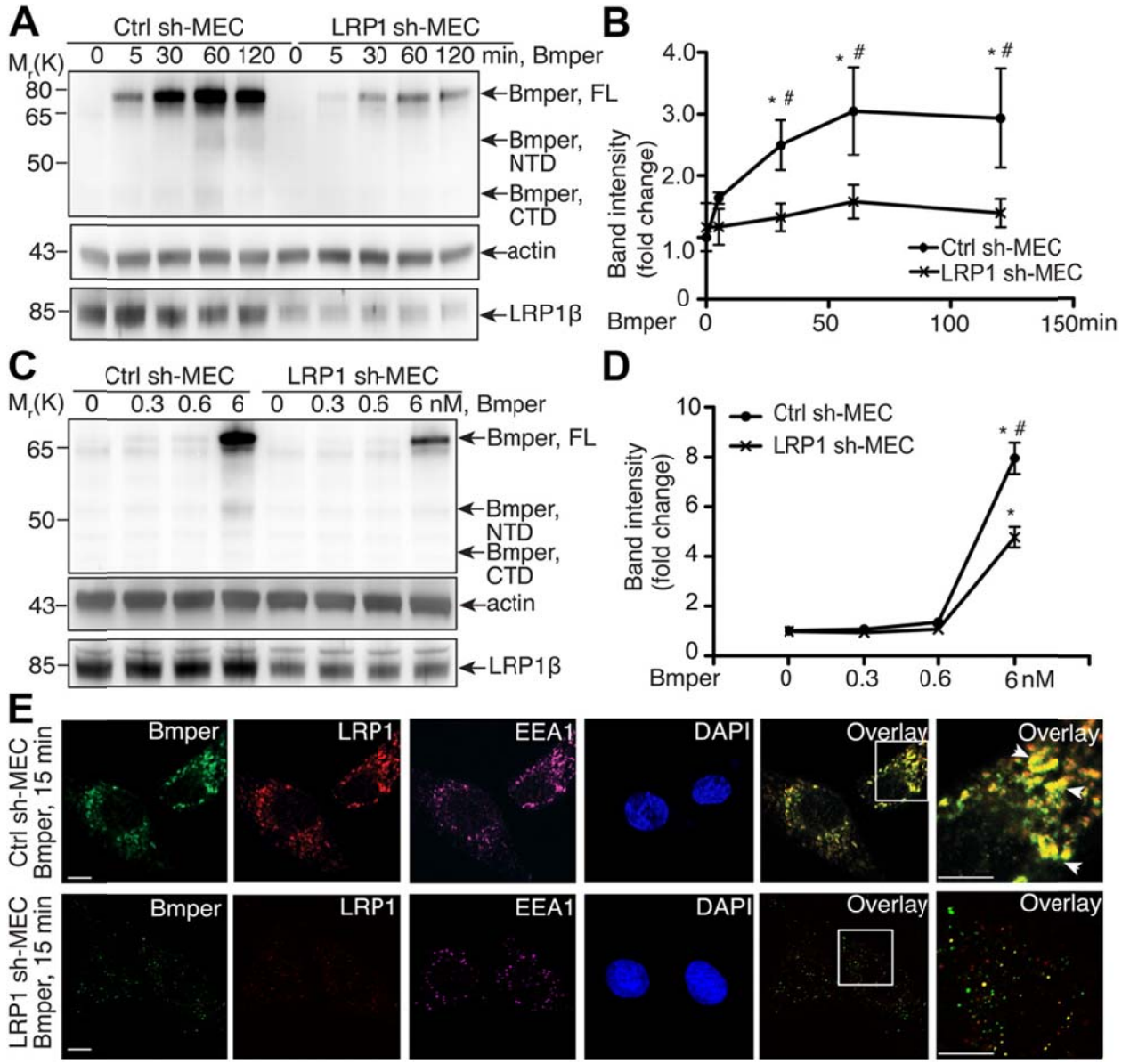
A
Ctrl sh-MEC
LRP1 sh-MEC
Mr(K)
0 5 30 60 120 0 5 30 60 120 min, Bmper
80
65
50
43
85
Bmper, FL
Bmper, NTD
Bmper, CTD
actin
LRP1β
B
Band intensity (fold change)
4.0
3.0
2.0
1.0
0
Bmper 0 50 100 150min
Ctrl sh-MEC
LRP1 sh-MEC
C
Ctrl sh-MEC
LRP1 sh-MEC
Mr(K)
0 0.3 0.6 6 0 0.3 0.6 6 nM, Bmper
65
50
43
85
Bmper, FL
Bmper, NTD
Bmper, CTD
actin
LRP1β
D
Band intensity (fold change)
10
8
6
4
2
0
Bmper 0 0.3 0.6 6nM
Ctrl sh-MEC
LRP1 sh-MEC
E
Ctrl sh-MEC Bmper, 15 min
LRP1 sh-MEC Bmper, 15 min
Bmper
LRP1
EEA1
DAPI
Overlay

Figure 6.2: LDL receptor-related protein 1 (LRP1) is required for bone morphogenetic protein endothelial cell precursor-derived regulator (Bmper) endocytosis.

(A) Time course of nondenatured cell lysates from Bmper-treated mouse endothelial cells (MECs) (6 nmol/L) were analyzed by Western blotting. (B) Quantification of Bmper protein band intensity in A. *, compared to nontreated control (Ctrl) sh-MECs, $P<0.02$, $n=3$; #, compared to LRP1-knockdown MECs treated similarly, $P<0.05$, $n=3$. (C) Nondenatured cell lysates from MECs treated with increasing doses of Bmper were analyzed by Western blotting. (D) Quantification of Bmper protein band intensity in C. *, compared to nontreated control sh-MECs, $P<0.05$; #, compared to LRP1-knockdown MECs treated similarly,$P<0.02$, $n=3$. (E) Bmper-treated MECs (15 min) were analyzed by confocal imaging for the colocalization of Bmper (green), LRP1 (red), and EEA1 (purple), indicated by the arrows. Scale bars: 5 μm. NTD indicates amino-terminal domain; CTD, carboxyl-terminal domain; DAPI, 4,6-diamidino-2-phenylindole.

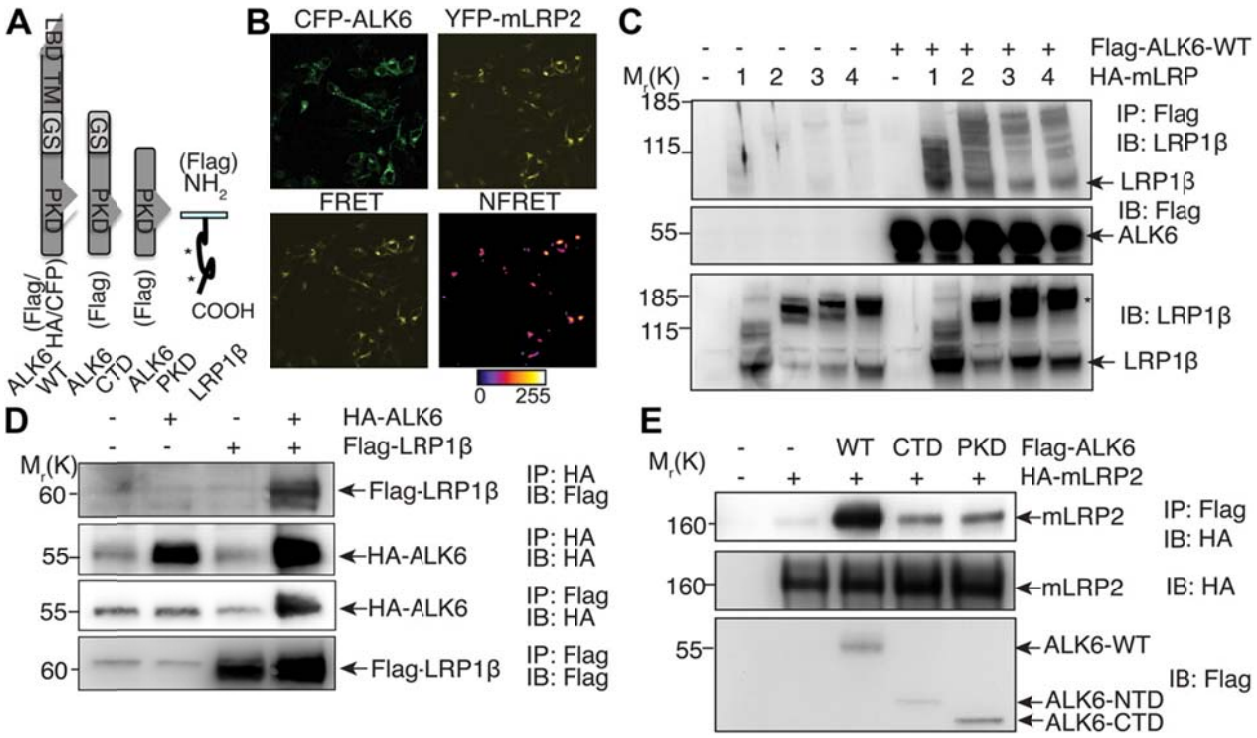

Figure 6.3: The association of LDL receptor-related protein 1 (LRP1) and activin-like kinase receptor (ALK)6.

(A) A schematic representation of wild type ALK6, its deletion mutants ALK6-carboxyl-terminal domain (CTD) and ALK6-protein kinase domain (PKD), and LRP1β constructs. (B) HEK 293 cells were transfected with cyan fluorescent protein (CFP)-ALK6 and yellow fluorescent protein (YFP)-mini-LRP (mLRP)2 and analyzed by fluorescence energy transfer (FRET). The calibration bar indicates fluorescence signal level with white being highest intensity in normalized FRET channel (NFRET). Scale bar: 10 µm. (C) Lysates of HEK 293 cells transfected with plasmids encoding Flag-ALK6-WT and HA-mLRP1-4 were immunoprecipitated with an anti-Flag antibody and analyzed by Western blotting. The asterisk (*) indicates precursor ER and fully glycosylated Golgi forms of mLRPs[15]. (D) Lysates of HEK293 cells transfected with HA-ALK6-WT and Flag-LRP1β were immunoprecipitated with anti-HA or Flag antibody and analyzed by Western blotting. (E) Lysates of HEK 293 cells transfected with Flag-ALK6-CTD/PKD and HA-mLRP2 were immunoprecipitated with an anti-Flag antibody and analyzed by Western blotting.

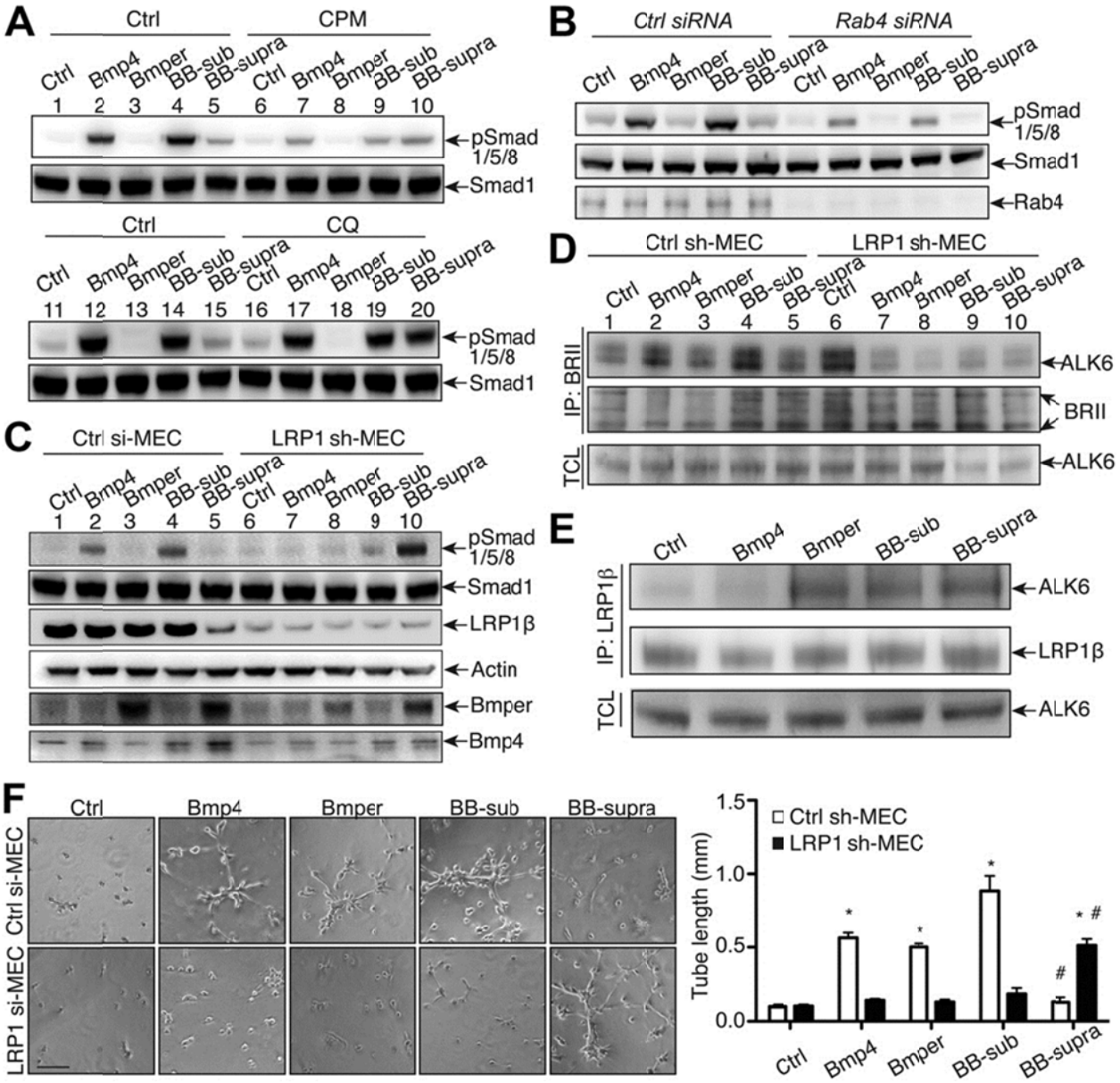
A
Ctrl
CPM
Ctrl Bmp4 Bmper BB-sub BB-supra Ctrl Bmp4 Bmper BB-sub BB-supra
1 2 3 4 5 6 7 8 9 10
pSmad 1/5/8
Smad1
Ctrl
CQ
Ctrl Bmp4 Bmper BB-sub BB-supra Ctrl Bmp4 Bmper BB-sub BB-supra
11 12 13 14 15 16 17 18 19 20
pSmad 1/5/8
Smad1
B
Ctrl siRNA
Rab4 siRNA
Ctrl Bmp4 Bmper BB-sub BB-supra Ctrl Bmp4 Bmper BB-sub BB-supra
pSmad 1/5/8
Smad1
Rab4
C
Ctrl si-MEC
LRP1 sh-MEC
Ctrl Bmp4 Bmper BB-sub BB-supra Ctrl Bmp4 Bmper BB-sub BB-supra
1 2 3 4 5 6 7 8 9 10
pSmad 1/5/8
Smad1
LRP1β
Actin
Bmper
Bmp4
D
Ctrl sh-MEC
LRP1 sh-MEC
Ctrl Bmp4 Bmper BB-sub BB-supra Ctrl Bmp4 Bmper BB-sub BB-supra
1 2 3 4 5 6 7 8 9 10
IP: BRII
ALK6
BRII
TCL
ALK6
E
Ctrl Bmp4 Bmper BB-sub BB-supra
IP: LRP1β
ALK6
LRP1β
TCL
ALK6
F
Ctrl Bmp4 Bmper BB-sub BB-supra
Ctrl si-MEC
LRP1 si-MEC
Ctrl sh-MEC
LRP1 sh-MEC
Tube length (mm)
1.5
1.0
0.5
0.0
Ctrl Bmp4 Bmper BB-sub BB-supra

Figure 6.4: LDL receptor-related protein 1 (LRP1)-mediated endocytosis is required for the bone morphogenetic protein endothelial cell precursor-derived regulator (Bmper)-dependent regulation of bone morphogenetic protein (Bmp)4 downstream signaling.

(A) Endocytosis is required for both promoting and inhibiting Bmp function of Bmper. Mouse endothelial cells (MECs) were pretreated with chlorpromazine (CPM) or chloroquine (CQ) and then treated with Bmp4 (0.6 nmol/L) and Bmper for 15 min (chlorpromazine [CPM]) or 120 min (CQ) at 10 nmol/L (Bmper alone); 0.3 nmol/L (BB-sub [substoichiometric Bmper]); 10 nmol/L (BB-supra [Bmper suprastoichiometric]). Cell lysates were analyzed by Western blotting. (B) Rab4 is required for Smad1/5/8 phosphorylation induced by Bmp4 and substoichiometric Bmper. Lysates of MECs transfected with control (Ctrl) or Rab4 siRNA and treated with Bmp4 and Bmper (15 min) were analyzed by Western blotting. (C) LRP1 is required for Bmper/Bmp internalization and Bmper-dependent Bmp downstream signaling. Lysates of LRP1-knockdown or control MECs treated with Bmp4 and Bmper (30 min) were analyzed by Western blotting. (D) Lysates of MECs treated with Bmp4 and Bmper for 15 min were immunoprecipitated with an anti-Bmp receptor (BMPR)II antibody and analyzed by Western blotting. (E) The association of LRP1 and ALK6 is regulated on the different treatment of Bmp4 and Bmper. Lysates of MECs following Bmp4 and Bmper treatments for 15 min were immunoprecipitated with the mouse anti-LRP1β antibody and analyzed by Western blotting. (F) MECs were subjected to the in vitro Matrigel angiogenesis assay. *, compared to the same MECs at control condition, $P<0.05$. #, compared to the same MECs treated with Bmp4, $P<0.01$. $n=3$. Scale bar: 100 μm.

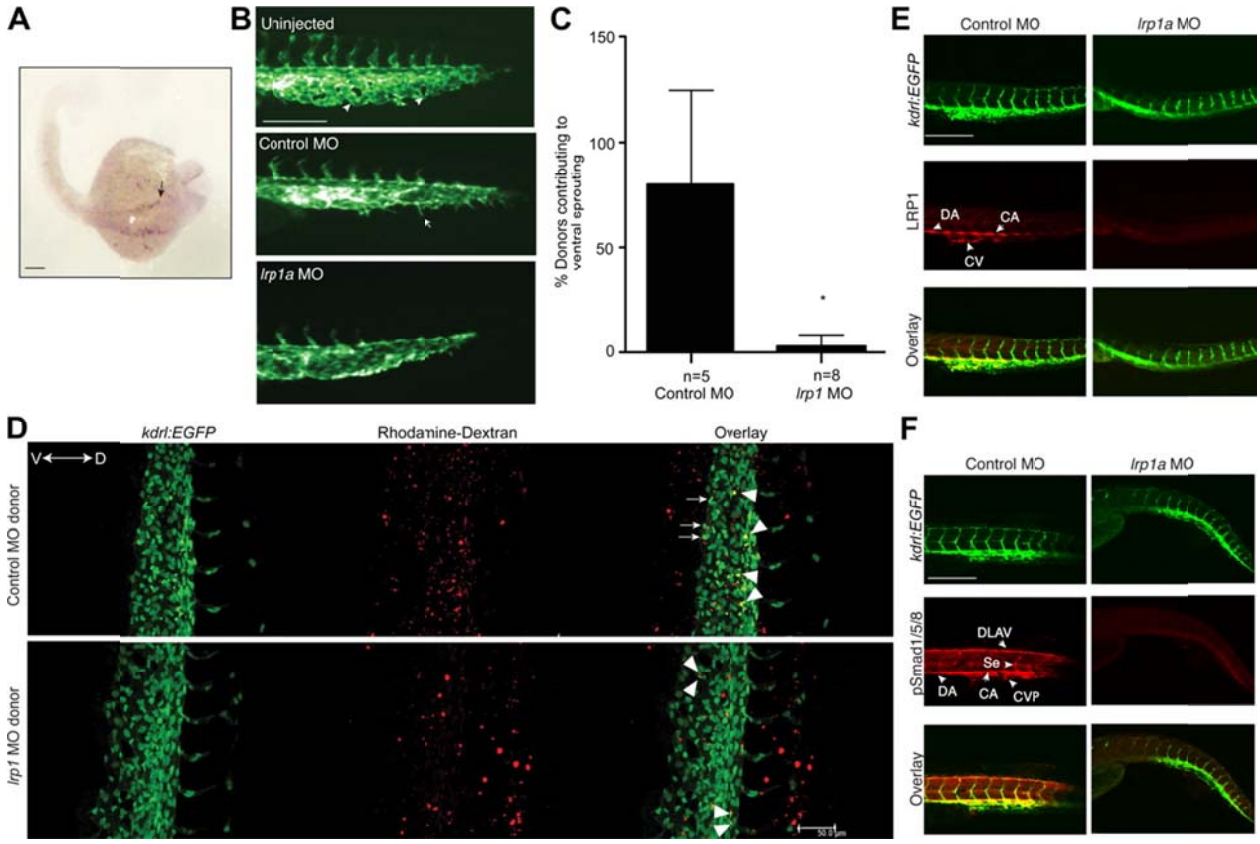

Figure 6.5: LDL receptor-related protein 1 (LRP1) is required for cardiovascular development in zebrafish.

(A) RNA expression of *lrp1a* in a whole-mount zebrafish embryo, analyzed by in situ hybridization using an *lrp1a*-specific antisense probe. The arrow represents the lateral dorsal aorta (LDA). (B) Loss of *lrp1a* results in a disrupted vascular phenotype. Images are lateral views of *Tg*(*kdrl:EGFP*)^{S843} zebrafish embryo tails at 24 hours postfertilization (hpf). The arrowheads represent the caudal vein plexus (CVP) with branches; the arrows represent filopodia located on the front edge of vessel plexus. (C) Quantitative analysis of the donor cells located at the tip cell region of cardinal vein plexus and contributing to ventral sprouting. *, compared to control morpholino oligonucleotides (MO)-injected donor cells, $P \leq 0.001$. n is the number of recipient embryos. (D) Representative lateral views of wild-type recipient embryos of *Tg*(*kdrl:EGFP*)^{s843} fish tail at 34 hpf. Confocal imaging was performed. In the control MO-donor cells-transplanted embryo, 3 donor cells (white arrows) participated in active ventral sprouting. However, in the *lrp1* MO-donor cells-transplanted embryo, donor cells remained in dorsal or axial vasculature (white arrowheads). (E, F) Confocal imaging analysis of whole mount *Tg*(*kdrl:EGFP*)^{s843} fish embryo tails at 48 hpf, with immunostaining for LRP1 (E) and phospho-Smad1/5/8 (F). Scale bars: 100 μm (A, B, E, F); 50 μm (D). DLAV indicates dorsal longitudinal anastomotic vessel; DA, dorsal aorta; CA, caudal artery; CV, caudal vein; CVP, caudal vein plexus; Se, intersegmental vessel.

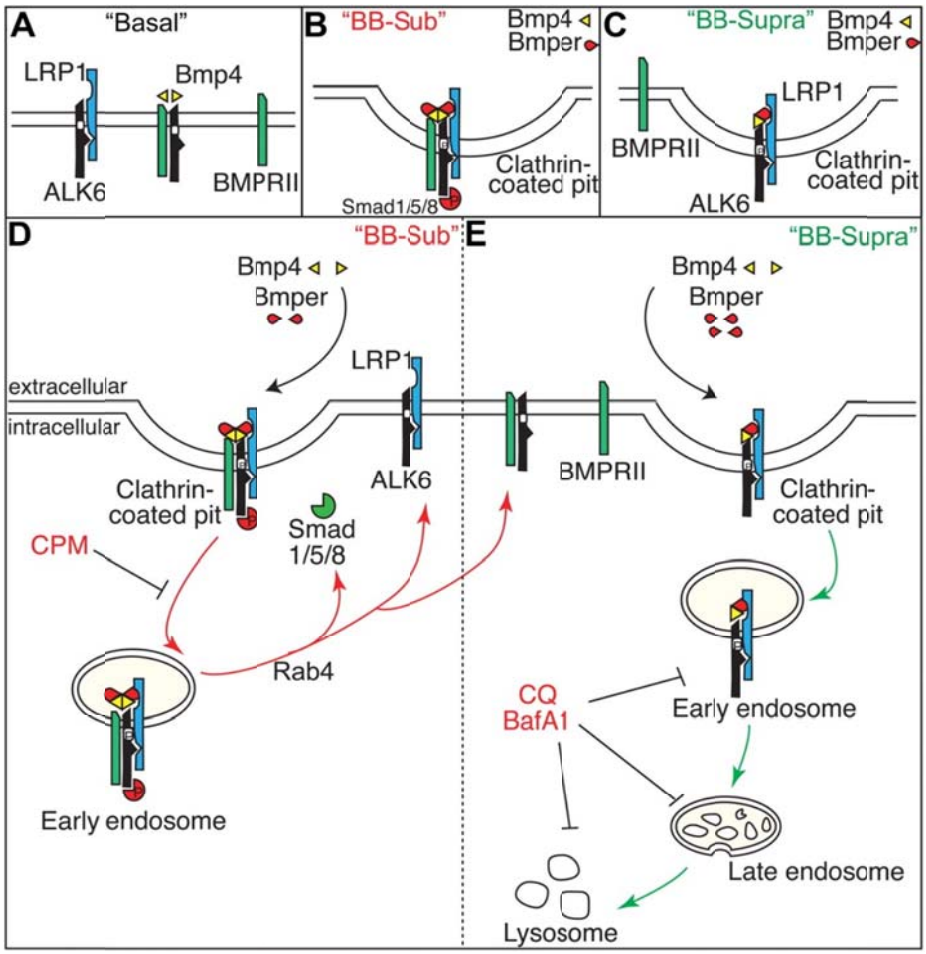

Figure 6.6: A schematic model shows how LDL receptor-related protein 1 (LRP1) is required for bone morphogenetic protein (Bmp)4/bone morphogenetic protein endothelial cell precursor-derived regulator (Bmper) signaling.

(A) left, In the absence of ligand, activin-like kinase receptor (ALK)6 and LRP1 are associated, blocking the assembly of an active Bmp receptor (BMPR)II/ALK6 complex. In the presence of Bmp4 (A, middle), ALK6 dissociates from LRP1 and heterodimerizes with BMPRII [20]. This Bmp4/BMPRII/ALK6 receptor complex is sequestered within endosomes where Bmp signaling occurs [30]. (B) When the concentration of Bmper is substoichiometric, Bmper/LRP1 forms a transient holocomplex of Bmp/ALK6/BMPRII, which promotes Rab4-dependent endocytic fast recycling and enhances downstream Bmp signaling (D, red route). (C) When the concentration of Bmper is suprastoichiometric, the association of LRP1 with ALK6 increases, but that of ALK6 with BMPRII decreases. The LRP1-dependent endocytosis of a transient Bmper/Bmp/ALK6/LRP1 holocomplex leads to the degradation of the Bmper/Bmp signaling complex and termination of Bmp signaling activity (E, green route).

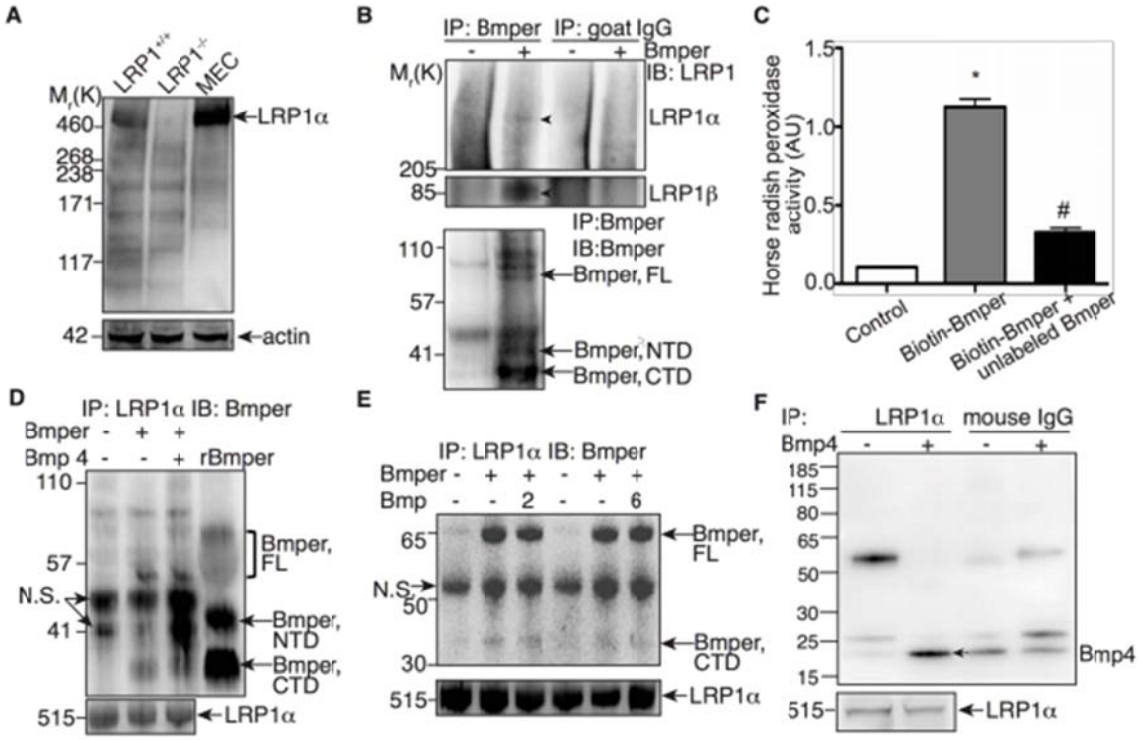

Figure 6.7: LRP1 is associated with Bmper.

(A) LRP1 was expressed in MECs. Lysates of cells were analyzed by Western blotting with an anti-LRP1α antibody. The expression of LRP1 was abundant in MEC and LRP1+/+ MEFs, with no LRP1 protein detected in LRP1-/- MEFs, indicating the specificity of the anti-LRP1 antibody. (B) Lysates of MECs were immunoprecipitated with an anti-Bmper antibody or goat control IgG and analyzed by Western blotting with anti-LRP1 antibody (the upper panel). The lower panel demonstrates the internalized Bmper detected in the total cell lysates. (C) Competitive inhibition of Bmper binding to LRP1-contained MEC Lysates. Competitive binding ELISA was performed in order to determine whether unlabeled Bmper competes with biotinylated Bmper for the binding of LRP1-contained MEC lysates. The reaction with lysates of LRP1-/- MEFs was used as a negative control. (D) Lysates of MECs treated with Bmper and Bmp4 were immunoprecipitated with anti-LRP1 antibody and analyzed by Western blotting with anti-Bmper antibody (the upper panel). The lower panel demonstrates the expression levels of LRP1α. N.S. means non-specific. (E) Lysates of MECs treated with Bmper and Bmp2 or 6 were immunoprecipitated with anti-LRP1 antibody and analyzed by Western blotting with biotinylated anti-Bmper antibody and avidin-HRP (the upper panel). The lower panel demonstrates the expression levels of LRP1α. N.S. means non-specific. (F) LRP1 is complexed with Bmp4. Lysates of MECs treated with Bmp4 were immunoprecipitated with an anti-LRP1 antibody or mouse IgG control, and then analyzed with Western blotting with the anti-Bmp4 antibody.

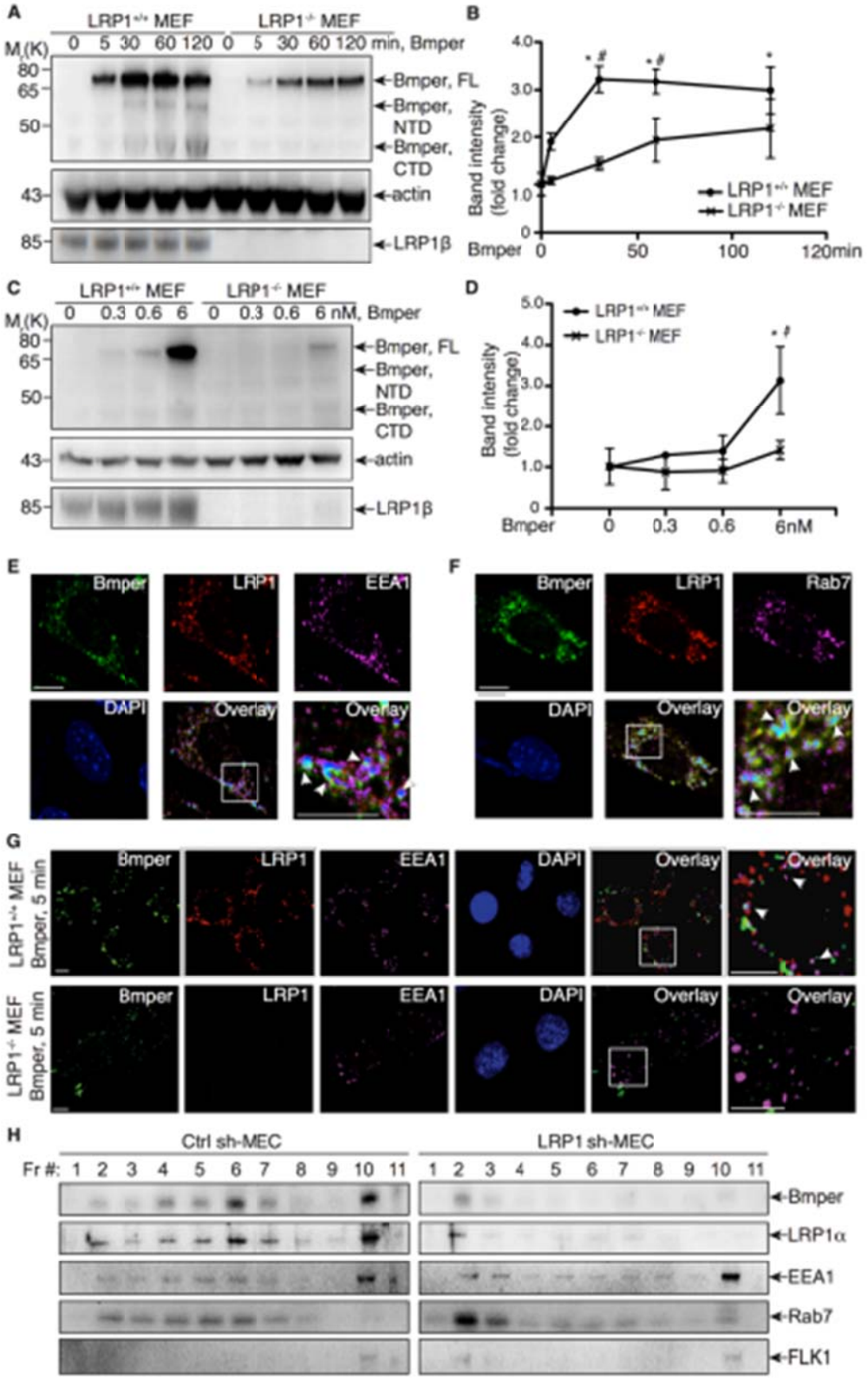
A
LRP1+/+ MEF
LRP1-/- MEF
0 5 30 60 120 0 5 30 60 120 min, Bmper
Mr(K)
80
65
50
43
85
Bmper, FL
Bmper, NTD
Bmper, CTD
actin
LRP1β
B
Band intensity (fold change)
LRP1+/+ MEF
LRP1-/- MEF
Bmper 0 50 100 120min
C
0 0.3 0.6 6 0 0.3 0.6 6 nM, Bmper
D
Bmper 0 0.3 0.6 6nM
E
Bmper
LRP1
EEA1
DAPI
Overlay
F
Rab7
G
LRP1+/+ MEF Bmper, 5 min
LRP1-/- MEF Bmper, 5 min
H
Ctrl sh-MEC
LRP1 sh-MEC
Fr #: 1 2 3 4 5 6 7 8 9 10 11
LRP1α
FLK1

Figure 6.8. LRP1 is required for Bmper endocytosis.

(A) Non-denatured cell lysates from cells treated with Bmper for different time periods were analyzed for Bmper protein level by Western blotting with an anti-Bmper antibody. (B) Quantification of Bmper protein band intensity in A. *, compared to non-treated wild-type MEFs, $P<0.02$, n=3; #, compared to LRP1 null MEFs treated similarly, $P<0.05$, n=3 independent experiments. (C) Non-denatured cell lysates from cells treated with increasing doses of Bmper were analyzed for Bmper protein level by western blotting with an anti-Bmper antibody. (D) Quantification of Bmper protein band intensity in C. *, compared to non-treated wild-type MEFs, $P<0.05$; #, compared to LRP1 null MEFs treated similarly, $P<0.02$, n=3 independent experiments. (E) Bmper-treated MECs (15 minutes) were analyzed by confocal imaging for the co-localization of Bmper (green), LRP1 (red) and EEA1 (purple). Colocalization of these three proteins is indicated by blue 14particles (arrow). These are the representative images of three independent experiments. (F) MECs treated with Bmper for 90 minutes were analyzed by confocal imaging for the co-localization of Bmper (green), LRP1 (red) and Rab7 (purple). Colocalization of these three proteins is indicated by blue particles (arrow). These are the representative images of three independent experiments. (G) MEFs treated with Bmper for 5 minutes were analyzed by confocal imaging for the co-localization of Bmper (green), LRP1 (red) and EEA1 (purple). Colocalization of these three proteins results in blue immunofluorescence, as indicated by the arrows. Scale bars: 5 μm. (H) Subcellular fractionation experiments were performed to confirm the location of Bmper and LRP1 in MECs. Eleven serial membrane fractions prepared from 5 nmol/L Bmper-treated control (Ctrl sh-MEC) or LRP1 shRNA stably transfected MECs (LRP1 sh-MEC) were fractionated on a self-generated Optiprep gradient (10%, 20%, 30%) and immunoblotted with antibodies against proteins-Bmper and LRP1α, and that enriched in plasma membrane (FLK1); early endosomes (EEA1); or late endosomes (Rab7). Optiprep gradient fractionation resulted in Bmper and LRP1α mainly cofractionating with Flk1 (plasma membrane marker), EEA1 (early endosome marker) and Rab7 (late endosome marker). In LRP1-knockdown MECs, we observed considerably less Bmper localized in plasma membrane and endosomal fractions.

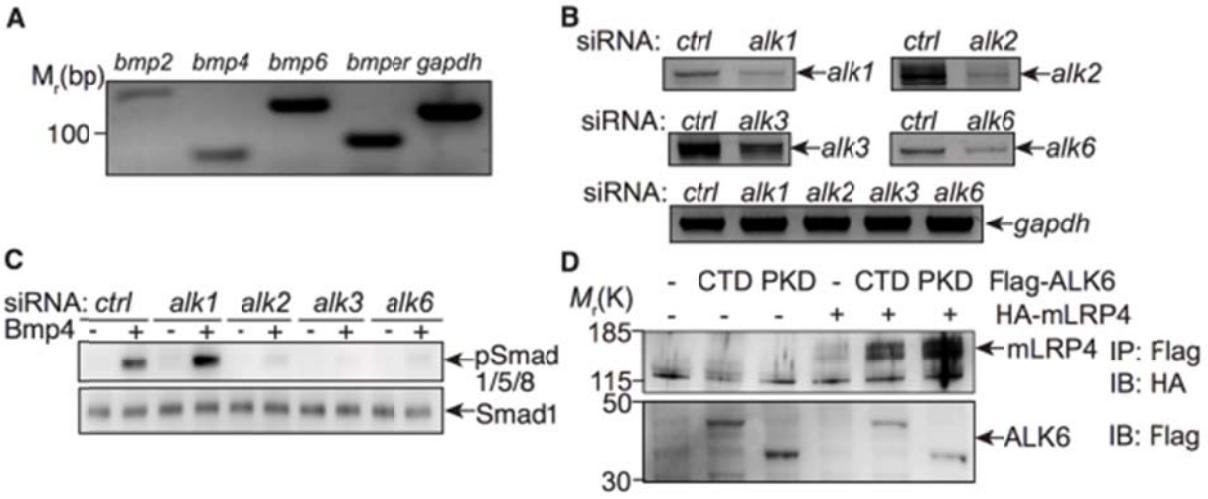

Figure 6.9: ALK2, 3 and 6 are required for Smad1/5/8 activation induced by Bmp4.

(A) The total RNA of MECs was reverse transcribed to cDNA and detected for the RNA levels of Bmp2, 4, 6, Bmper using their specific primers. GAPDH was used as a housekeeping gene control. (B) MECs were transfected with control (Ctrl) siRNA, alk1, alk2, alk3 or alk6 siRNAs. The total RNA obtained from these MECs were used for RT-PCR analysis with the specific primers of ALK1, 2, 3 and 6. GAPDH was used as an internal control. (C) MECs were transfected with alk1, 2, 3 or 6 siRNAs, or control siRNAs, and then treated with Bmp4 to activate Smad1/5/8. The cell lysates were immunoblotted with the antibodies against phospho-Smad1/5/8 and Smad1. (D) Lysates of HEK 293 cells transfected with FlagALK6-CTD/PKD and HA-mLRP4 were immunoprecipitated with an anti-Flag antibody and analyzed by Western blotting with an anti-HA antibody to detect mLRP4. The total cell lysates were also blotted with antibodies as indicated to show the equal loading of overexpressed proteins.

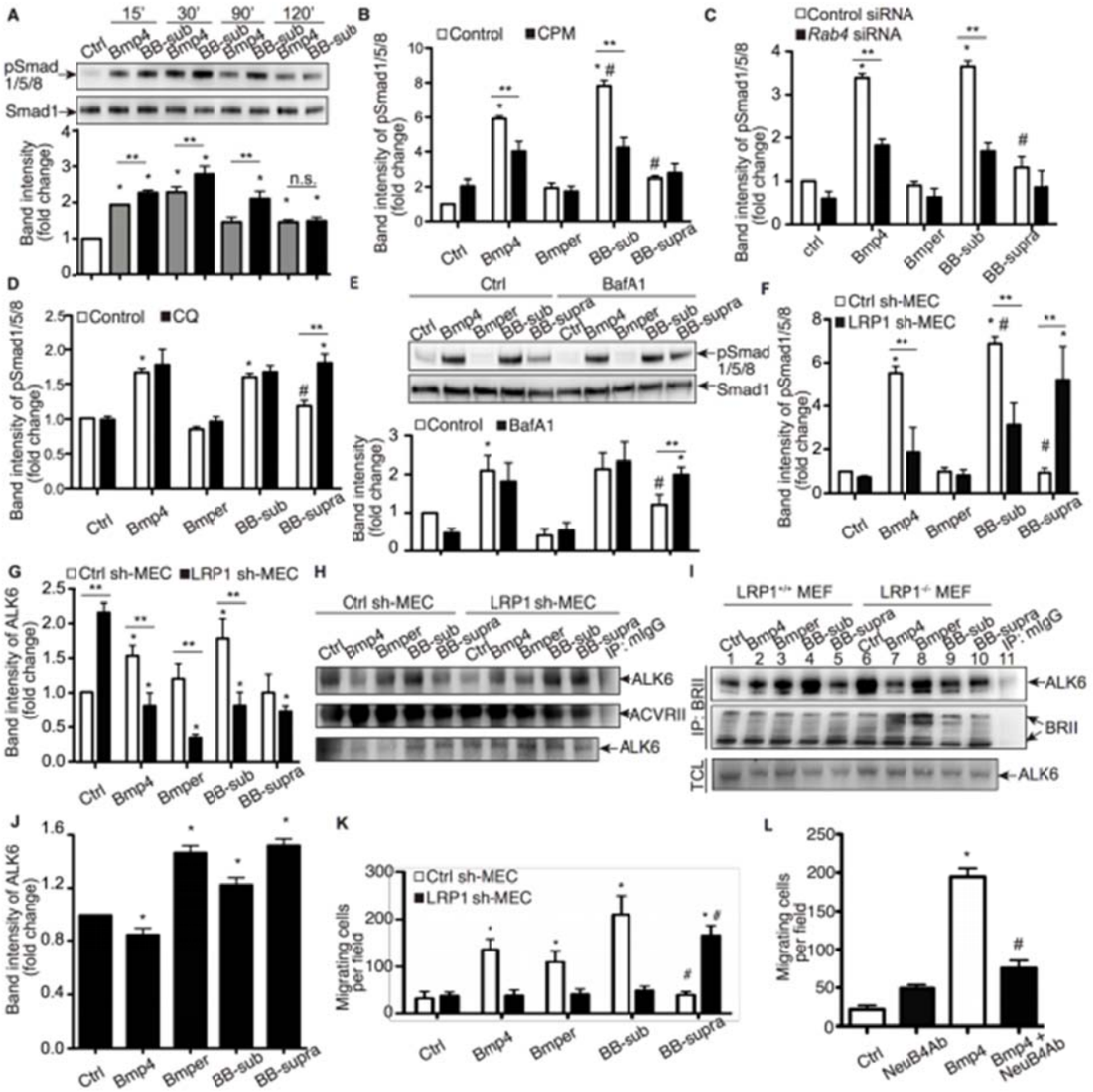

Figure 6.10: LRP1-mediated endocytosis is required for the Bmper-dependent regulation of Bmp4 downstream signaling.

(A) MECs were treated for indicated time periods with Bmp4 (0.6 nmol/L) or subjected to the "BB-sub" treatment in which the ratio of Bmper (0.3 nmol/L) to Bmp4 (0.6 nmol/L) concentration is substoichiometric. The "BB-supra" treatment is the treatment in which the ratio of Bmper (10 nmol/L) to Bmp4 (0.6 nmol/L) concentration is suprastoichiometric. Cell lysates were analyzed by Western blotting with antibodies for phosphorylated Smad1/5/8 (pSmad1/5/8) and Smad1. *, compared to MECs at control condition, P<0.05. **, P<0.05. n.s., not significant. n=3. (B) Quantitative analysis of Figure 4A "CPM" experiment (upper panel). *, compared to MECs at control condition, P<0.05. #, compared to MECs treated with Bmp4 alone, P<0.05. **, P<0.05. n=3. (C) Quantitative analysis of Figure 4B. *, compared to MECs at control condition, P<0.05.

#, compared to MECs treated with Bmp4 alone, P<0.05. **, P<0.05. n=3. (D) Quantitative analysis of Figure 4A "CQ" experiment (lower panel). *, compared to same MECs at control condition, P<0.05. #, compared to MECs treated with Bmp4 alone, P<0.05. **, P<0.05. n=3. (E) MECs were pretreated with 100 nmol/L bafilomycin A1(BafA1) for 6 hours and then subjected to the indicated treatments of Bmp4 and Bmper for 2 hours. The cell lysates were analyzed by Western blotting with antibodies for pSmad1/5/8 and Smad1. *, compared to same MECs at control condition, P<0.05. #, compared to MECs treated with Bmp4 alone, P<0.05. **, P<0.05. n=3. (F) Quantitative analysis of Figure 4C. *, compared to same MECs at control condition, P<0.05. #, compared to MECs treated with Bmp4 alone, P<0.05. **, P<0.05. n=3. (G) Quantitative analysis of Figure 4D. *, compared to same MECs at control condition, P<0.05. **, P<0.05. n=3. (H) The role of LRP1 in the regulation of ALK6 binding to other Bmp type II receptors such as the activin receptor type II (ACVRII) was examined. Lysates of MECs treated with Bmp4 (0.6 nmol/L) and Bmper (0.3 nmol/L or 10 nmol/L) for 15 minutes were immunoprecipitated with an anti-ACVRII antibody and analyzed by Western blotting with anti-ALK6 and ACVRII antibodies. Interestingly, the pattern of ALK6 binding to ACVRII was opposite from that of ALK6 and BMPRII (Figure 4D). At the basal state, ALK6 was associated with ACVRII, however the level of their binding significantly decreased in LRP1-knockdown MECs. Additionally, the binding of ALK6 and ACVRII was promoted upon Bmp4 and Bmper treatment in LRP1-knockdown MECs. Therefore, we speculate that LRP1 is required for the dynamic balance of Bmp receptors on the membrane. (I) Lysates of MEFs treated with Bmp4 (0.6 nmol/L) and Bmper (0.3 nmol/L or 10 nmol/L) for 15 minutes were immunoprecipitated with an antiBMPRII antibody and analyzed by Western blotting with anti-ALK6 and BMPRII antibodies. The binding of ALK6 and BMPRII was similar in MEFs, except samples treated with Bmper alone demonstrated no change in the association of ALK6 and BMPRII in MECs (Figure 4D) but an increased association in MEFs, suggesting that the expression levels of Bmp receptors and LRP1 possess subtle difference between MEFs and MECs. (J) Quantitative analysis of Figure 4E. *, compared to MECs at control condition, P<0.05. n=5. (K) MECs were subjected to the Boyden chamber migration analysis with Bmp4 (0.6 nmol/L) and Bmper as chemoattractants. *, compared to the same type of MECs at control condition, P<0.001. #, compared to the same type of MECs treated with Bmp4, P<0.001. n=4. (L) MECs were subjected to the Boyden chamber migration analysis with Bmp4 (4 nmol/L) as chemoattractants, and neutralizing Bmp4 antibody (10 μg/mL) was used to co-treat cells and block Bmp4 activity. *, compared to MECs at control condition, P<0.05. #, compared to MECs treated with Bmp4, P<0.05. n=3.

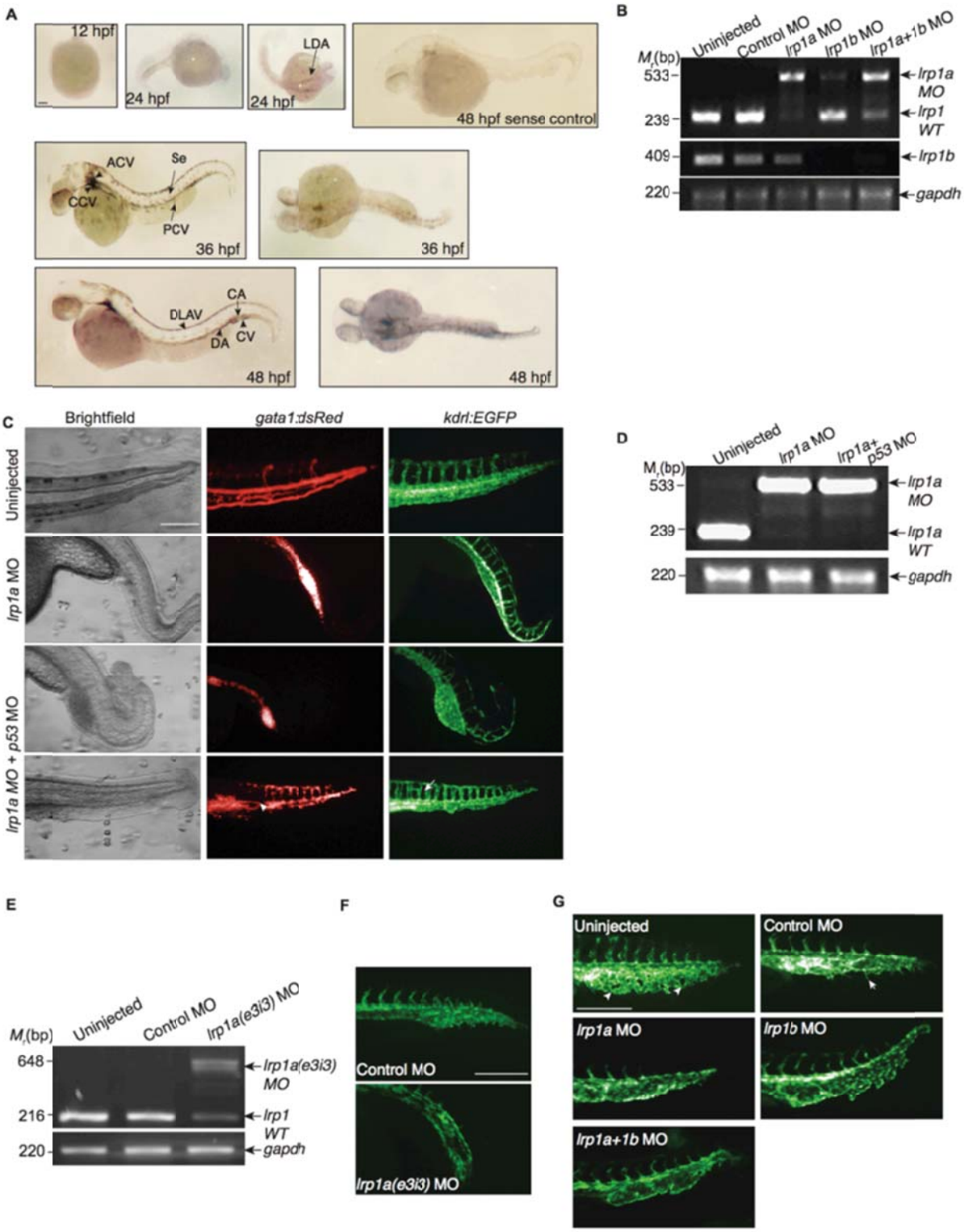
A
12 hpf
24 hpf
LDA
24 hpf
48 hpf sense control
ACV
Se
CCV
PCV
36 hpf
36 hpf
CA
DLAV
DA
CV
48 hpf
48 hpf
B
Uninjected
Control MO
lrp1a MO
lrp1b MO
lrp1a+1b MO
Mr(bp)
533
239
409
220
lrp1a MO
lrp1 WT
lrp1b
gapdh
C
Brightfield
gata1:dsRed
kdrl:EGFP
Uninjected
lrp1a MO
lrp1a MO + p53 MO
D
Uninjected
lrp1a MO
lrp1a+ p53 MO
Mr(bp)
533
239
220
lrp1a MO
lrp1a WT
gapdh
E
Mr(bp)
Uninjected
Control MO
lrp1a(e3i3) MO
648
216
220
lrp1a(e3i3) MO
lrp1 WT
gapdh
F
Control MO
lrp1a(e3i3) MO
G
Uninjected
Control MO
lrp1a MO
lrp1b MO
lrp1a+1b MO

Figure 6.11. *LRP1* is required for vascular development in zebrafish.

(A) RNA expression of lrp1a in a whole-mount zebrafish embryo, analyzed by in-situ hybridization using a lrp1a-specific antisense probe. The sense probe of lrp1a was used as a negative control Scale bar: 100 µm. (B) PCR analysis of zebrafish embryo RNAs demonstrates the knockdown of lrp1a or lrp1b or both with their specific MOs. (C) Loss of *lrp1a* and *p53* results in a similar vascular phenotype to the loss of *lrp1a*, suggesting there is no off-targeting effect with *lrp1a* MO. lateral views of *Tg(kdrl:EGFP)*^{s843};*Tg(gata1:dsRed)*^{sd2} fish embryo tails at 48 hpf were presented. The arrowhead represents the blood circulation with a changed route; the arrow represents the disrupted intersegmental vessel. Scale bar: 100µm. (D) PCR analysis of zebrafish embryo RNAs demonstrates the knockdown of lrp1a after injection of lrp1a and p53 MOs. (E) PCR analysis of zebrafish embryo RNAs demonstrates the knockdown of lrp1a(e3i3) with its specific MOs. (F) The cardiovascular defects observed with lrp1a MO targeting the e1i1 splice site were confirmed with an alternative MO -lrp1a(e3i3), targeting the e3i3 splice site. It suggests that lrp1a MO is specific. Images are lateral views of *Tg(kdrl:EGFP)*^{s843};*Tg(gata1:dsRed)*^{sd2} zebrafish embryo tails at 24 hpf. Scale bar: 100 µm. (G) Loss of lrp1a, lrp1b or both results in a similarly disrupted vascular phenotype. Images are lateral views of *Tg(kdrl:EGFP)*^{s843} zebrafish embryo tails at 24 hpf. The arrowheads represent the causal vein plexus with branches; the arrows represent filopodia located on the front edge of vessel plexus. Scale bar: 100 µm. (H) The wild-type recipient embryos *of Tg(kdrl:EGFP)*^{s843} were transplanted with control or lrp1 MO-injected donor cells (labeled with rhodamine-dextran). At 32 hpf, images of lateral views were taken with fluorescent microscopy. White arrowheads represent the donor cells located at cardinal vein plexus. Scale bar: 75 µm. LDA, lateral dorsal aorta. CCV, common cardinal vein. ACV, anterior cardinal vein. Se, intersegment vessel. DLAV, dorsal longitudianl anastomotic vessel. DA, dorsal aorta. CV, caudal vein. CA, caudal artery. PCV, posterior cardinal vein.

REFERENCES

1. Lowery JW, de Caestecker MP: **BMP signaling in vascular development and disease**. *Cytokine Growth Factor Rev*. 2010, **21**: 287–298.

2. Umulis D, O'Connor MB, Blair SS: **The extracellular regulation of bone morphogenetic protein signaling**. *Development* 2009, **136**: 3715–3728.

3. Heinke J, Wehofsits L, Zhou Q, Zoeller C, Baar KM, Helbing T, Laib A, Augustin H, Bode C, Patterson C, Moser M: **BMPER is an endothelial cell regulator and controls bone morphogenetic protein-4–dependent angiogenesis**. *Circ Res*. 2008, **103**:804–812.

4. Moser M, Binder O, Wu Y, Aitsebaomo J, Ren R, Bode C, Bautch VL, Conlon FL, Patterson C: **BMPER, a novel endothelial cell precursor-derived protein, antagonizes bone morphogenetic protein signaling and endothelial cell differentiation**. *Mol Cell Biol*. 2003, **23**:5664–5679.

5. Moser M, Yu Q, Bode C, Xiong JW, Patterson C: **BMPER is a conserved regulator of hematopoietic and vascular development in zebrafish**. *J Mol Cell Cardiol*. 2007, **43**:243–253.

6. Moreno-Miralles I, Ren R, Moser M, Hartnett ME, Patterson C; **Bone morphogenetic protein endothelial cell precursor-derived regulator regulates retinal angiogenesis in vivo in a mouse model of oxygen-induced retinopathy**. *Arterioscler Thromb Vasc Biol*. 2011, **31**:2216–2222.

7. Kelley R, Ren R, Pi X, Wu Y, Moreno I, Willis M, Moser M, Ross M, Podkowa M, Attisano L, Patterson C: **A concentration-dependent endocytic trap and sink mechanism converts Bmper from an activator to an inhibitor of Bmp signaling**. *J Cell Biol*. 2009, **184**:597–609.

8. Bu G, Geuze HJ, Strous GJ, Schwartz AL: **39 kDa receptor-associated protein is an ER resident protein and molecular chaperone for LDL receptor-related protein**. *EMBO J*. 1995, **14**:2269–2280.

9. Xia Z, Liu Y: **Reliable and global measurement of fluorescence resonance energy transfer using fluorescence microscopes**. *Biophys J*. 2001, **81**:2395–2402.

10. Pi X, Ren R, Kelley R, Zhang C, Moser M, Bohil AB, Divito M, Cheney RE, Patterson C: **Sequential roles for myosin-X in BMP6-dependent filopodial extension, migration, and activation of BMP receptors**. *J Cell Biol*. 2007, **179**:1569–1582.

11. Nasevicius A, Ekker SC: **Effective targeted gene 'knockdown' in zebrafish**. *Nat Genet*. 2000, **26**:216–220.

12. Wiley DM, Kim JD, Hao J, Hong CC, Bautch VL, Jin SW: **Distinct signalling pathways regulate sprouting angiogenesis from the dorsal aorta and the axial vein**. *Nat Cell Biol*. 2011, **13**:687–693.

13. Zhang JL, Qiu LY, Kotzsch A, Weidauer S, Patterson L, Hammerschmidt M, Sebald W, Mueller TD: **Crystal structure analysis reveals how the Chordin family member crossveinless 2 blocks BMP-2 receptor binding**. *Dev Cell*. 2008, **14**:739–750.

14. Lillis AP, Van Duyn LB, Murphy-Ullrich JE, Strickland DK: **LDL receptor-related protein 1: unique tissue-specific functions revealed by selective gene knockout studies**. *Physiol Rev*. 2008, **88**:887–918.

15. Obermoeller-McCormick LM, Li Y, Osaka H, FitzGerald DJ, Schwartz AL, Bu G: **Dissection of receptor folding and ligand-binding property with functional minireceptors of LDL receptor-related protein**. *J Cell Sci*. 2001, **114**:899–908.

16. Lillis AP, Mikhailenko I, Strickland DK: **Beyond endocytosis: LRP function in cell migration, proliferation and vascular permeability**. *J Thromb Haemost*. 2005, **3**:1884–1893.

17. Liu Q, Huang SS, Huang JS: **Function of the type V transforming growth factor beta receptor in transforming growth factor beta-induced growth inhibition of mink lung epithelial cells**. *J Biol Chem*. 1997, **272**:18891–18895.

18. May P, Rohlmann A, Bock HH, Zurhove K, Marth JD, Schomburg ED, Noebels JL, Beffert U, Sweatt JD, Weeber EJ, Herz J: **Neuronal LRP1 functionally associates with postsynaptic proteins and is required for normal motor function in mice**. *Mol Cell Biol*. 2004, **24**:8872–8883.

19. Shi Y, Massague J: **Mechanisms of TGF-beta signaling from cell membrane to the nucleus**. *Cell*. 2003, **113**:685–700.

20. Massague J: **TGF-beta signal transduction**. *Annu Rev Biochem*. 1998, **67**:753–791.

21. Southwood M, Jeffery TK, Yang X, Upton PD, Hall SM, Atkinson C, Haworth SG, Stewart S, Reynolds PN, Long L, Trembath RC, Morrell NW: **Regulation of bone morphogenetic protein signalling in human pulmonary vascular development**. *J Pathol*. 2008, **214**:85–95.

22. Robu ME, Larson JD, Nasevicius A, Beiraghi S, Brenner C, Farber SA, Ekker SC: **p53 activation by knockdown technologies**. *PLoS Genet*. 2007, 3:e78.

23. Rentzsch F, Zhang J, Kramer C, Sebald W, Hammerschmidt M: **Crossveinless 2 is an essential positive feedback regulator of Bmp signaling during zebrafish gastrulation**. *Development* 2006, **133**:801–811.

24. Di Fiore PP, De Camilli P: **Endocytosis and signaling: an inseparable partnership**. *Cell* 2001, **106**:1–4.

25. O'Connor MB, Umulis D, Othmer HG, Blair SS: **Shaping BMP morphogen gradients in the Drosophila embryo and pupal wing**. *Development* 2006, **133**:183–193.

26. Serpe M, Umulis D, Ralston A, Chen J, Olson DJ, Avanesov A, Othmer H, O'Connor MB, Blair SS: **The BMP-binding protein Crossveinless 2 is a short-range, concentration-dependent, biphasic modulator of BMP signaling in Drosophila**. *Dev Cell* 2008, **14**:940–953.

27. Yao Y, Jumabay M, Ly A, Radparvar M, Wang AH, Abdmaulen R, Bostrom KI: **Crossveinless 2 regulates bone morphogenetic protein 9 in human and mouse vascular endothelium**. *Blood* 2012, **119**:5037–5047.

28. van Kerkhof P, Lee J, McCormick L, Tetrault E, Lu W, Schoenfish M, Oorschot V, Strous GJ, Klumperman J, Bu G: **Sorting nexin 17 facilitates LRP recycling in the early endosome**. *EMBO J*. 2005, **24**:2851–2861.

29. Li Y, van Kerkhof P, Marzolo MP, Strous GJ, Bu G: **Identification of a major cyclic AMP-dependent protein kinase A phosphorylation site within the cytoplasmic tail of the low-density lipoprotein receptor-related protein: implication for receptor-mediated endocytosis**. *Mol Cell Biol*. 2001, **21**:1185–1195.

30. Hartung A, Bitton-Worms K, Rechtman MM, Wenzel V, Boergermann JH, Hassel S, Henis YI, Knaus P: **Different routes of bone morphogenic protein (BMP) receptor endocytosis influence BMP signaling**. *Mol Cell Biol*. 2006, **26**:7791–7805.

CHAPTER 7

Vascular Endothelial Growth Factor Signaling Regulates the Segregation of Artery and Vein via ERK Activity During Vascular Development

Summary

Vasculogenesis is the formation of a vascular cord, which is followed by arterio-venous segregation and lumenization of axial vessels. Little is known about the cues that promote this early separation of progenitors into differentiated, functional vessels. Here we further define the role of Vegf-A signaling in this process. Furthermore, we show interrogate the role of downstream effectors of Kdrl, Extracellular-signal-signal-related kinase (Erk) and phosphatidylinositol-3 kinase (PI3K), in this process using chemical genetic methods.

Introduction

The vascular network, which provides the essential functions of delivering oxygen and removing metabolic waste products, is one of the first organs to emerge in embryos. In vertebrates, the vascular system is formed by two distinct processes, vasculogenesis, de novo formation of blood vessels, and angiogenesis, the formation of new blood vessels from preexisting vessels. During development, endothelial cells, the innermost lining of the vascular network, form transient aggregates known as the vascular cord in the midline [1,2]. Endothelial cells within

the vascular cord start to express arterial and venous specific markers as early as E11.5 in mouse [3], and as early as 18 hours post-fertilization (hpf) in zebrafish [1,4], preceding the emergence of morphologically distinct arteries and veins [5]. Subsequently, developing vasculature acquires the stereotypic hierarchy; arteries and veins are physically separated and only connected by the capillaries. Failure to segregate arteries and veins results in ectopic shunts connecting these two types of vessels, a pathological condition known as arteriovenous malformation (AVM) [6]. While the etiology of AVM remains largely unknown, recent advances start to unravel the molecular and cellular mechanisms that underlie the sorting of arterial and venous endothelial cells. Attenuation of several genes has shown to cause failure in segregation of axial vessels in vertebrates. For instance, mutation in Dll4 in mice causes improper segregation of the dorsal aorta and the cardinal vein, creating arteriovenous shunts [7,8]. Similarly, simultaneous reduction of sox7 and sox18 genes resulted in improper segregation of the dorsal aorta and the cardinal vein[9,10,11]. In all cases, both differentiation of arterial/venous endothelial cells and the segregation of the axial vessels were affected, suggesting that these two events are tightly linked developmental processes.

Recent studies have shown that arterial and venous endothelial cells respond differently to various signaling molecules, which might be the main driving force for the segregation of arteries and veins during development. For instance, Vascular Endothelial Growth Factor-A (Vegf-A) and Vascular Endothelial Growth Factor-C (Vegf-C) signaling preferentially activates dorsal migration of arterial endothelial cells and ventral migration of venous endothelial cells respectively, within the vascular

cord, therefore, synergistically promoting the segregation of axial vessels in zebrafish embryos [2]. In addition, the repulsive interaction between EphrinB2 and EphB4 has been shown to be critical in regulating the segregation of arterial endothelial cells from the venous endothelial cells in developing mouse embryo. The dorsal aorta in mice lacking EphrinB2 or EphB4 contained venous endothelial cells, leading to the enlarged dorsal aorta at the expense of the cardinal vein [12]. Later in development, we have recently demonstrated that arterial and venous endothelial cells exhibit different responses to Vegf-A and Bone Morphogenetic Protein (Bmp) signaling [13]. While Bmp signaling induces angiogenesis within venous endothelial cells, arterial endothelial cells remain unaffected. Conversely, Vegf-A signaling preferentially facilitates angiogenesis within arterial endothelial cells without activating venous endothelial cells. Collectively, these reports indicate distinct molecular nature of arterial and venous endothelial cells. However, it is unclear how differences in molecular characteristics of arterial and venous endothelial cells contribute to the segregation of axial vessels. Moreover, it is unknown which signaling pathways regulate the segregation of axial vessels during development. Considering its importance during vascular development, it is likely that VEGF-A signaling may provide a pivotal function in this process.

In this study, we used zebrafish as a model system to investigate the role of Vegf-A signaling during the segregation of axial vessels. We find that reduction in Vegf-A signaling activity led to a failure in the segregation of arteries and veins. Moreover, we find that inhibition of Erk, which are known to function downstream of Vegf-A signaling pathway [4] yield similar defects in developing zebrafish, while

activation of Erk in embryos with a reduced level of Vegf-A activity can restore the segregation defects, indicating that activation of Erk by Vegf- A signaling is essential for the proper segregation of axial vessels. Taken together, our data demonstrate the critical role of Vegf-A signaling during the segregation of axial vessels.

Experimental Methods

Zebrafish Husbandry

Zebrafish (Danio rerio) embryos and adults were raised and maintained as previously described under IACUC guidelines[14].

Microinjection and chemical treatment

Morpholinos (MO) (Gene Tools, LLC) were injected into 1-cell-stage Tg(kdrl:EGFP) embryos as previously described [1]. The sequences of MOs used in this study are; kdrl: 5'- CACAAAAAGCGCACACTTACCATGT-3',
vegf-aa: 5'-CTCGTCTTATTTCCGTGACTGTTTT-3'[15],
kdr: 5'- GTTTTCTTGATCTCACCTGAACCCT-3',
ephrinb2a: 5'- CGGTCAAATTCCGTTTCGCGGGA-3'[16],
plcγ: 5'-ATTAGCATAGGGAACTTACTTTCG-3' [17].
For chemical treatment, embryos were treated from the 10 somite stage to 30 hours post fertilization (hpf) unless noted otherwise, and fixed overnight in 4% paraformaldehyde (PFA). To transiently express constitutively active MEK (CA-MEK) [18] in endothelial cells, CA-MEK was subcloned into the Gateway middle entry vector and recombined into kdrl promoter containing vector. The resulting

construct allows kdrl promoter regulated, transient expression of CA-MEK in a subset of endothelial cells in injected embryos.

IP3 uncaging and analysis

Caged IP_3 (800μM) was co-injected with caged-fluorescein (0.2% w/v) dextran to assess uncaging and Vegf-a morpholino. Uncaging was done using the UV channel of a Leica Confocal Microscope (Michael Hooker Miscroscopy Institute) at the 18-somite stage. Rescue of morphant phenotype was assessed at the 30 hpf stage.

Immunohistochemistry, western blot, and in situ hybridization

Immunohistochemistry and in situ hybridization were performed as previously described [1]. Anti-β-catenin antibody (1:150, BD Biosciences) was used to show cell boundaries.

Phenotypic analyses

30 hpf zebrafish embryos were analyzed by fluorescent stereomicroscope to examine the vascular morphology. For those appear to contain a single axial vessels, transverse sections from 10th somite to 18th somite of 30 hpf zebrafish embryos were analyzed by confocal microscopy. Minimum of ten sections per embryos were analyzed. If the embryo had more than seven sections with single axial vessels, it was counted as ‘embryos with a single axial vessel’.

Quantitative RT-PCR

Quantitative RT-PCR was performed as previously reported [19]. The trunk region (above the yolk extension) of the embryos was dissected and RNA was

extracted, and pre-tested qRT-PCR primers (Applied biosystems) were used to detect the gene expression

Results and Discussion

To examine the function of Vegf-A signaling during segregation of axial vessels, we attenuated the function of well characterized components of Vegf-A signaling in *Tg(kdrl:EGFP)*^{s843} embryos[1]. Blocking Vegf-A signaling by injecting morpholino (MO) against vegf-aa or plcγ caused failure in segregation of axial vessels (Figure 7.1A to C), indicating that Vegf-A signaling plays an important role in the segregation of axial vessels.

In zebrafish genome, two functional orthologs of Vascular Endothelial Growth Factor Receptor 2 (VEGFR2/KDR), vegfr2/kdr and vegfr4/kdrl are present [20]. Previously, it has been shown that the function of Kdr appears to be largely dispensable for the specification of arterial endothelial cells, although Kdrl and Kdr might function redundantly to promote segmental artery formation [21]. Therefore, it is plausible that Kdrl and Kdr may have a distinct role in transducing the activity of Vegf-A signaling during axial vessel segregation in zebrafish. To examine this possibility, we selectively inhibited Kdrl or Kdr during development, and analyze the resulting vascular phenotype (Figure 7.2).

While embryos injected with kdrl MO contained only a single axial vessel, those injected with kdr MO injected embryos had a distinct dorsal aorta and axial vein, suggesting that the function of Kdr may be dispensable for the segregation of axial vessels (Figure 7.2B and 7.2C). Furthermore, the severity and penetrance of

defects on axial vessel segregation in embryos co-injected with *kdrl* and *kdr* MO were comparable to those of embryos injected with *kdrl* MO alone, suggesting that the contribution of Kdr to the segregation of axial vessels is likely to be minor.

Interestingly, blocking either Kdrl or Kdr function led a significant reduction in the expression level of arterial and venous specific genes, indicating that both Vegfr2/KDR orthologs are required to promote or maintain the expression of differentiated endothelial cell markers (Figure 7.2D). Taken together, it seems that both Kdr and Kdrl are required to maintain and/or initiate differentiation of endothelial cells, while Kdrl appears to be the main Vegf-A receptor during segregation of axial vessels.

One of the main downstream effector of Vegf-A signaling is Protein Kinase C (PKC), which is activated by diacylglycerol (DAG) [22]. It has been shown that inhibition of PKC by chemical antagonists blocks the pro-angiogenic effects of Vegf-A signaling. To test whether PKC is also involved in transducing Vegf-A signaling during segregation of axial vessels, we attenuated the level of PKC activity. 14 hpf wild-type zebrafish embryos were treated with 60μM Bisindolylmaleimide, a known antagonist of PKC, for 16 hours [23]. As a positive control, SU5416, a well characterized chemical antagonist of VEGFR2, was used. In embryos treated with SU5416, the axial vessels failed to segregate as expected (n=20) (Figure 7.3A and 7.E). Similarly, we find that failure in segregation of axial vessels failed in embryos with reduced PKC activity (n=75) (Figure 7.3B and 7.3E), indicating that PKC is an essential mediator for Vegf-A signaling during segregation of axial vessels.

Two prominent downstream effectors of PKC activity in the Vegf-A signaling cascade is Map2k1/Erk and Akt/PI3K, which elicit a variety of cellular responses including increased vascular permeability, elevated eNOS production, and initiation of Vegf-A target genes [24]. To determine the function of these two signaling pathways in transducing Vegf-A signaling during the segregation of axial vessels, we also attenuated the activity of Map2k1/Erk or Akt/PI3K, and examined the resulting vascular phenotype.

When embryos were treated with 25μM U0126, a chemical antagonist of Map2k1/Erk [25], from 14 to 30 hpf, a significant portion of the embryos had a single axial vessel with impaired circulation, which was reminiscent of the phenotype of embryos with compromised Vegf-A signaling (n=105), suggesting that the Map2k1/Erk activity is required to mediate Vegf-A signaling during the segregation of axial vessels (Figure 3C and E).

Similarly, to investigate the contribution of Akt/PI3K in antagonizes Map2k1/Erk in a similar manner to modulate Vegf-A signaling during the segregation of axial vessels, we treated embryos from 14 to 30 hpf with 30μM LY294002, a chemical antagonist that inhibits phosphorylation of Akt therefore attenuating PI3K activity (n=98) [26]. Inhibition of PI3K activity at this stage caused vascular defects comparable to Map2k1/Erk inhibition (Figure 7.3D and 7.3E). Approximately 70 percent of the embryos treated with LY294002 displayed a single axial vessel (Figure 7.33E). Taken together, our data indicate that effects of Vegf-A signaling during the segregation of the axial vessels require the activity of PKC, Erk, and PI3K.

To determine if the effect seen when PI3K was inhibited was mediated by IP3, we used UV-photoactivation caged IP3 in small two somite segments at 18.5 hpf. Activation of IP3 in the developing vascular cord did not rescue the effect of the *kdrl* morpholinos. That is, rescue of arteriovenous segregation was never observed within the uncaged region (N=54) similar to mock control with only caged fluorescein dextran (N=34).

To examine whether activation of these downstream effectors is sufficient to initiate segregation of axial vessels in embryos with a reduced level of Vegf-A signaling, we utilized chemical genetics approach. To test whether the activation of PKC is sufficient to bypass the requirement of Vegf-A signaling, *kdrl* MO injected embryos were incubated with 16μM 12- O-tetradecanoylphorbol-13-acetate (TPA) [27], a chemical agonist of PKC from 14 to 30 hpf. As a positive control, we used GS4012, a chemical agonist of Vegf-A signaling. While *kdrl* MO injected embryos incubated with DMSO (empty vehicle) contained a single axial vessel (n=40, Figure 7.4A and 7.4B), 77 percent of *kdrl* MO injected embryos treated with GS4012, and 86 percent of *kdrl* MO injected embryos incubated with TPA had a clearly separate dorsal aorta and axial vein (n=55 for GS4012, and n=42 for TPA, Figure 7.4A and 7.4B). Therefore, activation of PKC is sufficient to alleviate defects on the segregation of axial vessels caused by reduced Vegf-A signaling.

To further examine the function of Map2k1/Erk in the segregation of axial vessels, constitutively active MEK (CA-MEK) was selectively expressed in endothelial cells in *kdrl* MO injected embryos (Figure 7.4C and 7.4D) [18]. Since MEK induces activation of Map2k1/Erk, ectopic expression of CA-MEK in endothelial

cells should alleviate the phenotype of kdrl MO injected embryos. While less than two percent of embryos co-injected with a vector encoding Blue Fluorescent Protein (BFP) and kdrl MO contained two axial vessels at 28 hpf (Figure 7.4E), a significant portion (38%) of embryos co-injected with the CA-MEK construct and *kdrl* MO had clearly distinguishable axial vessels (Figure 7.4E), suggesting that Map2k1/Erk activity is critical for the segregation of the axial vessels, but dispensable for the maintenance of the arterial or venous specific gene expression downstream of Vegfr signaling.

FIGURES:

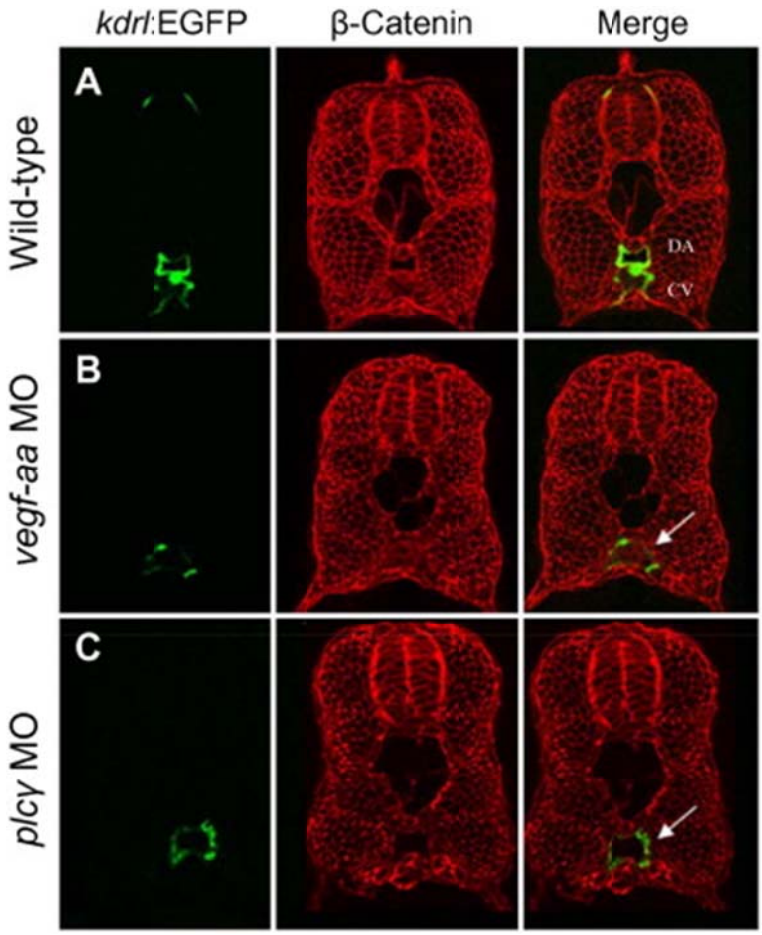

Figure 7.1: Attenuation of Vegf-A signaling components causes defects in axial vessel segregation as observed in *kdrl*^{s828} mutants.

Transverse sections taken at the level of the 14th somite were analyzed by confocal microscopy. 36 hpf wild-type (A), *vegf-aa* MO injected (B), and *plcγ* MO injected (C) embryos in *Tg(kdrl:*EGFP*)*^{s843} background. Endothelial cells are visualized by the expression of EGFP transgene (green), cell boundaries are shown by Anti-β-catenin staining (red). White arrows in panels B and C point to the single axial vessel. Abbreviations: DA, dorsal aorta, CV, caudal vein.

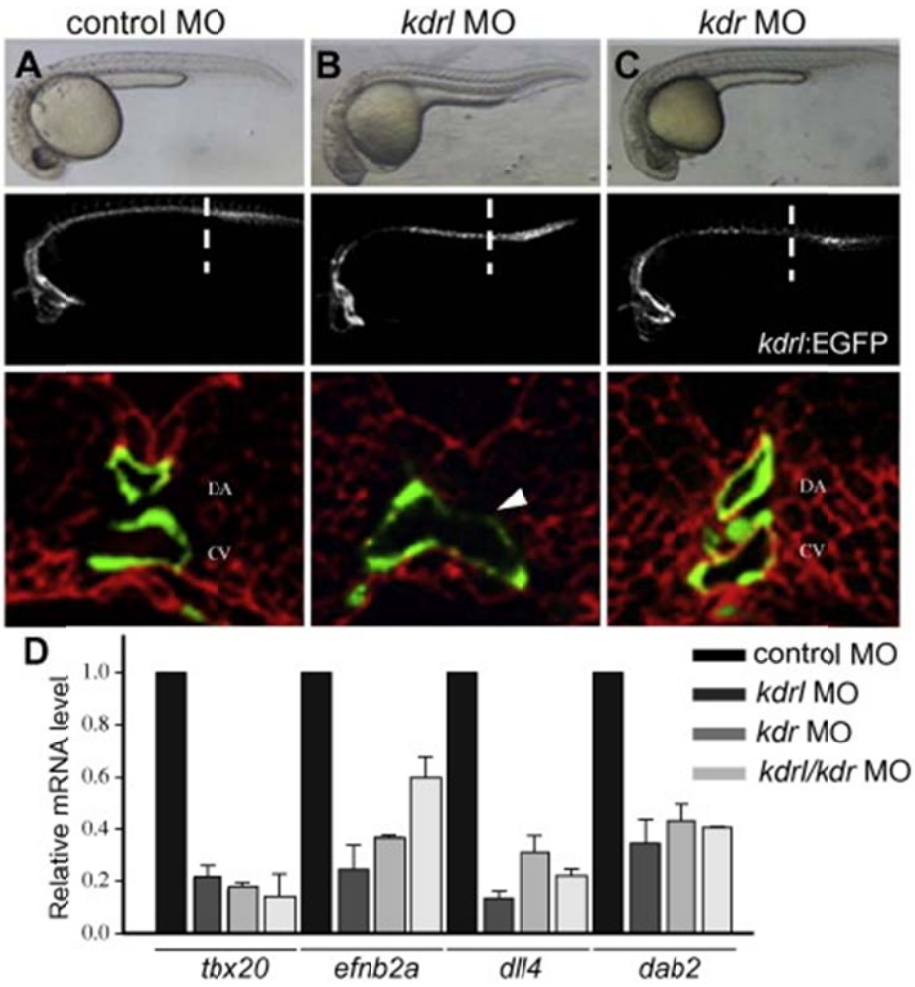

Figure 7.2: Kdrl functions as the main receptor for Vegf-A signaling during the segregation of axial vessels.

Bright field micrographs (top row), epifluorescence micrographs (middle row), and confocal images of a transverse section at the 14th somite level (bottom row) of 36 hpf embryos injected with control MO (A), *kdrl* MO (B), or *kdr* MO (C) in *Tg(kdrl:*EGFP*)*^{s843} background. Endothelial cells are visualized by the expression of EGFP transgene (green), cell boundaries are shown by Anti-β-catenin staining (red). White arrowhead in panel B points to the single axial vessel. (D) Quantitative RT-PCR of endothelial specific genes in 36 hpf MO injected embryos. Attenuation of either *kdrl* or *kdr* significantly reduced the expression of arterial and venous marker expression. Abbreviations: DA, dorsal aorta, CV, caudal vein.

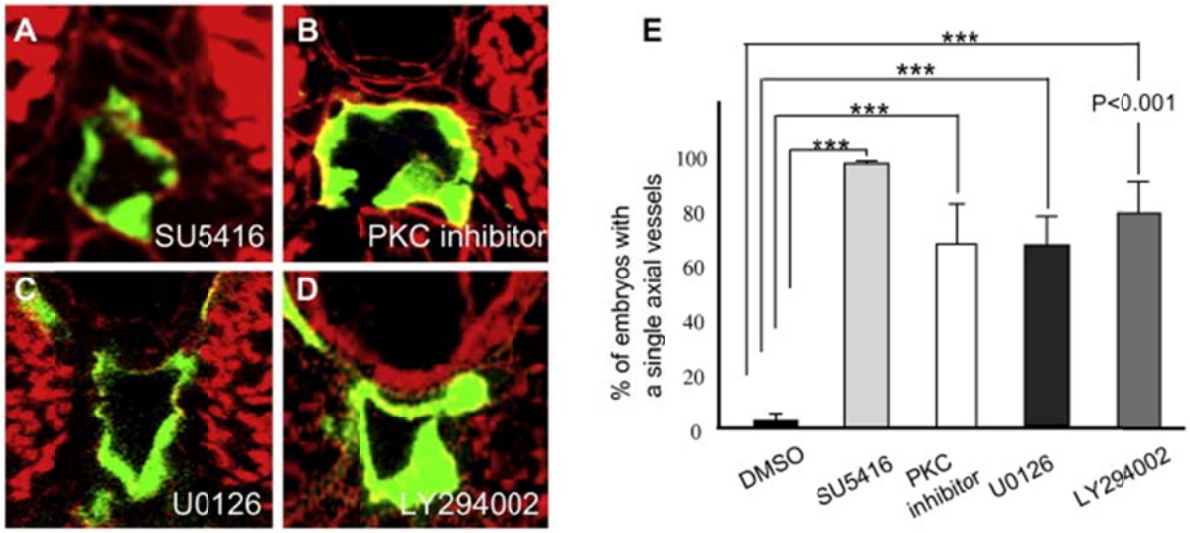

Figure 7.3: Attenuation of Vegf-A downstream effectors caused defects in segregation of axial vessels.

Transverse sections taken at the level of the 14th somite were analyzed by confocal microscopy. 36 hpf *Tg(kdrl:*EGFP*)s843* embryos treated with 1μM SU5416 (A), 60μM Bisindolylmaleimide, a chemical antagonist of PKC (B), 25μM U0126 (C), or 30μM LY294002 (D). (E) Quantification of chemical treatments. Compared to DMSO treated embryos, the percentage of embryos with a single axial vessel was significantly increased in embryos treated with SU5416, Bisindolylmaleimide, U0126, or LY294002 (P<0.001).

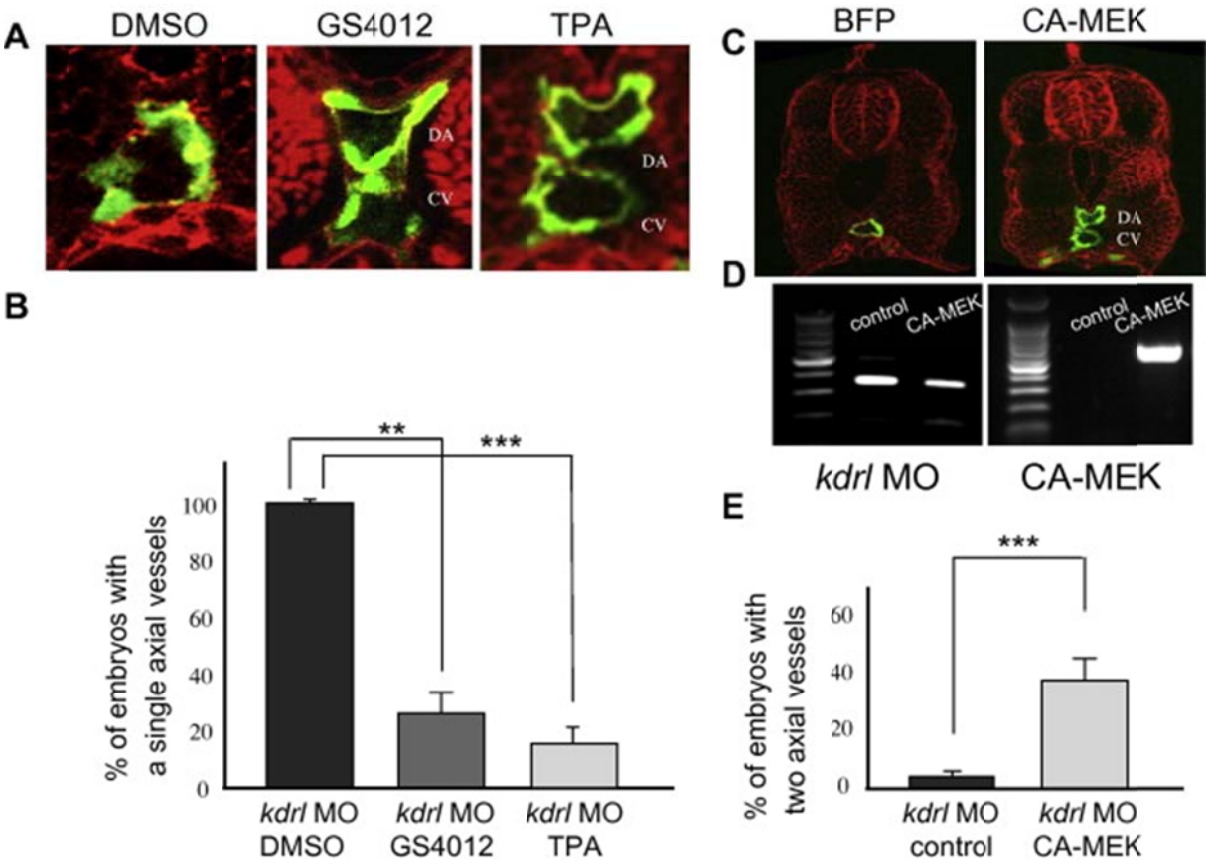

Figure 7.4: Activation of PKC or Erk activity can rescue the defects in segregation of axial vessels in embryos with compromised Vegf-A signaling.

Transverse sections taken at the level of the 14th somite were analyzed by confocal microscopy. 36 hpf *Tg(kdrl:*EGFP*)^{s843}* embryos treated with DMSO (left), 7.5μg/ml GS4012 (middle), and 16μM 12-O-tetradecanoylphorbol-13-acetate (right). (B) Treatment with 16μM 12-O-tetradecanoylphorbol-13-acetate restored the defects in segregation of axial vessels better than GS4012, a positive control. (C) Transverse sections taken at the level of the 14th somite from *kdrl* MO injected embryos, co-injected with either vector containing Blue Fluorescent Protein (BFP) or constitutively active MEK (CA-MEK). (D) PCR confirmation showing the validity of *kdrl* MO (left) and expression of CA-MEK construct (right). (E) The defect in axial vessel segregation in *kdrl* MO injected embryos was substantially rescued by ectopic activation of MEK, which can increase the level of Erk activity. Abbreviations: DA, dorsal aorta, CV, caudal vein.

uncaged & activated

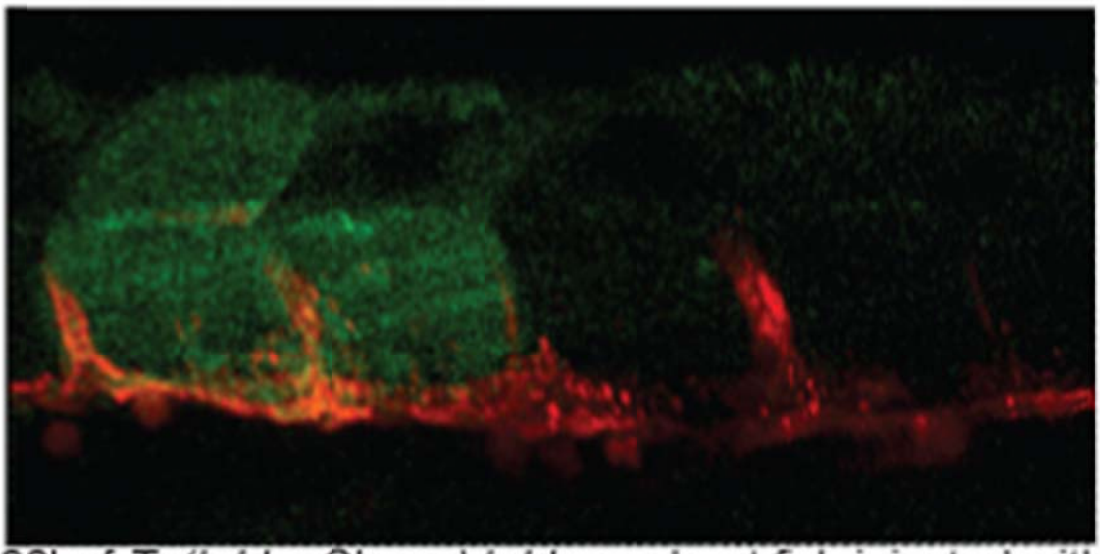

36hpf *Tg(kdrl:mCherry) kdrl* morphant fish injected with caged IP_3/caged fluorescein dextran

Figure 7.5: Photoactivation of IP_3 does not rescue the vessel defect in *kdrl* morphants.

Embryos were injected with caged IP_3 with caged fluorescein-dextran as a tracer. Segments two somites in length were activate using a UV laser. Activation of IP_3 was never found to rescue the arterio-venous segregation defect seen in *kdrl* morphant embryos (N=54). Black line on left indicates the single axial vessel.

REFERENCES

1. S.W. Jin, D. Beis, T. Mitchell, J.N. Chen, D.Y. Stainier: **Cellular and molecular analyses of vascular tube and lumen formation in zebrafish**. Development 132 (2005) 5199-5209.

2. S.P. Herbert, J. Huisken, T.N. Kim, M.E. Feldman, B.T. Houseman, R.A. Wang, K.M.Shokat, D.Y. Stainier: **Arterial-venous segregation by selective cell sprouting: an alternative mode of blood vessel formation**. Science 2009, **326**:294-298.

3. R.H. Adams, G.A. Wilkinson, C. Weiss, F. Diella, N.W. Gale, U. Deutsch, W. Risau, R. Klein: **Roles of ephrinB ligands and EphB receptors in cardiovascular development: demarcation of arterial/venous domains, vascular morphogenesis, and sprouting angiogenesis**. *Genes Dev* 1999, **13**:295-306.

4. C.C. Hong, Q.P. Peterson, J.Y. Hong, R.T. Peterson: **Artery/vein specification is governed by opposing phosphatidylinositol-3 kinase and MAP kinase/ERK signaling**. *Curr Biol* 2006, **16**:1366-1372.

5. S.W. Jin, C. Patterson: **The opening act: vasculogenesis and the origins of circulation**. *Arterioscler Thromb Vasc Biol* 2009, **29**:623-629.

6. G.G. Leblanc, E. Golanov, I.A. Awad, W.L. Young: **Biology of vascular malformations of the brain**. *Stroke* 2009, **40**:e694-702.

7. A. Duarte, M. Hirashima, R. Benedito, A. Trindade, P. Diniz, E. Bekman, L. Costa, D. Henrique, J. Rossant**: Dosage-sensitive requirement for mouse Dll4 in artery development**. *Genes Dev* 2004, 18:2474-2478.

8. N.W. Gale, M.G. Dominguez, I. Noguera, L. Pan, V. Hughes, D.M. Valenzuela, A.J. Murphy, N.C. Adams, H.C. Lin, J. Holash, G. Thurston, G.D. Yancopoulos: **Haploinsufficiency of delta-like 4 ligand results in embryonic lethality due to major defects in arterial and vascular development**. *Proc Natl Acad Sci* 2004, **101**:15949-15954.

9. H. Pendeville, M. Winandy, I. Manfroid, O. Nivelles, P. Motte, V. Pasque, B. Peers, I. Struman, J.A. Martial, M.L. Voz: **Zebrafish Sox7 and Sox18 function together to control arterial-venous identity**. *Dev Biol* 2008, **317**:405-416.

10. R. Herpers, E. van de Kamp, H.J. Duckers, S. Schulte-Merker: **Redundant roles for sox7 and sox18 in arteriovenous specification in zebrafish**. *Circ Res* 2008, **102**:12-15.

11. S. Cermenati, S. Moleri, S. Cimbro, P. Corti, L. Del Giacco, R. Amodeo, E. Dejana, P. Koopman, F. Cotelli, M. Beltrame: **Sox18 and Sox7 play redundant roles in vascular development**. *Blood* 2008, **111**:2657-2666.

12. Y.H. Kim, H. Hu, S. Guevara-Gallardo, M.T. Lam, S.Y. Fong, R.A. Wang: **Artery and vein size is balanced by Notch and ephrin B2/EphB4 during angiogenesis**. *Development* 2008, **135**:3755-3764.

13. D.M. Wiley, J.D. Kim, H. J., C.C. Hong, V.L. Bautch, S.W. Jin: **Distinct Signaling Pathways Regulate Sprouting Angiogenesis from the Dorsal Aorta and Axial Vein**. *Nat Cell Biol* 2011,

14. M. Westerfield: **The zebrafish book, A Guide for the laboratory use of zebrafish (Danio rerio)**. 4th Ed., *University of Oregon Press*, Eugene, 2000.

15. A. Nasevicius, S.C. Ekker: **Effective targeted gene 'knockdown' in zebrafish**. *Nat Genet* 2000, **26**:216-220.

16. J.E. Cooke, H.A. Kemp, C.B. Moens: **EphA4 is required for cell adhesion and rhombomere-boundary formation in the zebrafish**. *Curr Biol* 2005, **15**:536-542.

17. N.D. Lawson, J.W. Mugford, B.A. Diamond, B.M. Weinstein: **phospholipase C gamma-1 is required downstream of vascular endothelial growth factor during arterial development**. *Genes Dev* 2003, **17**:1346-1351.

18. F.A. Scholl, P.A. Dumesic, P.A. Khavari: **Mek1 alters epidermal growth and Differentiation**. *Cancer Res* 2004, **64**: 6035-6040.

19. C.Y. Lee, K.M. Vogeli, S.H. Kim, S.W. Chong, Y.J. Jiang, D.Y. Stainier, S.W. Jin, **Notch signaling functions as a cell-fate switch between the endothelial and hematopoietic lineages**. *Curr Biol* 2009,**19**:1616-1622.

20. J. Bussmann, N. Lawson, L. Zon, S. Schulte-Merker: **Zebrafish VEGF receptors: a guideline to nomenclature**. *PLoS Genet* 2008, **4**:e1000064.

21. L.D. Covassin, J.A. Villefranc, M.C. Kacergis, B.M. Weinstein, N.D. Lawson: **Distinct genetic interactions between multiple Vegf receptors are required for development of different blood vessel types in zebrafish**. *Proc Natl Acad Sci* 2006,**103**:6554-6559.

22. C.C. Hong, T. Kume, R.T. Peterson: **Role of crosstalk between phosphatidylinositol 3-kinase and extracellular signal-regulated kinase/mitogen-activated protein kinase pathways in artery-vein specification**. *Circ Res* 2008, **103**:573-579.

23. D. Toullec, P. Pianetti, H. Coste, P. Bellevergue, T. Grand-Perret, M. Ajakane, V. Baudet, P. Boissin, E. Boursier, F. Loriolle, et al.: **The bisindolylmaleimide GF109203X is a potent and selective inhibitor of protein kinase C**. *J Biol Chem* 1991, **266**:15771-15781.

24. I. Zachary: **VEGF signalling: integration and multi-tasking in endothelial cell biology**. *Biochem Soc Trans* 2003, **31**:1171-1177.

25. M.F. Favata, K.Y. Horiuchi, E.J. Manos, A.J. Daulerio, D.A. Stradley, W.S. Feeser, D.E. Van Dyk, W.J. Pitts, R.A. Earl, F. Hobbs, R.A. Copeland, R.L. Magolda, P.A. Scherle, J.M. Trzaskos: **Identification of a novel inhibitor of mitogen-activated protein kinase kinase**. *J Biol Chem* 1998, **273**:18623-18632.

26. C.J. Vlahos, W.F. Matter, K.Y. Hui, R.F. Brown: **A specific inhibitor of phosphatidylinositol 3-kinase, 2-(4-morpholinyl)-8-phenyl-4H-1-benzopyran-4-one (LY294002)**. *J Biol Chem* 1994, **269**:5241-5248.

27. R.M. Bell, Y.A. Hannun, C.R. Loomis: **Mechanism of regulation of protein kinase C by lipid second messengers**. *Symp Fundam Cancer Res* 1986, **39**:145-156.